APPENDIX – C

DERIVATION OF EQUATIONS RELATED TO THE GAMMA CURVE

C.1 Equation of the Unit-Peak-at-Origin (UPO) Gamma curve used for deriving the parametric form of the characteristic flood hydrograph

Expressing *y* as a function of *x*, the equation of the standard Gamma distribution, having the start of rise at the origin (*x* = 0, *y* = 0) and enclosing unit volume under the curve, is given by

$$y = f(x) = \frac{1}{K\,\Gamma(n)}\left(\frac{x}{K}\right)^{n-1} Exp\left(-\frac{x}{K}\right) \qquad \text{… (C.1.1)}$$

where, *n* is the shape parameter, *K* is the scale parameter and *Γ*(*n*) is the Gamma function at *n*, with *n* ≥ 1.

If the start of rise of the curve is to be shifted/translated by '*T*' units to the left of the origin, for any value *T* > 0, the equation of the 3-parameter shifted Gamma curve has the form

$$y = f(x) = \frac{1}{K\,\Gamma(n)}\left(\frac{x+T}{K}\right)^{n-1} Exp\left(-\frac{x+T}{K}\right) \qquad \text{… (C.1.2)}$$

the parameters being *K*, *x* and *T*.

For the maximum or the minimum of this shifted curve, d*y*/d*x* = 0.

Differentiating equation (C.1.2) with respect to *x*, and setting d*y*/d*x* = 0 gives

$$\frac{dy}{dx} = \frac{1}{K\,K^{n-1}\Gamma(n)}\left\{(n-1)(x+T)^{n-2} Exp\left(-\frac{x+T}{K}\right) - \frac{1}{K}(x+T)^{n-1} Exp\left(-\frac{x+T}{K}\right)\right\} = 0$$

$$\Rightarrow \quad \frac{dy}{dx} = \frac{(x+T)^{n-1} Exp\left(-\frac{x+T}{K}\right)}{K^{n+1}\Gamma(n)}\left\{\frac{(n-1)K}{x+T} - 1\right\} = 0$$

i.e. $(x+T)^{n-1} = 0,$ or $Exp\left\{-\frac{(x+T)}{K}\right\} = 0$ or $\left\{\frac{(n-1)K}{x+T}\right\} - 1 = 0$

For $n > 1,\ (x+T)^{n-1} = 0 \ \Rightarrow\ x = -T$ and hence we have a minimum at that value of *x*.

It may be seen from equation (C.1.2) that *y* = 0 at *x* = -*T*, so that this minimum at *x* = -*T* clearly corresponds to the start of rise of the Gamma curve at the point (-*T*,0), which is consistent with the translation of the Gamma curve of equation (C.1.1) to the left by *T*.

For $Exp\left\{-\frac{x+T}{K}\right\} = 0,\quad \left\{-\frac{x+T}{K}\right\} = Log_e(0) = \infty$, which is impossible.

Hence, we must have $\left\{\frac{(n-1)K}{x+T}\right\} - 1 = 0$, giving $x = (n-1)K - T$ as the constraint on the value of *x*, for given *T*, *K* and *n* values, such that the corresponding *y* value is the peak value, i.e. this is the value on the abscissa at which the maximum, i.e. the peak, of the shifted Gamma curve of equation (C.1.2) occurs.

If, furthermore, we introduce the additional constraint that the peak ordinate of the shifted Gamma curve of equation (C.1.2) be located at the origin, then $x = \{(n-1)K - T\} = 0$ is the condition that must be satisfied. For given *K* and *n* values, the required value of the

shift/translation T to satisfy this 'peak-at-origin' condition, denoted by the symbol T_r, is given by

$$T_r = (n-1)K \qquad \text{… (C.1.3)}$$

Henceforth, we will call this 'Peak-at-Origin Gamma curve' the 'PO-Gamma curve'.

Thus, in terms of T_r, K and n, the equation for the shifted Gamma curve having its peak located at the origin, i.e. the PO-Gamma curve, is obtained from equation (C.1.2) simply by replacing T by T_r to give the 2-parameter curve

$$y = f(x) = \frac{1}{K\,\Gamma(n)}\left(\frac{x+T_r}{K}\right)^{n-1} Exp\left(-\frac{x+T_r}{K}\right) \qquad \text{(C.1.4)}$$

which, on using equation (C.1.3), may also be written explicitly in terms of the two parameters n and K as

$$y = f(x) = \frac{1}{K\,\Gamma(n)}\left(\frac{x+(n-1)K}{K}\right)^{n-1} Exp\left(-\frac{x+(n-1)K}{K}\right) \qquad \text{(C.1.5)}$$

Thus, in contrast to the 3-parameter Gamma curve of equation (C.1.2), the PO-Gamma curve of equations (C.1.4) and (C.1.5), like the standard Gamma curve of equation (C.1.1), is simply a 2-parameter curve. Whereas equation (C.1.1) has been widely applied in rainfall-runoff modelling and flood routing, as the Nash-cascade IUH (Nash, 1957) and the Kalinin-Milyukov routing method (Kalinin and Milyukov, 1957), it is the PO-Gamma that is appropriate in the context of WP3.1, i.e. for fitting a Gamma curve having its peak coincide with a given flood peak value.

For the PO-Gamma curve, having its origin at the location of its peak, the peak ordinate y_P is given by setting $x = 0$ in equations (C.1.4) and (C.1.5), i.e. as

$$y_P = \frac{1}{K\,\Gamma(n)}\left(\frac{T_r}{K}\right)^{n-1} Exp\left(-\frac{T_r}{K}\right) \qquad \text{… (C.1.6)}$$

$$y_P = \frac{1}{K\,\Gamma(n)}(n-1)^{n-1} Exp(1-n) \qquad \text{… (C.1.7)}$$

Dividing equations (C.1.4) and (C.1.5) by (C.1.6) and (C.1.7) respectively, i.e. rescaling the PO-Gamma curve to have unit peak, yields the ratio as

$$\frac{y}{y_P} = \left(\frac{x+T_r}{T_r}\right)^{n-1} Exp\left(-\frac{x+T_r}{K}+\frac{T_r}{K}\right) = \left(\frac{x+T_r}{T_r}\right)^{n-1} Exp\left(-\frac{x}{K}\right)$$

and also, on substituting for $T_r = K(n-1)$, as

$$\frac{y}{y_P} = \left(\frac{x+(n-1)K}{K(n-1)}\right)^{n-1} Exp\left(-\frac{x+(n-1)K}{K}+\frac{(n-1)K}{K}\right) = \left(\frac{x+(n-1)K}{K(n-1)}\right)^{n-1} Exp\left(-\frac{x}{K}\right)$$

Denoting this ratio $\frac{y}{y_P}$ by $\boldsymbol{y}$ gives

$$\boldsymbol{y} = \boldsymbol{y}(x) = \left(\frac{x+T_r}{T_r}\right)^{n-1} Exp\left(-\frac{x}{K}\right) \qquad \text{… (C.1.8)}$$

in terms of the T_r and K parameters.

In terms of the more familiar K and n parameters, this function $\boldsymbol{y}$ has the form

$$\boldsymbol{y} = \boldsymbol{y}(x) = \left(\frac{x+(n-1)K}{(n-1)K}\right)^{n-1} Exp\left(-\frac{x}{K}\right) \qquad \text{… (C.1.9)}$$

Similarly, substituting $1/K = (n-1)/T_r$ from equation (C.1.3) into Equation (C.1.8), we have $\boldsymbol{y}$ in terms of n and T_r as

$$\boldsymbol{y} = \boldsymbol{y}(x) = \left(\frac{x+T_r}{T_r}\right)^{n-1} Exp\left(-\frac{x(n-1)}{T_r}\right) \qquad \text{… (C.1.10)}$$

Equations (C.1.8) to (C.1.10) of the shifted (i.e. unit-peak-at-origin) Gamma curve, referred to as the **'UPO-Gamma' curve** in the main report and in the following sections of this appendix, has its peak located at the origin, the start of its rise at T_r units to the left of the origin (i.e. at x = $-T_r$), and a peak magnitude of unity. As n, K and T_r, are related by $T_r = K(n-1)$, from equation (C.1.3), where $n > 1.0$, the 'UPO-Gamma' curve of equation (C.1.10), like those of the PO-Gamma equations (C.1.6) to (D1.1.8) and the standard Gamma curve of equation (C.1.1), is a 2-parameter curve. Note that if $n = 1$, the UPO-Gamma curve would reduce to an exponential curve of recession parameter K and $T_r = 0$, having an unrealistic vertical jump from zero, at the start, to the peak value of unity. Hence, the value of the parameter n must always be greater than unity.

Note that while the 'unit peak at origin' constraint, which defines the 2-parameter UPO-Gamma curve, is obtained at the cost of relaxing the 'unit volume' constraint of the standard 2-parameter Gamma distribution, the volume above any selected percentile of the UPO-Gamma curve can easily be calculated by integration, as shown in section C.5.1 of this appendix.

The shapes of the 'UPO-Gamma' curve of equation (C.1.10), for different values of the shape parameter n and shift parameter T_r, are shown in Figs. C.1.1 and C.1.2. Note that the ordinates in these two figures are expressed as percentiles, e.g. the value of $\boldsymbol{y} = 0.5$ in equation (C.1.10) is plotted as $\boldsymbol{y} = 50$ percentile in these figures.

The 'UPO-Gamma' 2-parameter curve was tested as a potential parsimonious parametric form of derived hydrograph in the WP3.1 'Hydrograph Width Analysis' study. In application, although it generally performed quite well in matching the rising limb and the upper part of the recession, for both the non-parametric and observed flood hydrographs, it performed poorly in matching the lower part of the recession curves of many stations. To provide better overall matching, but at the expense of incorporating an additional parameter, the UPO-Gamma curve was subsequently coupled with a replacement 1-parameter recession curve which starts (for convenience and to avoid having to estimate a further parameter) at the point of inflection on the recession side of the UPO-Gamma curve. Up to that point, the coupled curve consists of the UPO-Gamma with the replacement recession curve taking over at that point, thereby preserving continuity of the coupled curve (but not of its 1st derivative) at the point.

The mathematics of this coupling procedure is considered in section C.2 of this appendix.

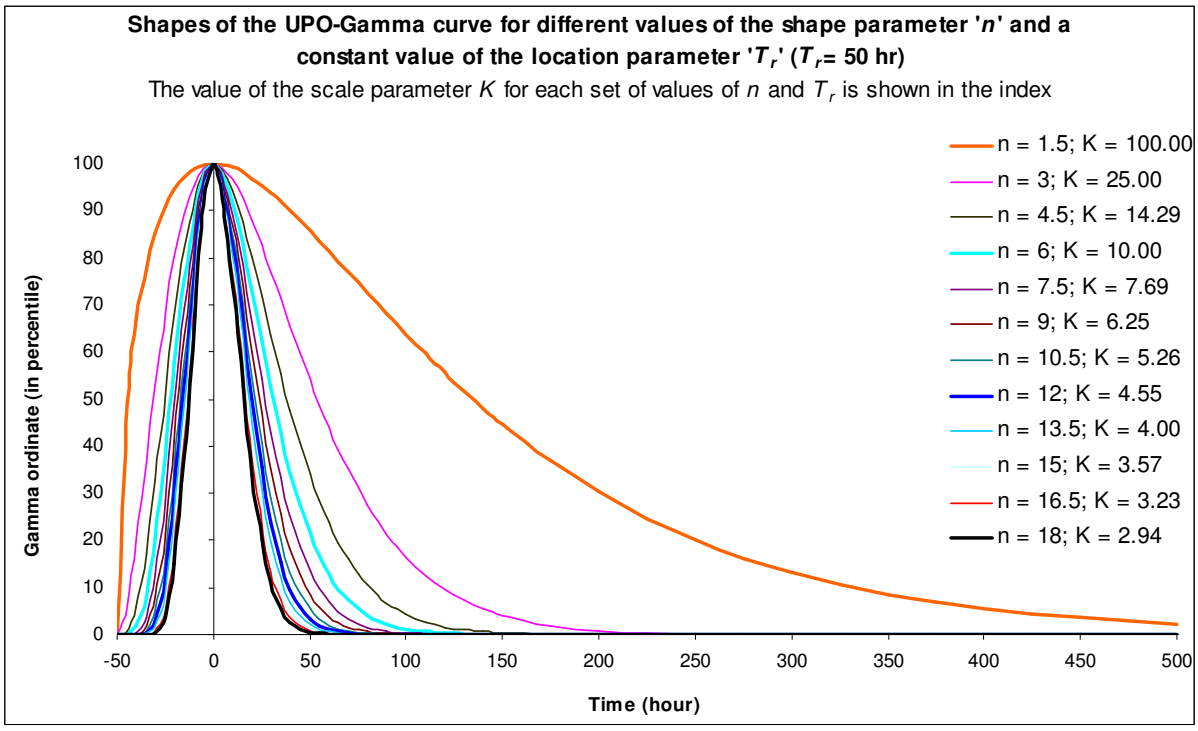

Fig. C.1.1 Variation of the shape of the UPO-Gamma hydrograph for different values of the shape parameter *n* and a constant value of the scale parameter T_r (the value of the scale parameter *K* corresponding to each set of values of *n* and T_r is also shown)

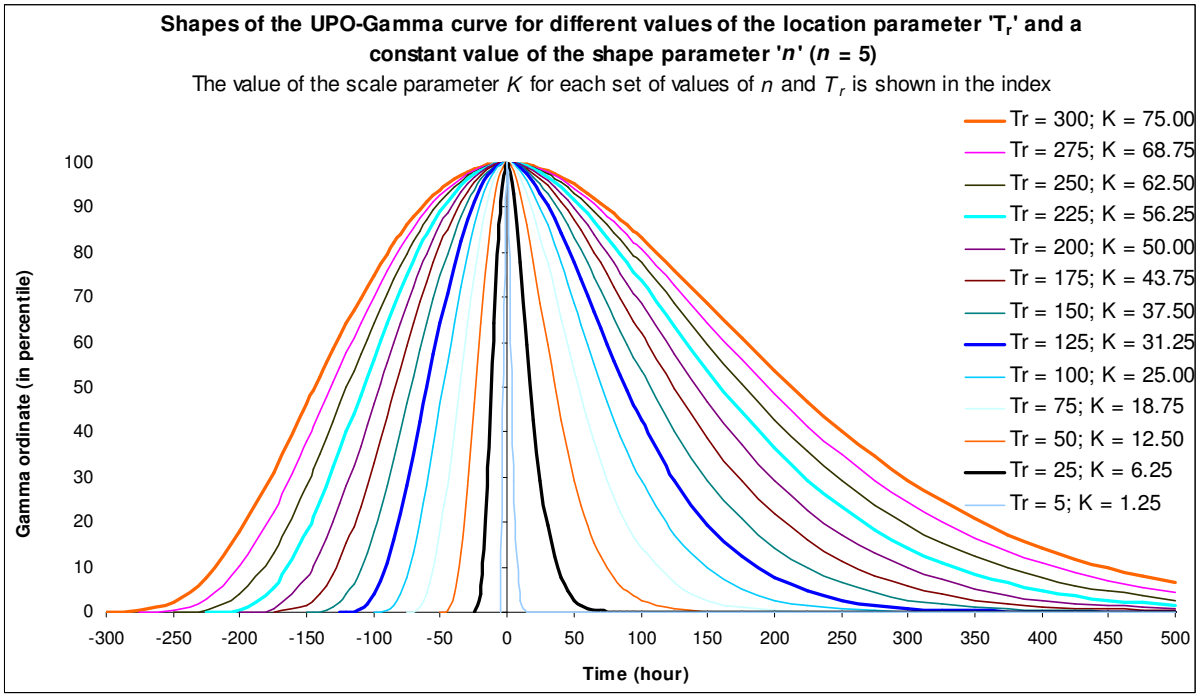

Fig. C.1.2 Variation of the shape of the UPO-Gamma hydrograph for different values of the scale parameter T_r and a constant value of the shape parameter *n* (the value of the scale parameter *K* corresponding to each set of values of *n* and T_r is also shown)

C.2 Equation for the point of inflection on the receding side of the UPO-Gamma curve

The equation of the UPO-Gamma curve applicable to 'Hydrograph Width Analysis', as given in equation (C.1.10), is

$$\boldsymbol{y} = \left(\frac{x+T_r}{T_r}\right)^{n-1} Exp\left(-\frac{x(n-1)}{T_r}\right),\ n > 1.0 \qquad \text{...(C.2.1)}$$

For determining the point of inflection of this curve, equation (C.2.1) is differentiated with respect to x to give

$$\frac{d\boldsymbol{y}}{dx} = \left(\frac{x+T_r}{T_r}\right)^{n-1} Exp\left(-\frac{x(n-1)}{T_r}\right)\left(-\frac{n-1}{T_r}\right) + \frac{(n-1)}{T_r} Exp\left\{-\frac{x(n-1)}{T_r}\right\}\left(\frac{x+T_r}{T_r}\right)^{n-2}$$

$$= \frac{n-1}{T_r} Exp\left(-\frac{x(n-1)}{T_r}\right)\left(\frac{x+T_r}{T_r}\right)^{n-2} - \frac{n-1}{T_r} Exp\left(-\frac{x(n-1)}{T_r}\right)\left(\frac{x+T_r}{T_r}\right)^{n-1}$$

Differentiating again,

$$\frac{d^2\boldsymbol{y}}{dx^2} = \frac{n-1}{T_r}\left(\frac{x+T_r}{T_r}\right)^{n-2} Exp\left(-\frac{x(n-1)}{T_r}\right)\left(\frac{n-1}{T_r}\right) + \frac{n-1}{T_r} Exp\left(-\frac{x(n-1)}{T_r}\right)(n-2)\left(\frac{x+T_r}{T_r}\right)^{n-3}\frac{1}{T_r}$$

$$-\frac{n-1}{T_r}\frac{n-1}{T_r} Exp\left(-\frac{x(n-1)}{T_r}\right)\left(\frac{x+T_r}{T_r}\right)^{n-2} + \left(\frac{n-1}{T_r}\right)^2 Exp\left(-\frac{x(n-1)}{T_r}\right)\left(\frac{x+T_r}{T_r}\right)^{n-1}$$

Simplifying,

$$\frac{d^2\boldsymbol{y}}{dx^2} = \left(\frac{n-1}{T_r}\right)^2\left(\frac{x+T_r}{T_r}\right)^{n-3} Exp\left(-\frac{x(n-1)}{T_r}\right)\left[-2\frac{x+T_r}{T_r} + \frac{n-2}{n-1} + \left(\frac{x+T_r}{T_r}\right)^2\right]$$

that is, $$\frac{d^2\boldsymbol{y}}{dx^2} = \left(\frac{n-1}{T_r}\right)^2\left(\frac{x+T_r}{T_r}\right)^{n-3} Exp\left(-\frac{x(n-1)}{T_r}\right)\left[\frac{x^2}{T_r^{\,2}} - \frac{1}{n-1}\right] \qquad \text{...(C.2.2)}$$

For $d^2\boldsymbol{y}/dx^2$ to be equal to zero, from equation (C.2.2), then

$$\left(\frac{x+T_r}{T_r}\right)^{n-3} = 0 \quad \Rightarrow x = -T_r \qquad \text{...(C.2.3)}$$

or $Exp\left(-\frac{x(n-1)}{T_r}\right) = 0$ which is impossible

or $$\frac{x^2}{T_r^{\,2}} - \frac{1}{n-1} = 0 \quad \Rightarrow \quad x = \pm\frac{T_r}{\sqrt{n-1}} \qquad \text{...(C.2.4)}$$

The abscissa $x = -T_r$ corresponds to the starting point of the UPO-Gamma curve on its rising side. By studying the curvature of this gamma curve just on the left and the right side of the point corresponding to $x = \frac{T_r}{\sqrt{n-1}}$, it is concluded that $x = \frac{T_r}{\sqrt{n-1}}$ represents the point of inflection on the receding side. Hence, recalling equation (C.1.3), i.e. $T_r = K(n-1)$,we can express the coordinates of the point of inflection as (x_0, y_0) of the UPO-Gamma curve as

$$x_0 = \frac{T_r}{\sqrt{n-1}} = \sqrt{T_r K} = K\sqrt{n-1} \qquad \text{...(C.2.5)}$$

$$\left.\begin{aligned} y_0 &= \left(\frac{x_0+T_r}{T_r}\right)^{n-1} Exp\left\{-\frac{x_0(n-1)}{T_r}\right\} \\ &= \left\{\frac{1}{\sqrt{n-1}}+1\right\}^{n-1} Exp\left\{-\sqrt{n-1}\right\} \\ &= \left\{\sqrt{K/T_r}+1\right\}^{n-1} Exp\left\{-\sqrt{T_r/K}\right\} \end{aligned}\right\} \qquad \text{…(C.2.6)}$$

Interestingly, as seen in the middle equation of (C.2.6) above, the value of the ordinate (y_o) at the point of inflection of the UPO-Gamma curve is defined by the value of the single curve parameter *n*.

C.3 Expressions for the coupling of an Exponential Replacement Recession curve (ERR) with the UPO-Gamma curve, with the replacement recession curve starting at the point of inflection of the UPO-Gamma curve

The equation of the exponential replacement recession (ERR) curve, which starts at the point of inflection (x_0 , y_0) of the UPO-Gamma curve, i.e. with both curves having the point (x_0 , y_0) in common, has the form

$y = y_0 Exp\left(-\frac{x-x_0}{C}\right)$, where *C* is the parameter of the curve …(C.3.1)

This equation can also be rewritten as $C = -\frac{x-x_0}{Ln\left(y/y_0\right)}$ …(C.3.2)

For fitting this curve to a series of *N* points, having coordinates (x_1, y_1), (x_2, y_2), …, (x_N, y_N), with each coordinate pair (x_i, y_i) providing an estimate $\hat{C}_i$ provided the coordinates (x_0, y_0) are known, a global estimate of the parameter *C* can be taken as the simple average

$$\hat{C}_{av} = \sum_{i=1}^{N} \hat{C}_i = -\frac{1}{N}\left[\frac{x_1-x_0}{Ln\left(y_1/y_0\right)} + \frac{x_2-x_0}{Ln\left(y_2/y_0\right)} + \ldots + \frac{x_N-x_0}{Ln\left(y_N/y_0\right)}\right] \qquad \text{…(C.3.3)}$$

More elaborately, taking the estimate $\hat{C}_{av}$ from equation (C.3.3) as the initial estimate of *C* in equation (C.3.2), we can calculate the *y* value for each of the x_i values, for i = 1,*N*, as the series $\hat{y}_i$, and then optimise *C* , e.g. by using SOLVER in MS-Excel, to minimise *S*, the sum of squares of the differences $\left(y_i - \hat{y}_i\right)$, i.e.

$$S = \sum_{i=1}^{N} \left(y_i - \hat{y}_i\right)^2 \qquad \text{…(C.3.4)}$$

to give a least-squares estimate $\hat{C}_{LS}$ of the exponential recession parameter *C*.

Having estimated the parameter *C*, by whatever means, and using it in equation (C.3.1), the value on the abscissa for any give ordinate value for a point on the exponential recession curve can be derived as

$$x = x_0 - \hat{C} Ln\left(\frac{y}{y_0}\right) \qquad \text{...(C.3.5)}$$

In the case of a design food hydrograph obtained by coupling a UPO-Gamma curve together with an ERR curve, the expression of the area under the curve will be required to estimate the volume of flow above any chosen percentile of the peak flow.

Integrating equation (C.3.1) between $x = x_1$ and $x = x_2$, the area A_{exp} under the exponential recession curve between $x = x_1$ and $x = x_2$ is given by

$$A_{\exp} = -Cy_0\left[Exp\frac{x_0 - x_2}{C} - Exp\frac{x_0 - x_1}{C}\right] \qquad \text{...(C.3.6)}$$

The shapes of the exponential recession curve for different values of the parameter *C* are shown in Fig. C.3.1. Note that the ordinates of the recession curve in this figure are expressed in percentile. The curve asymptotically approaches the zero percentile.

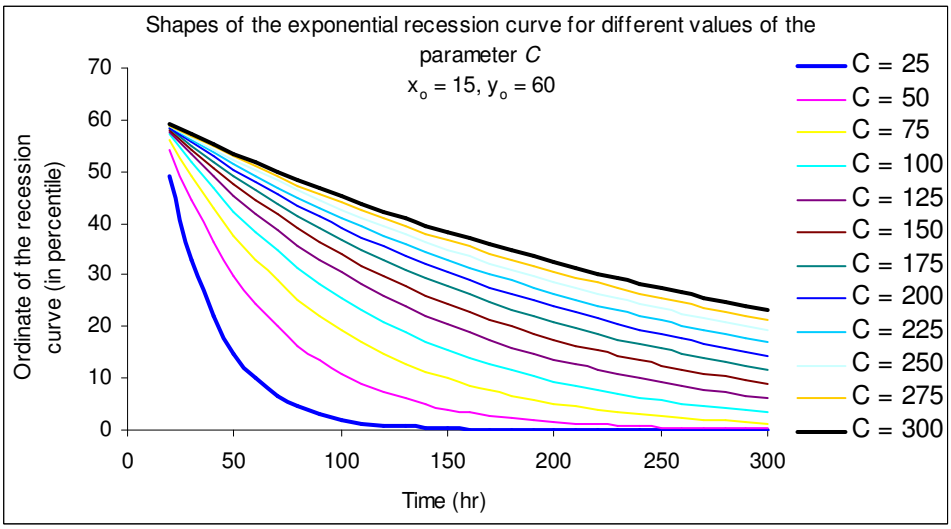

Fig. C.3.1 Variation of the shape of the hydrograph for different values of the parameter *C* of the exponential recession curve

While the above method for calibrating the replacement of the recession of the UPO-Gamma below its point of inflection (x_0, y_0), where the values of x_0 and y_0 *are* known, were used initially to demonstrate the efficacy of such a coupling, subsequently the UPO-Gamma parameters (*n* and T_r) and the ERR curve parameter *C*, i.e. 3 parameters in all, were optimised simultaneously, not in sequence.

C.4 Estimation of the width of exceedence at any specified percentile p of the peak flow of the UPO-Gamma curve coupled with an exponential replacement recession (ERR) curve drawn from the point of inflection of the Gamma curve, i.e. of the UPO-ERR-Gamma curve

Using the derivations in Appendices C.1 and C.3, the equations of the UPO-Gamma curve coupled with an exponential replacement recession curve drawn from the point of inflection of the Gamma curve, involving the three curve parameters, n, T_r and C, can be rewritten as follows:

For the part of the curve from the start of rise to the point of inflection on the receding side

$$p = \left(\frac{t+T_r}{T_r}\right)^{n-1} Exp\left(-\frac{t(n-1)}{T_r}\right)\times 100\,,\ n > 1 \qquad \text{… (C.4.1)}$$

where t is the symbol denoting time measured from the origin (rather than the symbol x used earlier in this appendix),

p is the percentile of the peak flow at time t, the origin of the time axis being at the point of occurrence of the peak flow, i.e. $p = p_0 = 100$ when $t = 0$.

T_r is the time of rise of the flood hydrograph, and is given by the location (or translation) parameter of the UPO- Gamma curve.

n is the shape parameter of that curve.

For the part of the curve from the point of inflection (t_{infl}, p_{infl}) on the receding side onwards (with (t_{infl}, p_{infl}) corresponding to (x_0, $100\times y_0$) in the notation used in C.1)

$$p = p_{\text{infl}}\, Exp\left(-\frac{t-t_{\text{infl}}}{C}\right) \qquad \text{… (C.4.2)}$$

where C is the parameter of the exponential replacement recession curve drawn from the point of inflection (t_{infl}, p_{infl}) on the receding side.

Corresponding to the point of inflection on the receding side, p_{infl} is the percentile of the peak flow at time t_{infl}, the expressions for t_{infl} and p_{infl} (see (C.3.5) and (C.3.6)) being as follows:

$$t_{\text{infl}} = \frac{T_r}{\sqrt{n-1}} \text{ and } p_{\text{infl}} = \left(\frac{t_{\text{infl}}+T_r}{T_r}\right)^{n-1} Exp\left(-\frac{t_{\text{infl}}(n-1)}{T_r}\right) \qquad \text{… (C.4.3)}$$

Note that the scale parameter K, which is not explicitly provided in equation (C.4.1) above for the derived formulation of the UPO-Gamma curve, is given from equation (C.1.3) as $K = \frac{T_r}{n-1}$.

As an illustration, figures C.4.1 and C.4.2 show the UPO-Gamma curve coupled with an exponential replacement recession curve drawn from the point of inflection of that Gamma curve for Station No. 7009 for two cases of the percentile p, i.e. $p > p_{infl}$ and $p < p_{infl}$, respectively where p_{infl} is as defined by equation (C.4.3). It can be seen from these two figures that there are two values of time t, i.e. $t_1 < 0$ and $t_2 > 0$, corresponding to each percentile p so that the width W_p at percentile p is given by $W_p = -t_1 + t_2$.

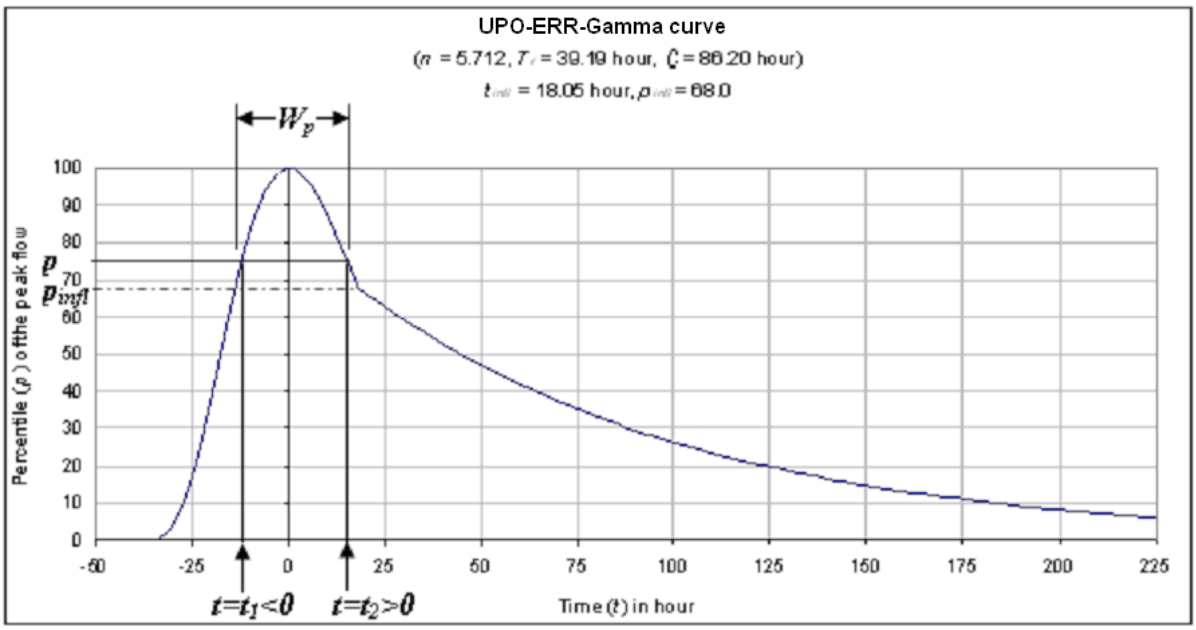

Fig. C.4.1 Illustration of the estimation of the width of exceedence at percentile p of the peak flow where $p > p_{infl}$

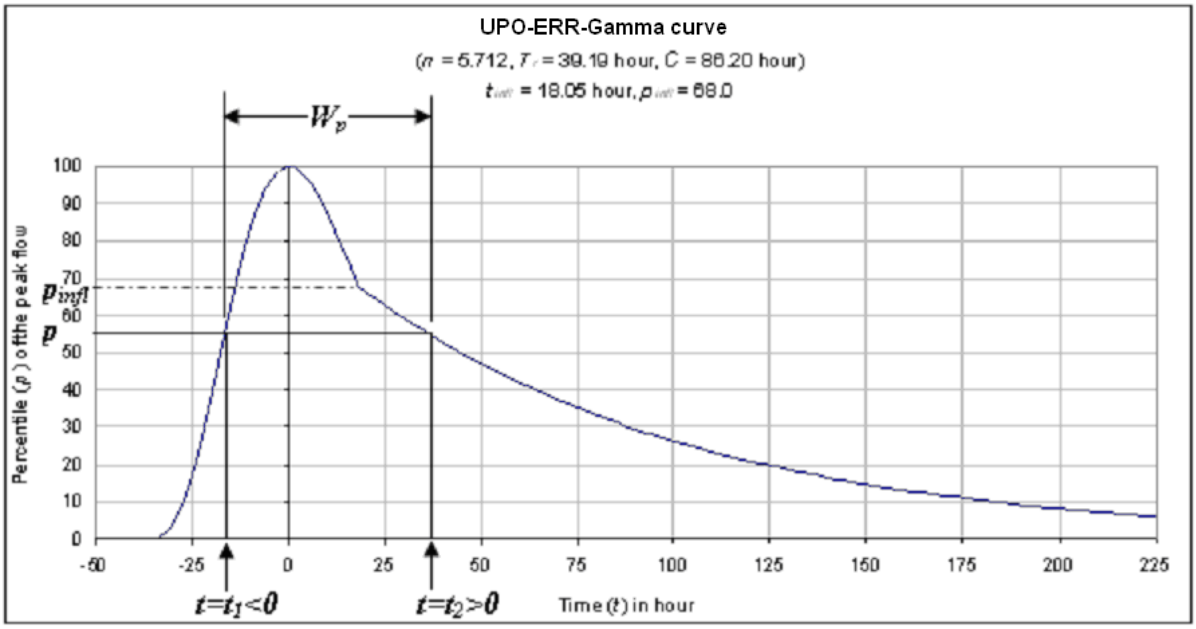

Fig. C.4.2 Illustration of the estimation of the width of exceedence at percentile p of the peak flow where $p < p_{infl}$

For the case when $p > p_{infl}$, both t_1 and t_2 correspond to two points on the UPO-Gamma curve given by the equation (C.4.1). However, for the case when $p < p_{infl}$, t_1 corresponds to a point on the rising side of the UPO-Gamma curve and t_2 corresponds to a point on the exponential recession curve given by the equation (C.4.2).

In each case, the calculation of t would require expressing t explicitly in terms of p and the two curve parameters n and T_r in equation (C.4.1). However, since such an expression for the UPO-Gamma curve cannot be easily derived, any suitable numerical method can be applied. Alternatively, if using MS-Excel, either the 'Goal Seek' or the 'Solver' tool can be

applied to obtain the value of *t* for a given value of *p*. In WP 3.1, the numerical method of interval-halving, also known as the Bolzano[1] or the Bisection Method, is used. The reader may refer to any standard book on numerical analysis for the details of the method. Programming codes for numerical approximation methods are also available in many books of software applications in engineering, e.g. *Numerical Recipes in Fortran* [2] (Press *et al.*, 1996).

For the case when $p < p_{infl}$, the value of $t=t_2$, which is on the exponential recession curve, can be obtained by rewriting equation (C.4.2) as follows:

$$t = t_{\text{infl}} - C \times Ln\left(\frac{p}{p_{\text{infl}}}\right) \qquad \text{… (C.4.4)}$$

[1] Brian Bradie, 2006. *A Friendly Introduciton to Numerical Analysis*, Pearson Prentice Hall, section 2.3, p. 53.

[2] Press, W.H., Teukolsky, S.A., Vetterling, W.H. and Flannery, B.P., 1996. *Numerical Recipes in Fortran 90*. Volume 1 and 2. Cambridge University Press, the UK.

C.5 Estimation of the volume of flow above any specified percentile p of the peak flow for the UPO-ERR-Gamma curve

An analytical expression for the volume under the UPO-Gamma curve coupled with an exponential replacement recession curve drawn from the point of inflection of the UPO-Gamma curve above any given percentile *p* of the peak flow can be derived for an integer value of the parameter *n* and approximated for a non-integer value of *n*. The formulae for calculating such a volume are given below:

C.5.1 Volume V_g under the UPO-Gamma curve

Using equation (C.1.10) of the UPO-Gamma curve and replacing *x* by *t* to indicate the width of exceedence along the abscissa in unit of time, the volume V_g under the UPO-Gamma curve bound by two ordinates corresponding to $t = -t_1$ and $t = t_2$ is given by,

$$V_g = \int_{-t_1}^{t_2} y\, dt = \int_{-t_1}^{t_2} \left(\frac{t+T_r}{T_r}\right)^{n-1} Exp\left(-\frac{t(n-1)}{T_r}\right) dt \qquad \text{… (C.5.1)}$$

Expressing the above integral by $I_{n\text{-}1}$, in which the subscript *n*-1 indicates the exponent of $\frac{t+T_r}{T_r}$, and considering only integer value n_{int} of *n*,

$$V_g = I_{n_{\text{int}}-1} \qquad \text{… (C.5.2)}$$

Integrating the integrand on the right hand side of equation (C.5.1) by parts,

$$I_{n_{\text{int}}-1} = \left(\frac{t+T_r}{T_r}\right)^{n_{\text{int}}-1} \left(-\frac{T_r}{n_{\text{int}}-1}\right) Exp\left(-\frac{t(n_{\text{int}}-1)}{T_r}\right)\Bigg|_{-t_1}^{t_2} \qquad \text{… (C.5.3)}$$

$$-\int_{-t_1}^{t_2} (n_{\text{int}}-1)\left(\frac{t+T_r}{T_r}\right)^{(n_{\text{int}}-2)} \left(\frac{1}{T_r}\right)\left(-\frac{T_r}{n_{\text{int}}-1}\right) Exp\left(-\frac{t(n_{\text{int}}-1)}{T_r}\right) dt$$

We can now express $I_{n\text{-}1}$ by $I_{n_{\text{int}}-1} = A_{n_{\text{int}}-1} + \frac{n_{\text{int}}-1}{n_{\text{int}}-1} I_{n_{\text{int}}-2}$ … (C.5.4)

where,

$$A_{n_{\text{int}}-1} = \left(\frac{t+T_r}{T_r}\right)^{n_{\text{int}}-1} \left(-\frac{T_r}{n_{\text{int}}-1}\right) Exp\left(-\frac{t(n_{\text{int}}-1)}{T_r}\right)\Bigg|_{-t_1}^{t_2} \qquad \text{… (C.5.5)}$$

and, following from equation (C.5.1) and (C.5.2), $I_{n_{\text{int}}-2} = \int_{-t_1}^{t_2} \left(\frac{t+T_r}{T_r}\right)^{(n_{\text{int}}-2)} Exp\left(-\frac{t(n_{\text{int}}-1)}{T_r}\right) dt$

… (C.5.6)

The subscripts n_{int}-1 and n_{int}-2 in $A_{n_{\text{int}}-1}$ and $I_{n_{\text{int}}-2}$ indicate the exponents of $\frac{t+T_r}{T_r}$ in the respective equations.

Now, integrating the integrand in equation (C.5.6) by the same way as for the integrand in equation (C.5.1),

$$I_{n_{\text{int}}-2} = A_{n_{\text{int}}-2} + \frac{n_{\text{int}}-2}{n_{\text{int}}-1} I_{n_{\text{int}}-3} \qquad \text{… (C.5.7)}$$

Combining equations (C.5.4) and (C.5.7),

$$I_{n_{\text{int}}-1} = A_{n_{\text{int}}-1} + \frac{n_{\text{int}}-1}{n_{\text{int}}-1}\left(A_{n_{\text{int}}-2} + \frac{n_{\text{int}}-2}{n_{\text{int}}-1} I_{n_{\text{int}}-3} \right) \qquad \text{… (C.5.8)}$$

$$\text{Or, } I_{n_{\text{int}}-1} = A_{n_{\text{int}}-1} + \frac{n_{\text{int}}-1}{n_{\text{int}}-1} A_{n_{\text{int}}-2} + \frac{n_{\text{int}}-1}{n_{\text{int}}-1}\frac{n_{\text{int}}-2}{n_{\text{int}}-1} I_{n_{\text{int}}-3}$$

$$Or, I_{n_{\text{int}}-1} = A_{n_{\text{int}}-1} + \frac{n_{\text{int}}-1}{(n_{\text{int}}-1)^1} A_{n_{\text{int}}-2} + \frac{(n_{\text{int}}-1)(n_{\text{int}}-2)}{(n_{\text{int}}-1)^2} I_{n_{\text{int}}-3}$$

$$Or, I_{n_{\text{int}}-1} = A_{n_{\text{int}}-1} + \frac{n_{\text{int}}-1}{(n_{\text{int}}-1)^{(n_{\text{int}}-1)-(n_{\text{int}}-2)}} A_{n_{\text{int}}-2} + \frac{(n_{\text{int}}-1)(n_{\text{int}}-2)}{(n_{\text{int}}-1)^{(n_{\text{int}}-1)-(n_{\text{int}}-3)}} I_{n_{\text{int}}-3} \qquad \text{… (C.5.9)}$$

Now, successively integrating the integrand in $I_{n_{\text{int}}-3}$, $I_{n_{\text{int}}-4}$, $I_{n_{\text{int}}-5}$, …, $I_{n_{\text{int}}-(n_{\text{int}}-1)}$, equation (C.5.9) can be written as,

$$I_{n-1} = A_{n_{\text{int}}-1} + \frac{n_{\text{int}}-1}{(n_{\text{int}}-1)^{(n_{\text{int}}-1)-(n_{\text{int}}-2)}} A_{n_{\text{int}}-2} + \frac{(n_{\text{int}}-1)(n_{\text{int}}-2)}{(n_{\text{int}}-1)^{(n_{\text{int}}-1)-(n_{\text{int}}-3)}} A_{n_{\text{int}}-3} + \frac{(n_{\text{int}}-1)(n_{\text{int}}-2)(n_{\text{int}}-3)}{(n_{\text{int}}-1)^{(n_{\text{int}}-1)-(n_{\text{int}}-4)}} I_{n_{\text{int}}-4}$$

$$I_{n_{\text{int}}-1} = A_{n_{\text{int}}-1} + \frac{n_{\text{int}}-1}{(n_{\text{int}}-1)^{(n_{\text{int}}-1)-(n_{\text{int}}-2)}} A_{n_{\text{int}}-2} + \frac{(n_{\text{int}}-1)(n_{\text{int}}-2)}{(n_{\text{int}}-1)^{(n_{\text{int}}-1)-(n_{\text{int}}-3)}} A_{n_{\text{int}}-3} + \frac{(n_{\text{int}}-1)(n_{\text{int}}-2)(n_{\text{int}}-3)}{(n_{\text{int}}-1)^{(n_{\text{int}}-1)-(n_{\text{int}}-4)}} A_{n_{\text{int}}-4} + \frac{(n_{\text{int}}-1)(n_{\text{int}}-2)(n_{\text{int}}-3)(n_{\text{int}}-4)}{(n_{\text{int}}-1)^{(n_{\text{int}}-1)-(n_{\text{int}}-5)}} I_{n_{\text{int}}-5}$$

… … … …
… … … …
… … … …

$$I_{n_{\text{int}}-1} = A_{n_{\text{int}}-1} + \frac{n_{\text{int}}-1}{(n_{\text{int}}-1)^{(n_{\text{int}}-1)-(n_{\text{int}}-2)}} A_{n_{\text{int}}-2} + \frac{(n_{\text{int}}-1)(n_{\text{int}}-2)}{(n_{\text{int}}-1)^{(n_{\text{int}}-1)-(n_{\text{int}}-3)}} A_{n_{\text{int}}-3} + \frac{(n_{\text{int}}-1)(n_{\text{int}}-2)(n_{\text{int}}-3)}{(n_{\text{int}}-1)^{(n_{\text{int}}-1)-(n_{\text{int}}-4)}} A_{n_{\text{int}}-4} + \ldots + \frac{(n_{\text{int}}-1)(n_{\text{int}}-2)(n_{\text{int}}-3)\ldots 5.4.3}{(n_{\text{int}}-1)^{n_{\text{int}}-3}} A_2 + \frac{(n_{\text{int}}-1)(n_{\text{int}}-2)(n_{\text{int}}-3)\ldots 4.3.2}{(n_{\text{int}}-1)^{n_{\text{int}}-2}} A_1 + \frac{(n_{\text{int}}-1)(n_{\text{int}}-2)(n_{\text{int}}-3)(n_{\text{int}}-4)\ldots 3.2.1}{(n_{\text{int}}-1)^{n_{\text{int}}-1}} I_0$$

… (C.5.10)

Using the expression for $I_{n_{\text{int}}-1}$ in equation (C.5.1),

$$I_0 = \int_{-t_1}^{t_2} \left(\frac{t+T_r}{T_r} \right)^0 Exp\left(-\frac{t(n_{\text{int}}-1)}{T_r} \right) dt = \int_{-t_1}^{t_2} Exp\left(-\frac{t(n_{\text{int}}-1)}{T_r} \right) dt$$

$$\text{Or, } I_0 = -\frac{T_r}{n_{\text{int}}-1} Exp\left(-\frac{t(n_{\text{int}}-1)}{T_r} \right)\Bigg|_{-t_1}^{t_2} \qquad \text{… (C.5.11)}$$

Combining equations (C.5.10) and (C.5.11),

$$I_{n_{\text{int}}-1} = A_{n_{\text{int}}-1} + \frac{n_{\text{int}}-1}{(n_{\text{int}}-1)^{(n_{\text{int}}-1)-(n_{\text{int}}-2)}} A_{n_{\text{int}}-2} + \frac{(n_{\text{int}}-1)(n_{\text{int}}-2)}{(n_{\text{int}}-1)^{(n_{\text{int}}-1)-(n_{\text{int}}-3)}} A_{n_{\text{int}}-3} +$$
$$\frac{(n_{\text{int}}-1)(n_{\text{int}}-2)(n_{\text{int}}-3)}{(n_{\text{int}}-1)^{(n_{\text{int}}-1)-(n_{\text{int}}-4)}} A_{n_{\text{int}}-4} + \ldots + \frac{(n_{\text{int}}-1)(n_{\text{int}}-2)(n_{\text{int}}-3)\ldots 5.4.3}{(n_{\text{int}}-1)^{n-3}} A_2 +$$
$$\frac{(n_{\text{int}}-1)(n_{\text{int}}-2)(n_{\text{int}}-3)\ldots 4.3.2}{(n_{\text{int}}-1)^{n_{\text{int}}-2}} A_1 - \frac{(n_{\text{int}}-1)!}{(n_{\text{int}}-1)^{n-1}} \frac{T_r}{n_{\text{int}}-1} Exp\left(-\frac{t(n_{\text{int}}-1)}{T_r} \right)\Bigg|_{-t_1}^{t_2}$$

… (C.5.12)

Now, using the expressions for $A_{n_{\text{int}}-1}$, $A_{n_{\text{int}}-2}$, …, A_2, A_1 (see equation C.5.5) and taking $-\frac{T_r}{n_{\text{int}}-1} Exp\left(-\frac{t(n_{\text{int}}-1)}{T_r} \right)$ common, equation (C.5.12) can be written as,

$$I_{n_{\text{int}}-1} = -\frac{T_r}{n_{\text{int}}-1} Exp\left(-\frac{t(n_{\text{int}}-1)}{T_r}\right)\times$$

$$\left[\begin{array}{l}
\left(\frac{t+T_r}{T_r}\right)^{n_{\text{int}}-1} + \\
\frac{n_{\text{int}}-1}{(n_{\text{int}}-1)^{(n_{\text{int}}-1)-(n_{\text{int}}-2)}}\left(\frac{t+T_r}{T_r}\right)^{n_{\text{int}}-2} + \\
\frac{(n_{\text{int}}-1)(n_{\text{int}}-2)}{(n_{\text{int}}-1)^{(n_{\text{int}}-1)-(n_{\text{int}}-3)}}\left(\frac{t+T_r}{T_r}\right)^{n_{\text{int}}-3} + \\
\frac{(n_{\text{int}}-1)(n_{\text{int}}-2)(n_{\text{int}}-3)}{(n_{\text{int}}-1)^{(n_{\text{int}}-1)-(n_{\text{int}}-4)}}\left(\frac{t+T_r}{T_r}\right)^{n_{\text{int}}-4} + \ldots + \\
\frac{(n_{\text{int}}-1)(n_{\text{int}}-2)(n_{\text{int}}-3)\ldots 5.4.3}{(n_{\text{int}}-1)^{n_{\text{int}}-3}}\left(\frac{t+T_r}{T_r}\right)^{2} + \\
\frac{(n_{\text{int}}-1)(n_{\text{int}}-2)(n_{\text{int}}-3)\ldots 4.3.2}{(n_{\text{int}}-1)^{n_{\text{int}}-2}}\left(\frac{t+T_r}{T_r}\right)^{1} + \\
\qquad + \frac{(n_{\text{int}}-1)!}{(n_{\text{int}}-1)^{n_{\text{int}}-1}}
\end{array}\right]\Bigg|_{-t_1}^{t_2} \qquad \ldots(C.5.13)$$

Expressing equation (C.5.13) in a simpler form, the total volume $V_{g_{\text{int}}}$ under the UPO-Gamma curve contained by two ordinates corresponding to $t = -t_1$ and $t = t_2$ is given by

$$V_{g_{n_{\text{int}}}} = V_t\big|_{\text{at } t=t_2} - V_t\big|_{\text{at } t=-t_1} \qquad \ldots (C.5.14)$$

where

$$V_t = -\frac{T_r}{n_{\text{int}}-1} Exp\frac{-(n_{\text{int}}-1)t}{T_r}\left[\left(\frac{t+T_r}{T_r}\right)^{n_{\text{int}}-1} + \frac{n_{\text{int}}-1}{(n_{\text{int}}-1)^1}\left(\frac{t+T_r}{T_r}\right)^{n_{\text{int}}-2}\right.$$
$$\left. + \frac{(n_{\text{int}}-1)(n_{\text{int}}-2)}{(n_{\text{int}}-1)^2}\left(\frac{t+T_r}{T_r}\right)^{n_{\text{int}}-3} + \ldots + \frac{(n_{\text{int}}-1)(n_{\text{int}}-2)\ldots 3.2}{(n_{\text{int}}-1)^{n_{\text{int}}-2}}\left(\frac{t+T_r}{T_r}\right)^{1} + \frac{(n_{\text{int}}-1)!}{(n_{\text{int}}-1)^{n_{\text{int}}-1}}\right] \qquad \ldots (C.5.15)$$

Here, T_r is the time of rise of the flood hydrograph, which is given by the translation (or location) parameter of the UPO-Gamma curve.

The following are the expressions of V_t for integer values from n_{int} = 2 to n_{int} = 8

For n_{int} = 2:

$$V_t = -T_r\left[\frac{t+T_r}{T_r}+1\right]Exp\left(\frac{-t}{T_r}\right) \quad \text{... (C.5.16)}$$

For n_{int} = 3:

$$V_t = -\frac{T_r}{2}\left[\left(\frac{t+T_r}{T_r}\right)^2+\frac{2}{2^1}\left(\frac{t+T_r}{T_r}\right)^1+\frac{2!}{2^2}\right]Exp\left(\frac{-2t}{T_r}\right) \quad \text{... (C.5.17)}$$

For n_{int} = 4:

$$V_t = -\frac{T_r}{3}\left[\left(\frac{t+T_r}{T_r}\right)^3+\frac{3}{3^1}\left(\frac{t+T_r}{T_r}\right)^2+\frac{3.2}{3^2}\left(\frac{t+T_r}{T_r}\right)^1+\frac{3!}{3^3}\right]Exp\left(\frac{-3t}{T_r}\right) \quad \text{... (C.5.18)}$$

For n_{int} = 5:

$$V_t = -\frac{T_r}{4}\left[\left(\frac{t+T_r}{T_r}\right)^4+\frac{4}{4^1}\left(\frac{t+T_r}{T_r}\right)^3+\frac{4.3}{4^2}\left(\frac{t+T_r}{T_r}\right)^2+\frac{4.3.2}{4^3}\left(\frac{t+T_r}{T_r}\right)^1+\frac{4!}{4^4}\right]Exp\left(\frac{-4t}{T_r}\right) \quad \text{... (C.5.19)}$$

For n_{int} = 6:

$$V_t = -\frac{T_r}{5}\left[\begin{array}{l}\left(\frac{t+T_r}{T_r}\right)^5+\frac{5}{5^1}\left(\frac{t+T_r}{T_r}\right)^4+\frac{5.4}{5^2}\left(\frac{t+T_r}{T_r}\right)^3+\frac{5.4.3}{5^3}\left(\frac{t+T_r}{T_r}\right)^2+ \\ \qquad\qquad \frac{5.4.3.2}{5^4}\left(\frac{t+T_r}{T_r}\right)^1+\frac{5!}{5^5}\end{array}\right]Exp\left(\frac{-5t}{T_r}\right) \quad \text{... (C.5.20)}$$

For n_{int} = 7:

$$V_t = -\frac{T_r}{6}\left[\begin{array}{l}\left(\frac{t+T_r}{T_r}\right)^6+\frac{6}{6^1}\left(\frac{t+T_r}{T_r}\right)^5+\frac{6.5}{6^2}\left(\frac{t+T_r}{T_r}\right)^4+\frac{6.5.4}{6^3}\left(\frac{t+T_r}{T_r}\right)^3+ \\ \qquad\qquad \frac{6.5.4.3}{6^4}\left(\frac{t+T_r}{T_r}\right)^2+\frac{6.5.4.3.2}{6^5}\left(\frac{t+T_r}{T_r}\right)^1+\frac{6!}{6^6}\end{array}\right]Exp\left(\frac{-6t}{T_r}\right) \quad \text{... (C.5.21)}$$

For n_{int} = 8:

$$V_t = -\frac{T_r}{7}\left[\begin{array}{l}\left(\frac{t+T_r}{T_r}\right)^7+\frac{7}{7^1}\left(\frac{t+T_r}{T_r}\right)^6+\frac{7.6}{7^2}\left(\frac{t+T_r}{T_r}\right)^5+\frac{7.6.5}{7^3}\left(\frac{t+T_r}{T_r}\right)^4+ \\ \qquad\qquad \frac{7.6.5.4}{7^4}\left(\frac{t+T_r}{T_r}\right)^3+\frac{7.6.5.4.3}{7^5}\left(\frac{t+T_r}{T_r}\right)^2+\frac{7.6.5.4.3.2}{7^6}\left(\frac{t+T_r}{T_r}\right)^1+\frac{7!}{7^7}\end{array}\right]Exp\left(\frac{-7t}{T_r}\right) \quad \text{... (C.5.22)}$$

From tests, it was found that, for non-integer values of n, equation (C.5.14) can be used to estimate the required volume approximately. In the case of n>2, the required volume can be obtained by linear interpolation using the volumes at two consecutive integer values, one smaller and the other larger than the given non-integer value of n. However, in the case of 1<n<2, the volume is to be linearly extrapolated using the volumes at n=2 and n=3. Thus, for

a non-integer value of n, where $n_1<n<n_2$, n_1 and n_2 being two consecutive integers, the volume V_g under the UPO-Gamma curve contained by two ordinates corresponding to $t = -t_1$ and $t = t_2$ is given by

$$V_g = V_{g_{n_1}} + \frac{V_{g_{n_2}} - V_{g_{n_1}}}{n_2 - n_1}(n - n_1) \qquad \text{… (C.5.23)}$$

where $V_{g_{n_1}}$ and $V_{g_{n_2}}$ are the volumes corresponding to the integer values n_1 and n_2 respectively which are obtained using the equation (C.5.15).

C.5.2 Volume V_e under the exponential recession curve

Using equation (C.2.5) of the exponential recession curve and replacing x, x_0 and y_0 by t, t_{infl} and p_{inf}, the volume V_e contained by any two ordinates corresponding to $t = t_3$ and $t = t_4$, where t_3 and t_4 lie beyond the point of inflection on the receding side of the UPO-Gamma curve, is given by

$$V_e = \int_{t_3}^{t_4} y\, dt = \int_{t_3}^{t_4} y_{\text{infl}}\, Exp\left(-\frac{t - t_{\text{infl}}}{C}\right) dt \qquad \text{… (C.5.24)}$$

Substituting $(-t + t_{\text{infl}})/C$ by z,

$$\left.\begin{array}{l} t = t_{\text{infl}} - Cz \text{ and } dt = -Cdz \\ \text{for } t = t_3,\ z = (t_{\text{infl}} - t_3)/C \text{ and for } t = t_4,\ z = (t_{\text{infl}} - t_4)/C \end{array}\right\} \qquad \text{… (C.5.25)}$$

$$\therefore V_e = -Cp_{\text{infl}} \int_{\frac{t_{\text{infl}} - t_3}{C}}^{\frac{t_{\text{infl}} - t_4}{C}} Exp(z)dz = -Cp_{\text{infl}}\left[Exp\left(\frac{t_{\text{infl}} - t_4}{C}\right) - Exp\left(\frac{t_{\text{infl}} - t_3}{C}\right)\right] \qquad \text{… (C.5.26)}$$

where C is the parameter of the exponential recession curve drawn from the point of inflection on the receding side of the UPO-Gamma curve and p_{infl} is the percentile of the peak flow at time t_{infl} corresponding to that point of inflection.

The expressions for t_{infl} and p_{infl} are as follows:

$$t_{\text{infl}} = \frac{T_r}{\sqrt{n-1}} \text{ and } p_{\text{infl}} = \left(\frac{t_{\text{infl}} + T_r}{T_r}\right)^{n-1} Exp\left(-\frac{t_{\text{infl}}(n-1)}{T_r}\right) \qquad \text{… (C.5.27)}$$

Illustrations of the estimation of volume for the cases when $p > p_{infl}$ and $p < p_{inf}$ for Station No. 7009 are given in Figures C.5.1 and C.5.2 respectively.

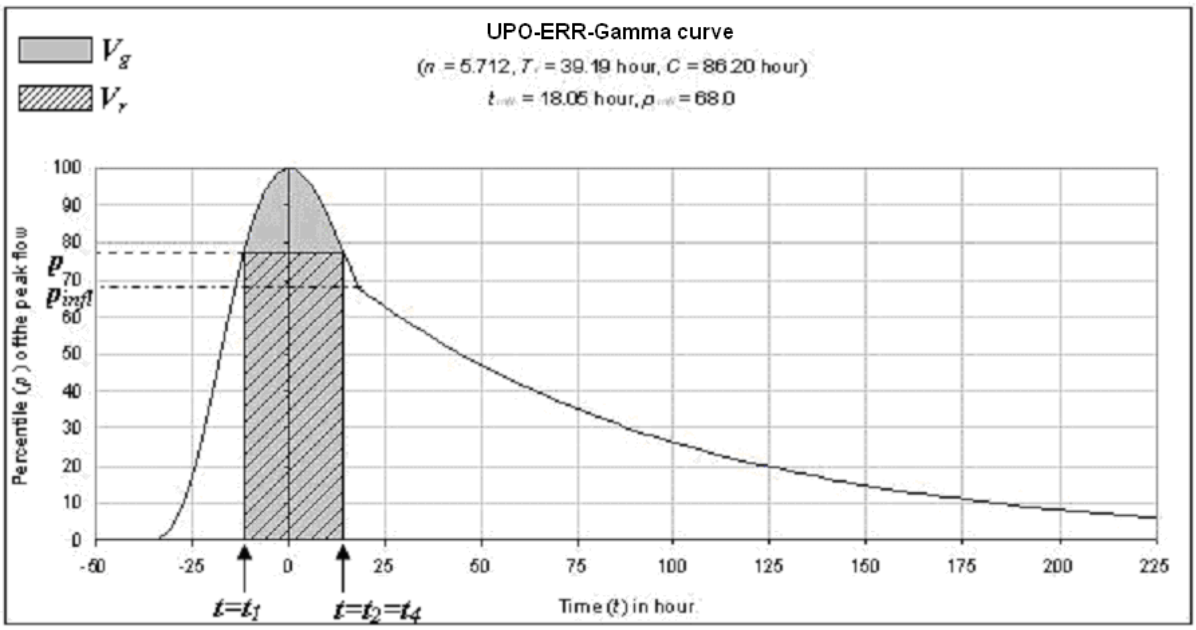

Fig. C.5.1 Illustration of the estimation of the volume above percentile *p* of the peak flow where $p > p_{infl}$

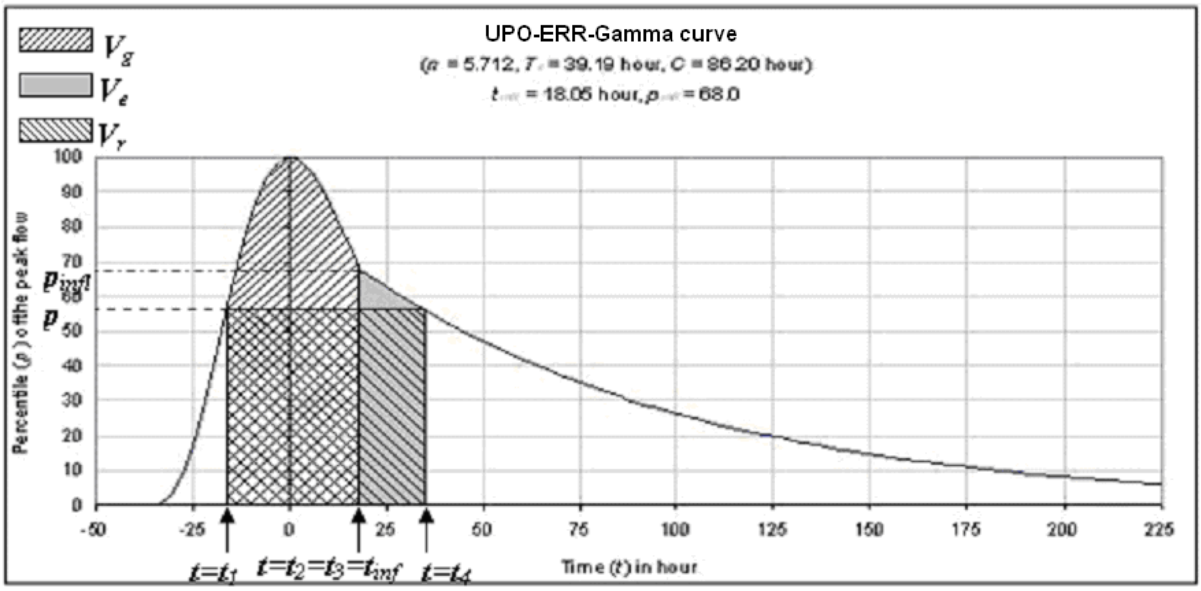

Fig. C.5.2 Illustration of the estimation of the volume above percentile *p* of the peak flow where $p < p_{infl}$

C.5.3 Volume *V* under the UPO-ERR-Gamma curve

Having estimated V_g and V_e by equations (C.5.23) and (C.5.26) respectively, the volume V above any specified percentile p of the peak flow for the UPO-Gamma curve coupled with an exponential recession curve drawn from the point of inflection of the UPO-Gamma curve can be calculated as $V = V_g + V_e - V_r$, where V_r is the volume contained by the ordinates at $t = t_1$ and $t = t_4$ under the specified percentile p of the peak flow.

C.6 Total volume V under the UPO-Gamma curve from the start of rise on the rising side to infinity on the receding side

Although not required in the context of the UPO-ERR-Gamma curve for application in the 'Hydrograph Width analysis', an expression for the total volume under the UPO-Gamma curve is given below for the completeness of the mathematical derivations related to the UPO-gamma curve (i.e. without the exponential replacement recession curve).

Like the standard Gamma distribution function, The 2-parameter translated Gamma function, i.e. the 'peak-at-origin Gamma', or PO-Gamma (see §C.1), having parameters T_r and n, with $T_r = K(n-1)$, has an integral value (volume) of 'unity'.

The peak-normalised PO Gamma, i.e. the 'unit-peak-at-origin Gamma', or the UPO-Gamma, has a volume

V_{Gamma_total} = 'unity'/y_p … (C.6.1)

where y_{pa} is the peak ordinate of the PO-Gamma curve as given by equations (C.1.6) and (C.1.7) in §C.1.

The expression of the total volume under the UPO-Gamma curve, given in equation (C.6.1), can also be alternatively derived by following the steps similar to those given in §C.5 for the estimation of volume under the UPO-ERR-Gamma curve. This derivation is given below.

Rewriting equation (C.5.1) in §C.5.1 by changing the limits t_1 and t_2 to T_r and ∞ respectively, and considering only integer value of the parameter n,

$$V_{Gamma\_Total} = I_{n-1} = \int_{-T_r}^{\infty} \left(\frac{t+T_r}{T_r}\right)^{n-1} Exp\left(-\frac{t(n-1)}{T_r}\right) dt \qquad \text{… (C.6.2)}$$

In this equation, the subscript n-1 of I_{n-1}indicates the exponent of $\frac{t+T_r}{T_r}$

Integrating the integrand on the right hand side of equation (C.6.2) by parts,

$$I_{n-1} = \left(\frac{t+T_r}{T_r}\right)^{n-1}\left(-\frac{T_r}{n-1}\right)Exp\left(-\frac{t(n-1)}{T_r}\right)\Bigg|_{-T_r}^{\infty} \qquad \text{… (C.6.3)}$$

$$-\int_{-T_r}^{\infty}(n-1)\left(\frac{t+T_r}{T_r}\right)^{(n-2)}\left(\frac{1}{T_r}\right)\left(-\frac{T_r}{n-1}\right)Exp\left(-\frac{t(n-1)}{T_r}\right)dt$$

We can now express I_{n-1} by $I_{n-1} = A_{n-1} + \frac{n-1}{n-1} I_{n-2}$ … (C.6.4)

where,

$$A_{n-1} = \left(\frac{t+T_r}{T_r}\right)^{n-1}\left(-\frac{T_r}{n-1}\right)Exp\left(-\frac{t(n-1)}{T_r}\right)\Bigg|_{-T_r}^{\infty} \qquad \text{… (C.6.5)}$$

and, following from equation (C.6.2) and (C.6.3), $I_{n-2} = \int_{-T_r}^{\infty}\left(\frac{t+T_r}{T_r}\right)^{(n-2)} Exp\left(-\frac{t(n-1)}{T_r}\right)dt$

… (C.6.6)

The subscripts *n*-1 and *n*-2 in A_{n-1} and I_{n-2} indicate the exponents of $\frac{t+T_r}{T_r}$ in the respective equations.

Now, considering the limit of ∞ for the expression of A_{n-1} in equation (C.6.5),

$$\lim_{t\to\infty}\left(\frac{t+T_r}{T_r}\right)^{n-1} Exp\left(-\frac{t(n-1)}{T_r}\right) = \lim_{t\to\infty}\frac{\left(\frac{t+T_r}{T_r}\right)^{n-1}}{Exp\left(\frac{t(n-1)}{T_r}\right)}$$ is of the form ∞/∞.

∴Using the l'Hôpital's rule,

$$\lim_{t\to\infty}\left(\frac{t+T_r}{T_r}\right)^{n-1} Exp\left(-\frac{t(n-1)}{T_r}\right) = \lim_{t\to\infty}\frac{\frac{n-1}{T_r}\left(\frac{t+T_r}{T_r}\right)^{n-2}}{\frac{n-1}{T_r}Exp\left(\frac{t(n-1)}{T_r}\right)}$$

$$= \lim_{t\to\infty}\frac{\frac{(n-1)(n-2)}{T_r^{\,2}}\left(\frac{t+T_r}{T_r}\right)^{n-3}}{\left(\frac{n-1}{T_r}\right)^{2} Exp\left(\frac{t(n-1)}{T_r}\right)}$$

$$= \lim_{t\to\infty}\frac{\frac{(n-1)(n-2)(n-3)}{T_r^{\,3}}\left(\frac{t+T_r}{T_r}\right)^{n-4}}{\left(\frac{n-1}{T_r}\right)^{3} Exp\left(\frac{t(n-1)}{T_r}\right)}$$

… … …
… … …
… … …

$$= \lim_{t\to\infty} \frac{\dfrac{(n-1)(n-2)(n-3)\ldots 3.2.1}{T_r^{\,n-1}}\left(\dfrac{t+T_r}{T_r}\right)^0}{\left(\dfrac{n-1}{T_r}\right)^{n-1} Exp\left(\dfrac{t(n-1)}{T_r}\right)}$$

$$= \lim_{t\to\infty} \frac{\dfrac{(n-1)(n-2)(n-3)\ldots 3.2.1}{T_r^{\,n-1}}}{\left(\dfrac{n-1}{T_r}\right)^{n-1} Exp\left(\dfrac{t(n-1)}{T_r}\right)}$$

$$= 0 \qquad \ldots \text{(C.6.7)}$$

Next, entering the value of $-T_r$ for t in the expression of A_{n-1} in equation (C.6.5),

The expression $\left(\dfrac{t+T_r}{T_r}\right)^{n-1}\left(-\dfrac{T_r}{n-1}\right)Exp\left(-\dfrac{t(n-1)}{T_r}\right)$ at $t = -T_r$ equals to 0.

Therefore, considering the limits of ∞ and $-T_r$ for t the value of A_{n-1} in equation (C.6.4), A_{n-1} evaluates to zero, and equation (C.6.4) takes the form

$$I_{n-1} = \frac{n-1}{n-1} I_{n-2} \qquad \ldots \text{(C.6.8)}$$

From equations (C.6.3) and (C.6.8), it follows that,

$$I_{n-1} = \frac{(n-1)(n-2)}{(n-1)^2} I_{n-3}$$

$$= \frac{(n-1)(n-2)(n-3)}{(n-1)^3} I_{n-4}$$

$$\ldots \quad \ldots \quad \ldots \quad \ldots$$

$$\ldots \quad \ldots \quad \ldots \quad \ldots$$

$$\ldots \quad \ldots \quad \ldots \quad \ldots$$

$$I_{n-1} = \frac{(n-1)(n-2)(n-3)\ldots 3.2.1}{(n-1)^{n-1}} I_0$$

$$\text{Or, } I_{n-1} = \frac{(n-1)!}{(n-1)^{n-1}} I_0 \qquad \ldots \text{(C.6.9)}$$

Now,

$$I_0 = \int_{-T_r}^{\infty} Exp\left(-\frac{t(n-1)}{T_r}\right) dt$$

$$= -\frac{T_r}{n-1} Exp\left(-\frac{t(n-1)}{T_r}\right)\Bigg|_{-T_r}^{\infty}$$

$$= -\frac{T_r}{n-1}\left\{Exp\left(-\frac{\infty(n-1)}{T_r}\right) - Exp\left(-\frac{-T_r(n-1)}{T_r}\right)\right\}$$

$$= -\frac{T_r}{n-1}\{0 - Exp(n-1)\} = \frac{T_r Exp(n-1)}{n-1}$$

Therefore equation (C.6.9) can now be written as,

$$I_{n-1} = \frac{(n-1)!}{(n-1)^{n-1}} \frac{T_r}{n-1} Exp(n-1)$$

Simplifying further,

$$I_{n-1} = \frac{(n-2)!}{(n-1)^{n-1}} T_r Exp(n-1) \qquad \text{… (C.6.10)}$$

Therefore the total volume under the UPO-Gamma curve for an integer value of *n* is given by,

$$V_{Gamma\_Total} = \frac{(n-2)!}{(n-1)^{n-1}} T_r Exp(n-1) \qquad \text{… (C.6.11)}$$

For a non-integer value of *n*, the total volume under the UPO-Gamma curve can be approximately computed by using interpolation or extrapolation using suitable integer values of *n* as outlined in §C.5.1 and as expressed by equation (C.5.23).

Replacing T_r by $K(n\text{-}1)$, $(n\text{-}1)!$ by $\Gamma(n)$, and Exp(n-1) by 1/Exp(1-n), the equation (C.6.11) can be written as

$$V_{Gamma\_Total} = \frac{K\Gamma(n)}{(n-1)^{n-1} Exp(1-n)} \qquad \text{… (C.6.12)}$$

Noting from equation (C.1.7) that $y_P = \frac{1}{K\,\Gamma(n)}(n-1)^{n-1} Exp(1-n)$, equation (C.6.12) can be written as

$$V_{Gamma\_Total} = \frac{1}{y_P} \qquad \text{… (C.6.13)}$$

This expression is the same as that shown in equation (C.6.1).

If the Design Peak y_{DP} is that given, for a specified return period, by the procedure developed in work-package WP2.1, then the parametric Gamma form of the Design Hydrograph for that value of y_{DP} is the UPO-Gamma curve rescaled by multiplying it by y_{DP}. Hence, its volume (i.e. the total volume under the UPO-Gamma hydrograph) is ('unity × y_{DP})/ y_P. The conventional dimension of y_{DP} being [L^3T^{-1}], the volume, thus computed, can be expressed in m^3 or in cumec-hours or in mm.

APPENDIX – D

GRAPHS AND TABLES SHOWING RESULTS IN SPLIT-SAMPLE CALIBRATION AND VERIFICATION USING 37 A1 CATEGORY STATIONS

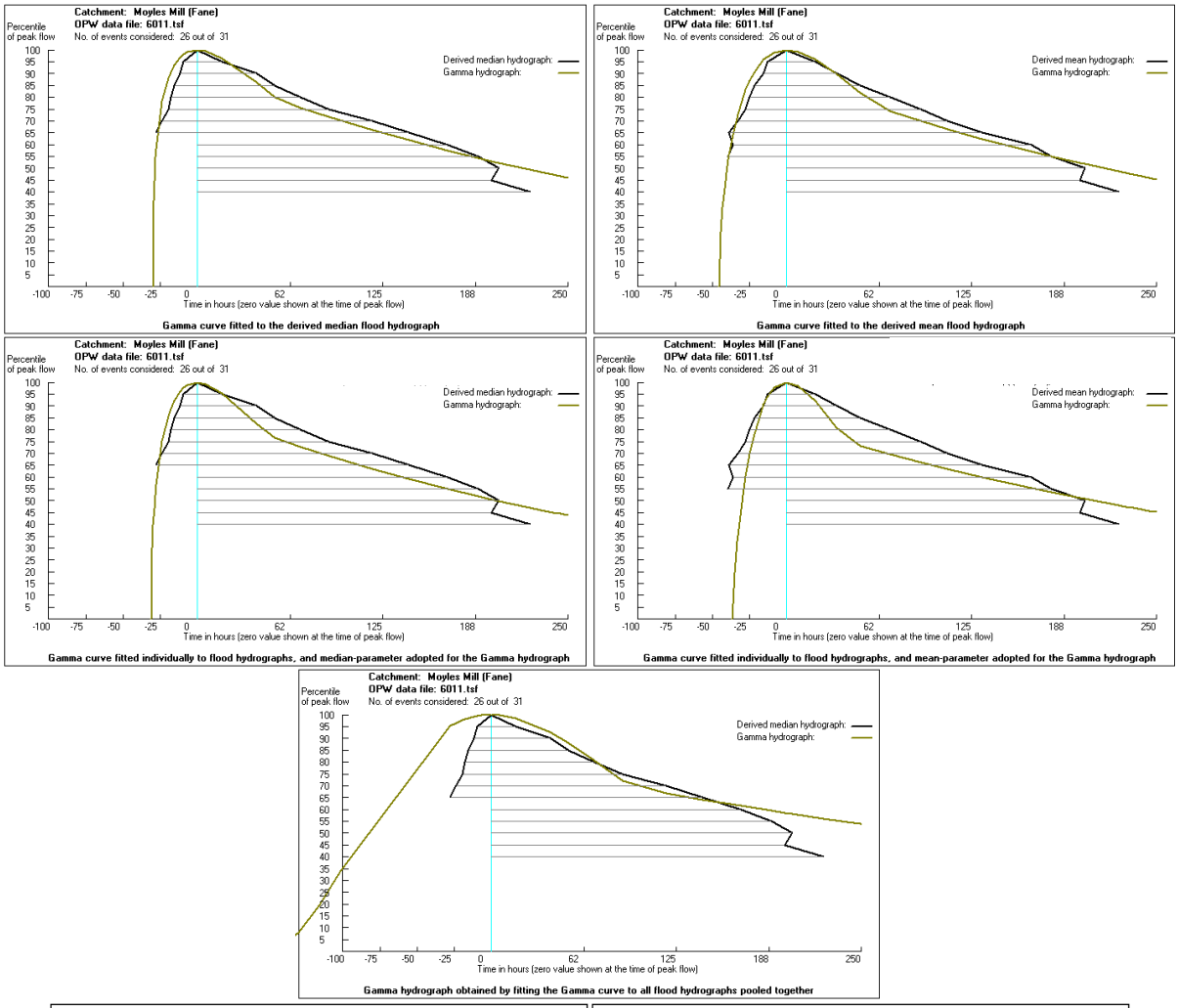

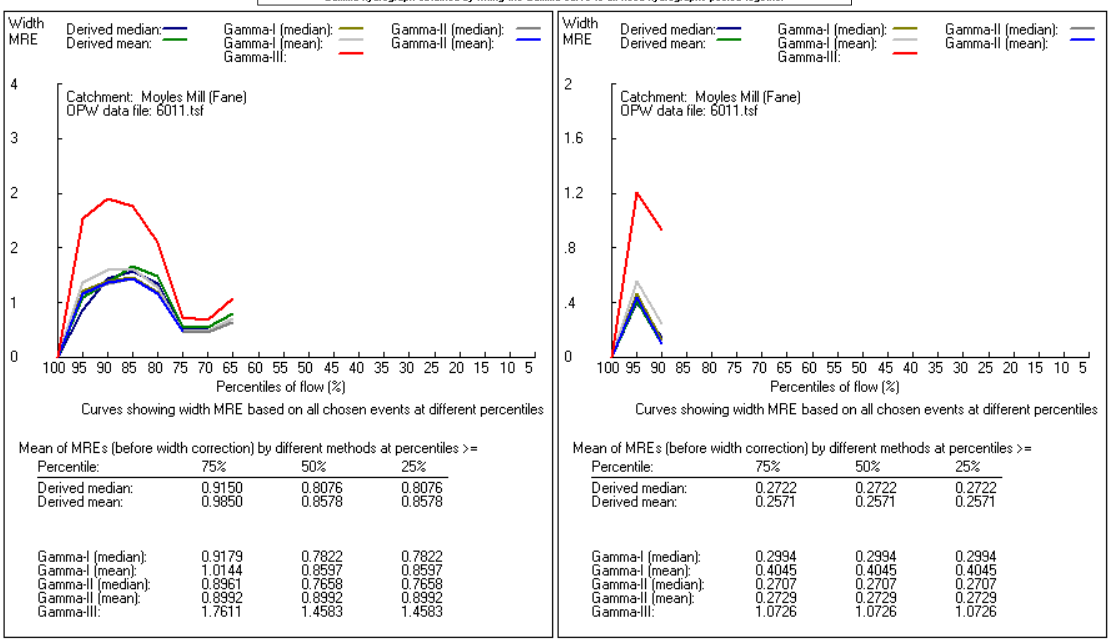

Fig. D.1.1 Calibration results for Station No. 6011

Parametric hydrographs, i.e. the modified Gamma curve coupled with an exponential replacement recession curve, as calibrated for the five alternative methods, are shown in the top five figures together with the derived median and mean hydrographs The bottom two figures display the variation of the Mean Relative Error (MRE) with percentiles of the peak flow and the values of the MRE at and above the 75, 50 and 25 percentiles of the peak flow in calibration (left) and verification (right)

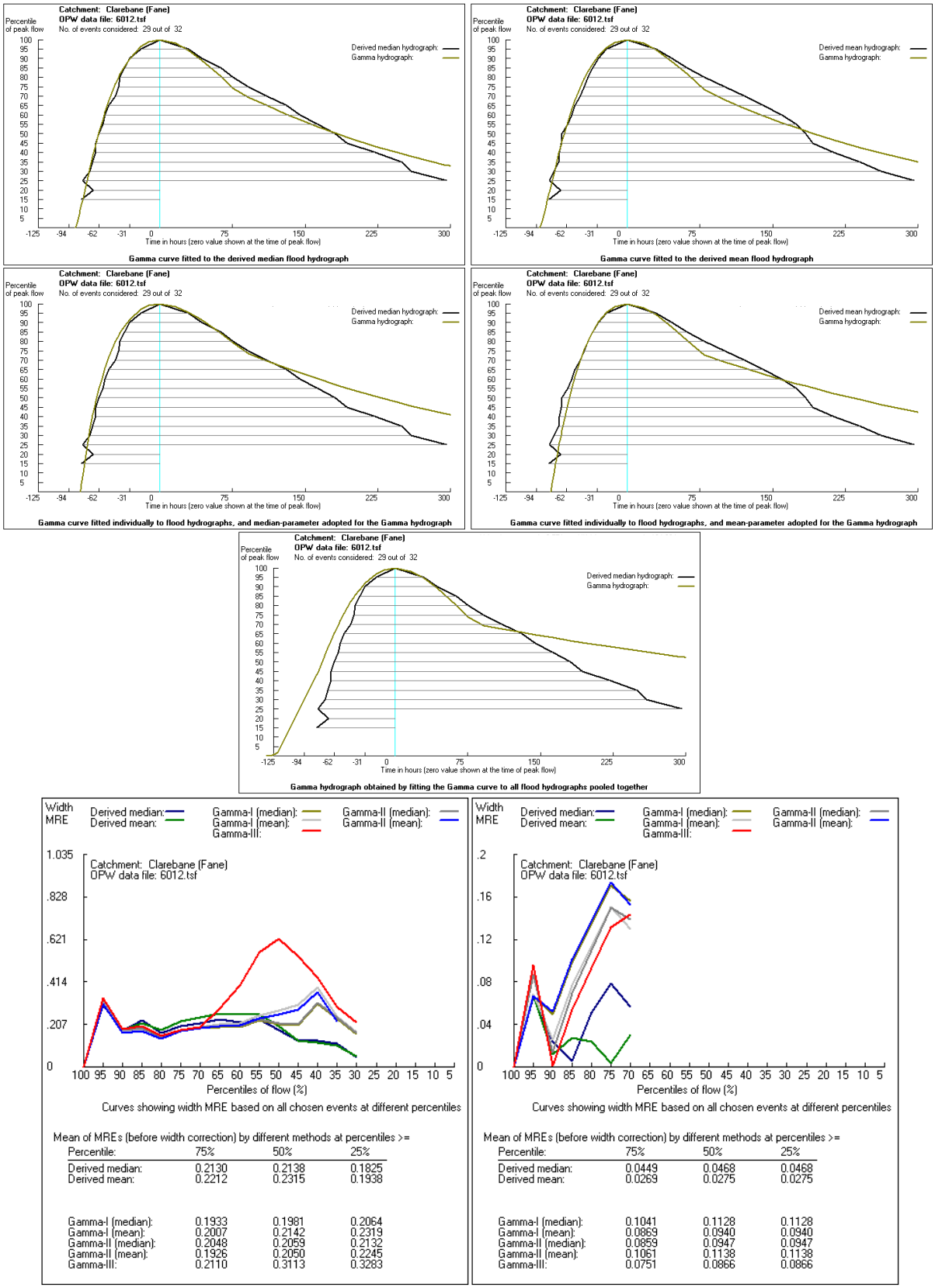

Fig. D.1.2 Calibration results for Station No. 6012

Parametric hydrographs, i.e. the modified Gamma curve coupled with an exponential replacement recession curve, as calibrated for the five alternative methods, are shown in the top five figures together with the derived median and mean hydrographs The bottom two figures display the variation of the Mean Relative Error (MRE) with percentiles of the peak flow and the values of the MRE at and above the 75, 50 and 25 percentiles of the peak flow in calibration (left) and verification (right)

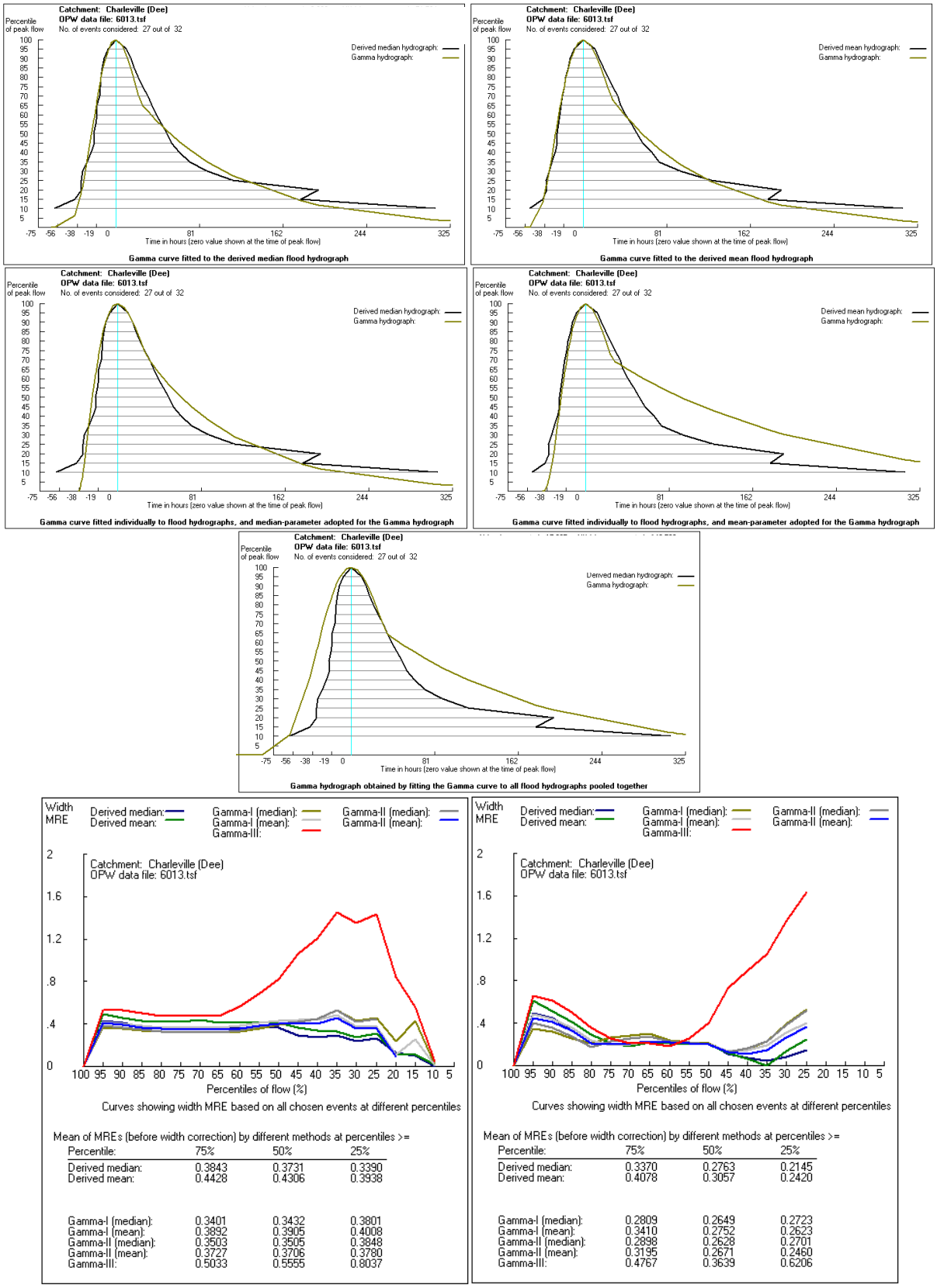

Fig. D.1.3 Calibration results for Station No. 6013

Parametric hydrographs, i.e. the modified Gamma curve coupled with an exponential replacement recession curve, as calibrated for the five alternative methods, are shown in the top five figures together with the derived median and mean hydrographs The bottom two figures display the variation of the Mean Relative Error (MRE) with percentiles of the peak flow and the values of the MRE at and above the 75, 50 and 25 percentiles of the peak flow in calibration (left) and verification (right)

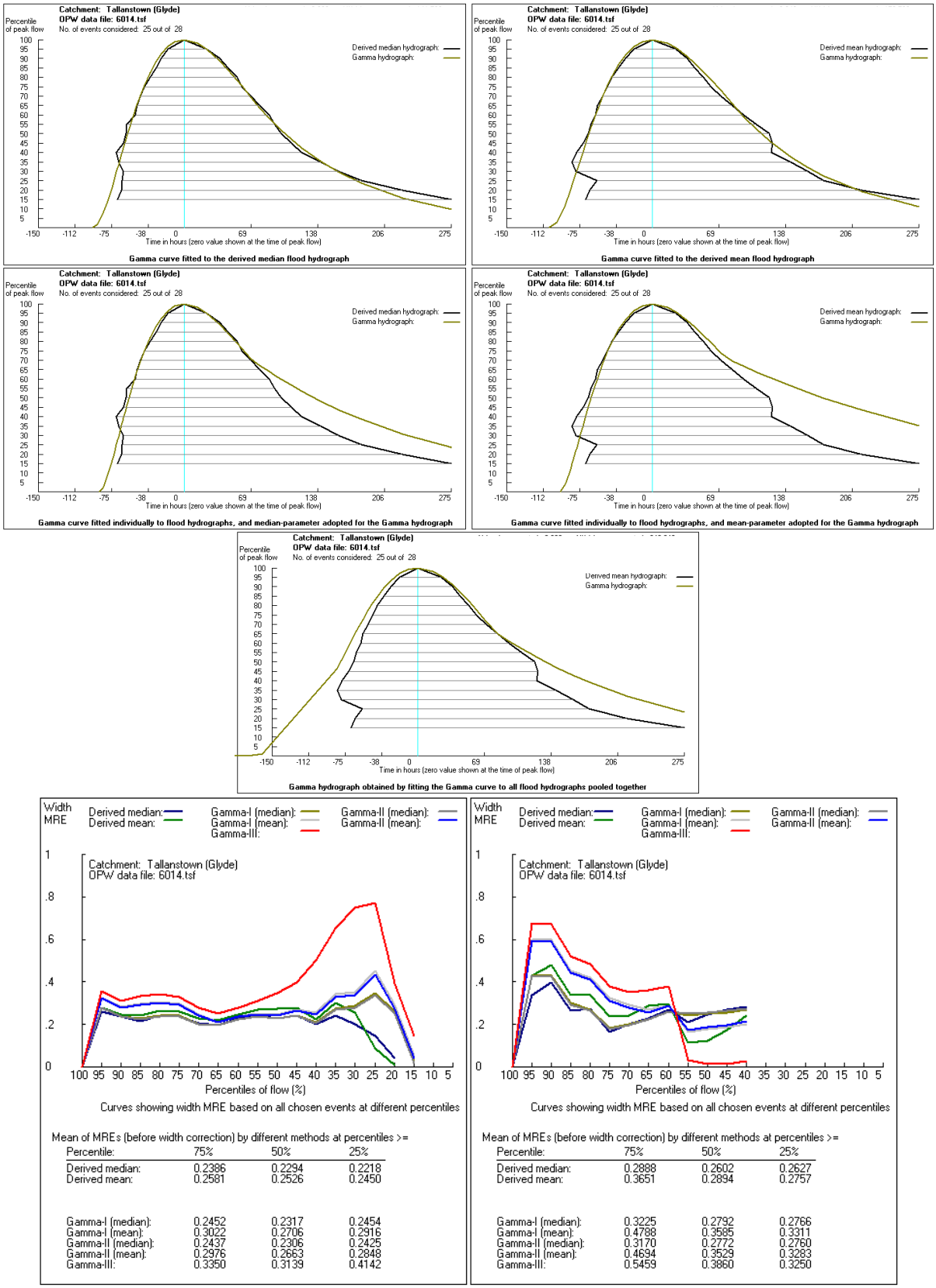

Fig. D.1.4 Calibration results for Station No. 6014

Parametric hydrographs, i.e. the modified Gamma curve coupled with an exponential replacement recession curve, as calibrated for the five alternative methods, are shown in the top five figures together with the derived median and mean hydrographs The bottom two figures display the variation of the Mean Relative Error (MRE) with percentiles of the peak flow and the values of the MRE at and above the 75, 50 and 25 percentiles of the peak flow in calibration (left) and verification (right)

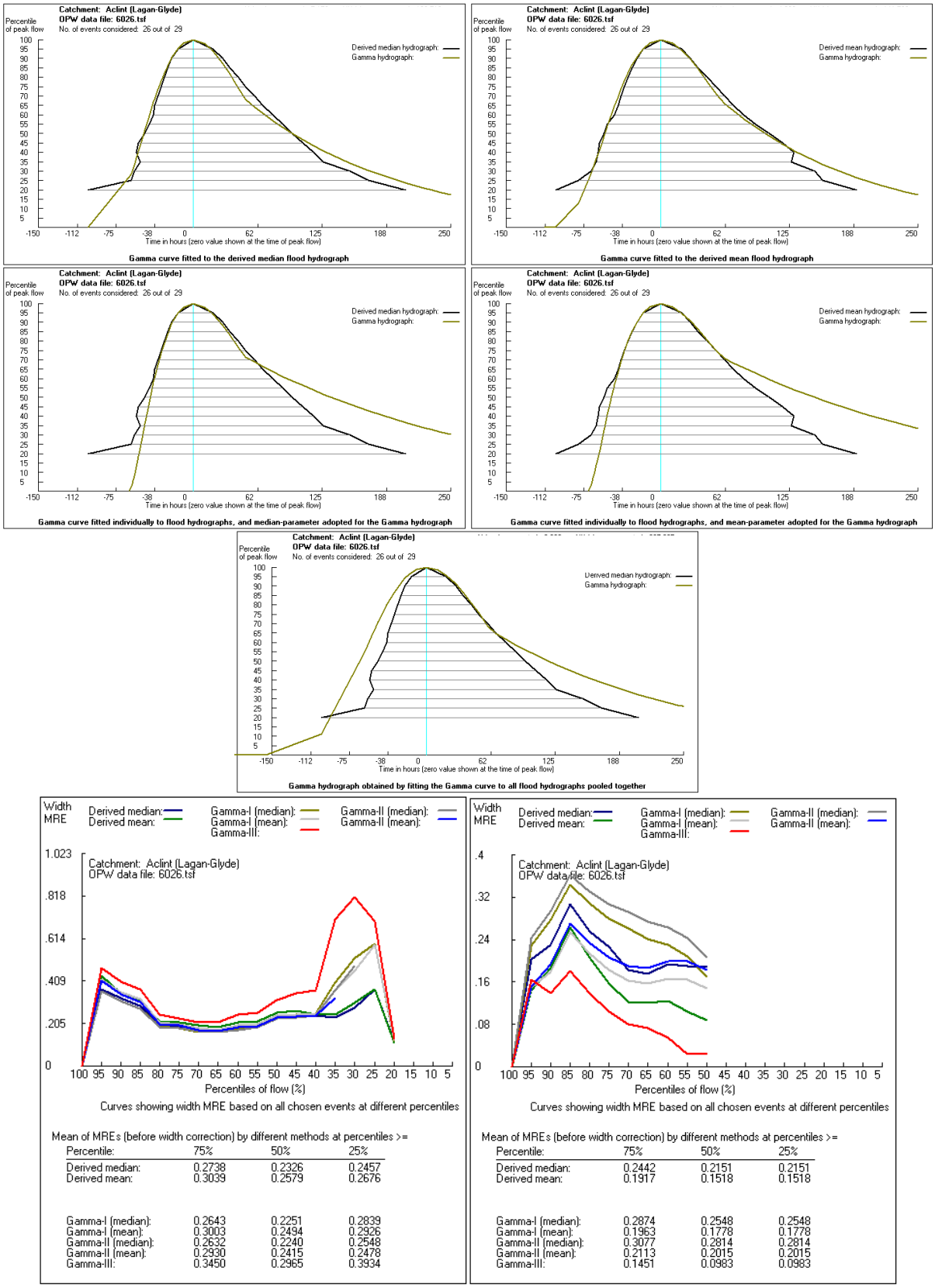

Fig. D.1.5 Calibration results for Station No. 6026

Parametric hydrographs, i.e. the modified Gamma curve coupled with an exponential replacement recession curve, as calibrated for the five alternative methods, are shown in the top five figures together with the derived median and mean hydrographs The bottom two figures display the variation of the Mean Relative Error (MRE) with percentiles of the peak flow and the values of the MRE at and above the 75, 50 and 25 percentiles of the peak flow in calibration (left) and verification (right)

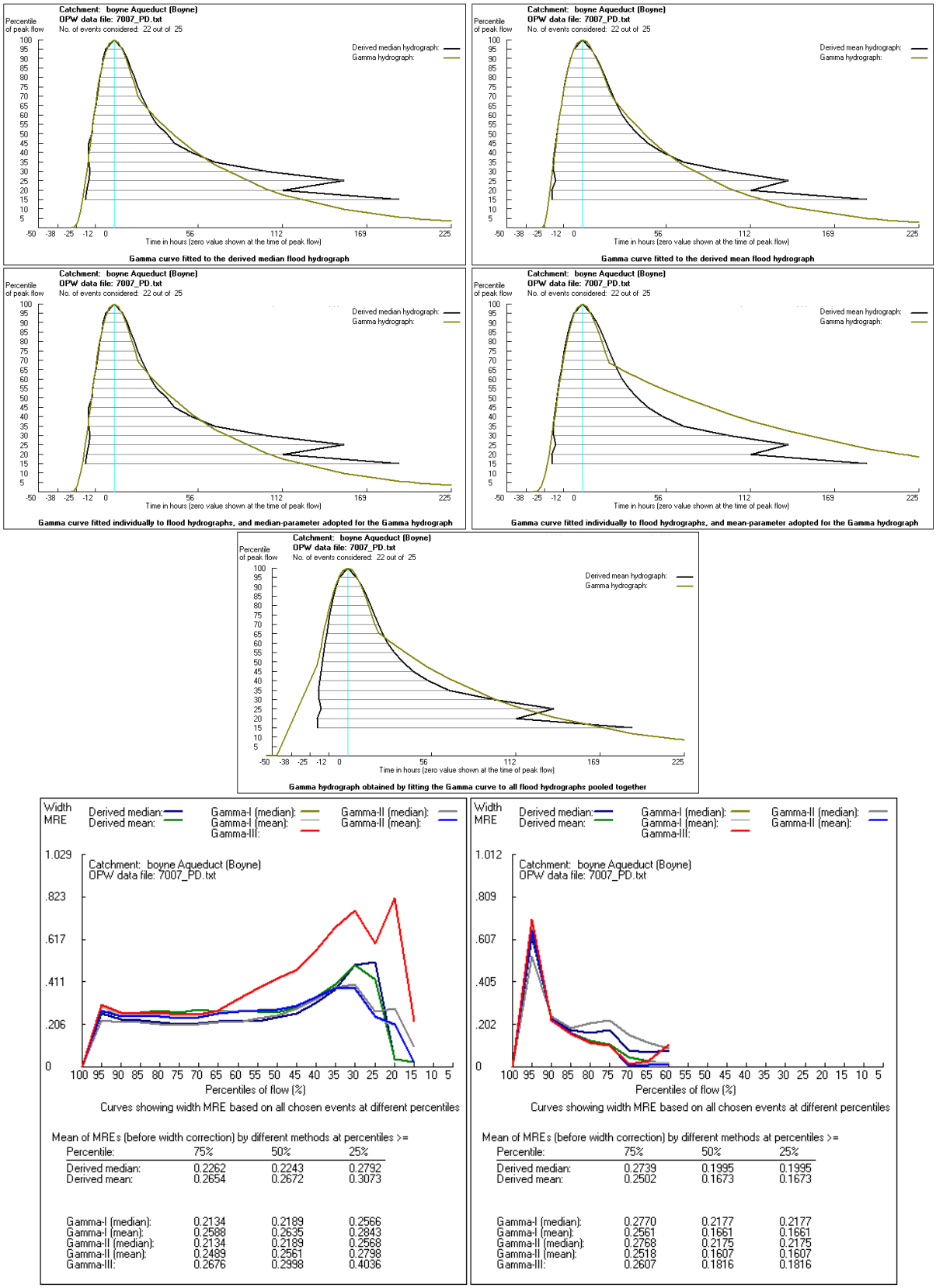

Fig. D.1.6 Calibration results for Station No. 7007 (post-drainage period)

Parametric hydrographs, i.e. the modified Gamma curve coupled with an exponential replacement recession curve, as calibrated for the five alternative methods, are shown in the top five figures together with the derived median and mean hydrographs The bottom two figures display the variation of the Mean Relative Error (MRE) with percentiles of the peak flow and the values of the MRE at and above the 75, 50 and 25 percentiles of the peak flow in calibration (left) and verification (right)

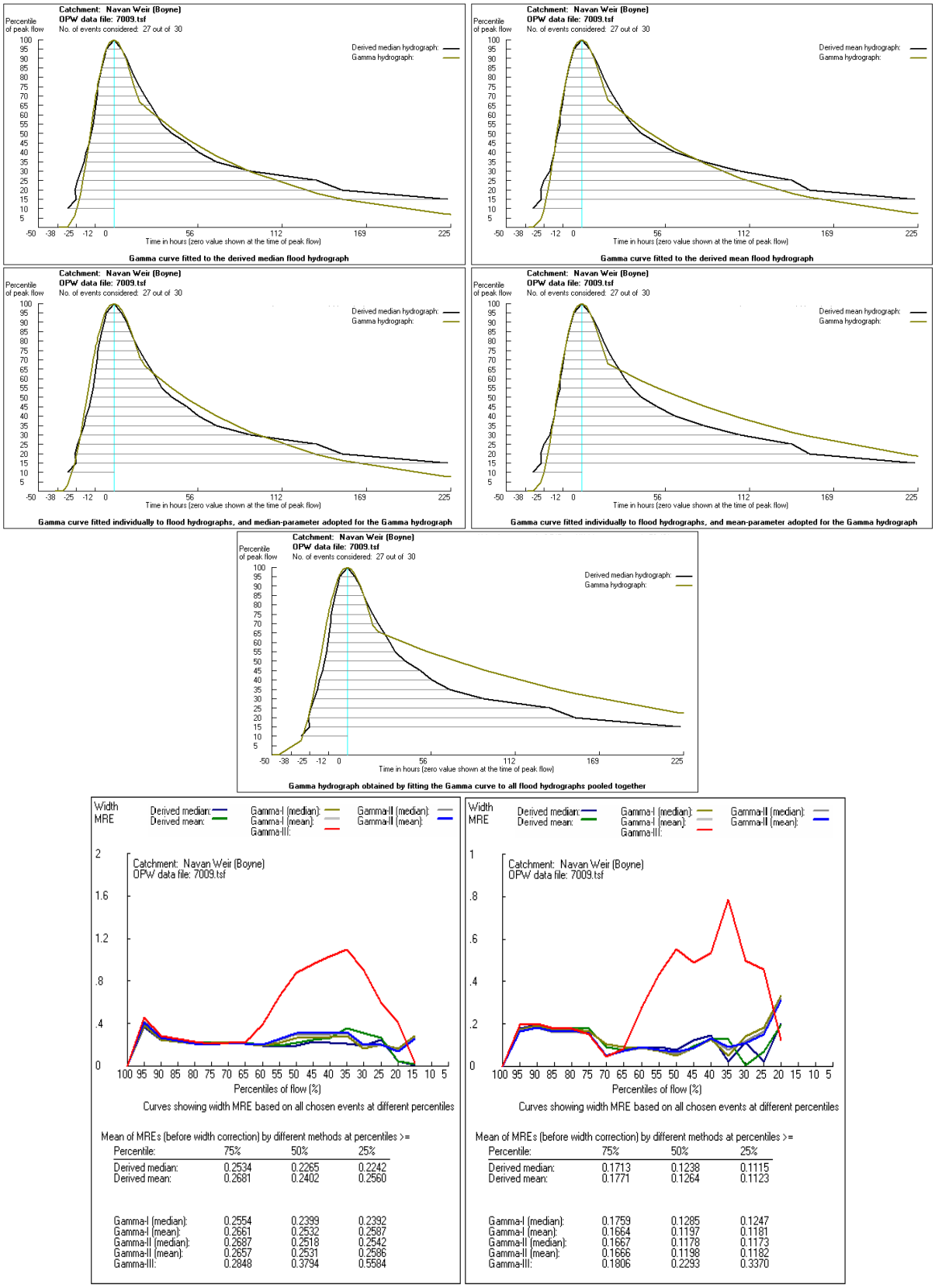

Fig. D.1.7 Calibration results for Station No. 7009

Parametric hydrographs, i.e. the modified Gamma curve coupled with an exponential replacement recession curve, as calibrated for the five alternative methods, are shown in the top five figures together with the derived median and mean hydrographs The bottom two figures display the variation of the Mean Relative Error (MRE) with percentiles of the peak flow and the values of the MRE at and above the 75, 50 and 25 percentiles of the peak flow in calibration (left) and verification (right)

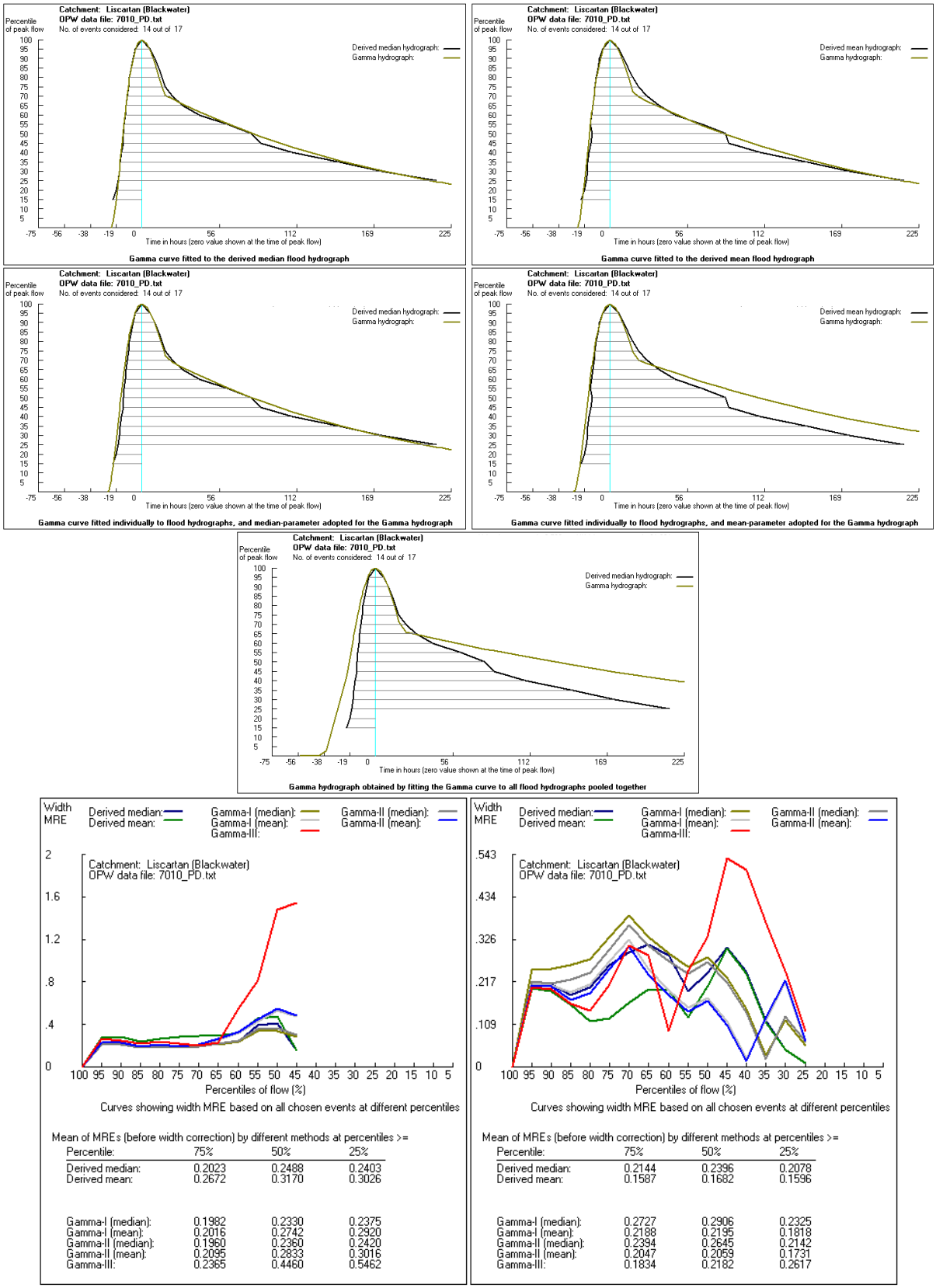

Fig. D.1.8 Calibration results for Station No. 7010 (post-drainage period)

Parametric hydrographs, i.e. the modified Gamma curve coupled with an exponential replacement recession curve, as calibrated for the five alternative methods, are shown in the top five figures together with the derived median and mean hydrographs The bottom two figures display the variation of the Mean Relative Error (MRE) with percentiles of the peak flow and the values of the MRE at and above the 75, 50 and 25 percentiles of the peak flow in calibration (left) and verification (right)

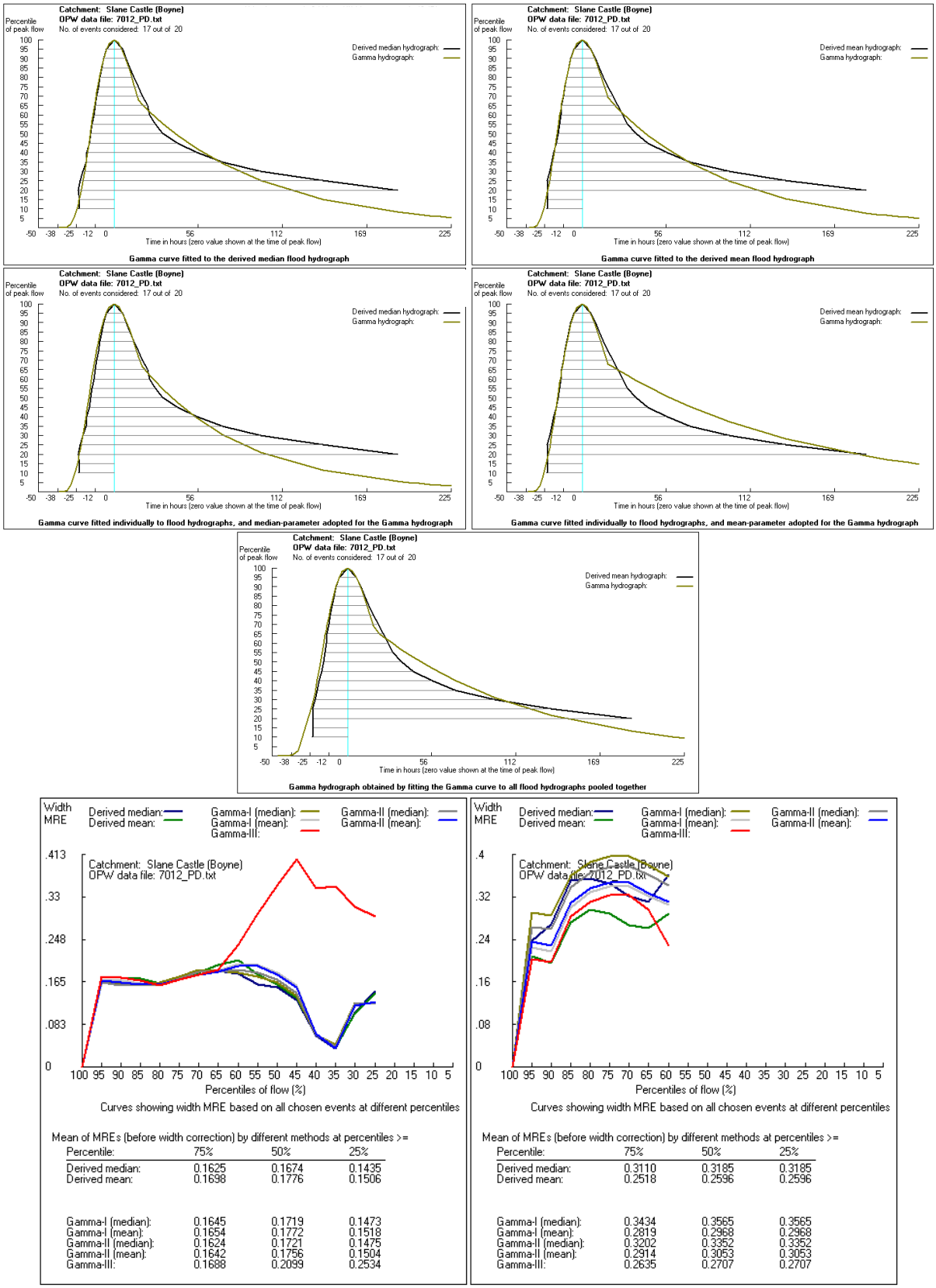

Fig. D.1.9 Calibration results for Station No. 7012 (post-drainage period)

Parametric hydrographs, i.e. the modified Gamma curve coupled with an exponential replacement recession curve, as calibrated for the five alternative methods, are shown in the top five figures together with the derived median and mean hydrographs The bottom two figures display the variation of the Mean Relative Error (MRE) with percentiles of the peak flow and the values of the MRE at and above the 75, 50 and 25 percentiles of the peak flow in calibration (left) and verification (right)

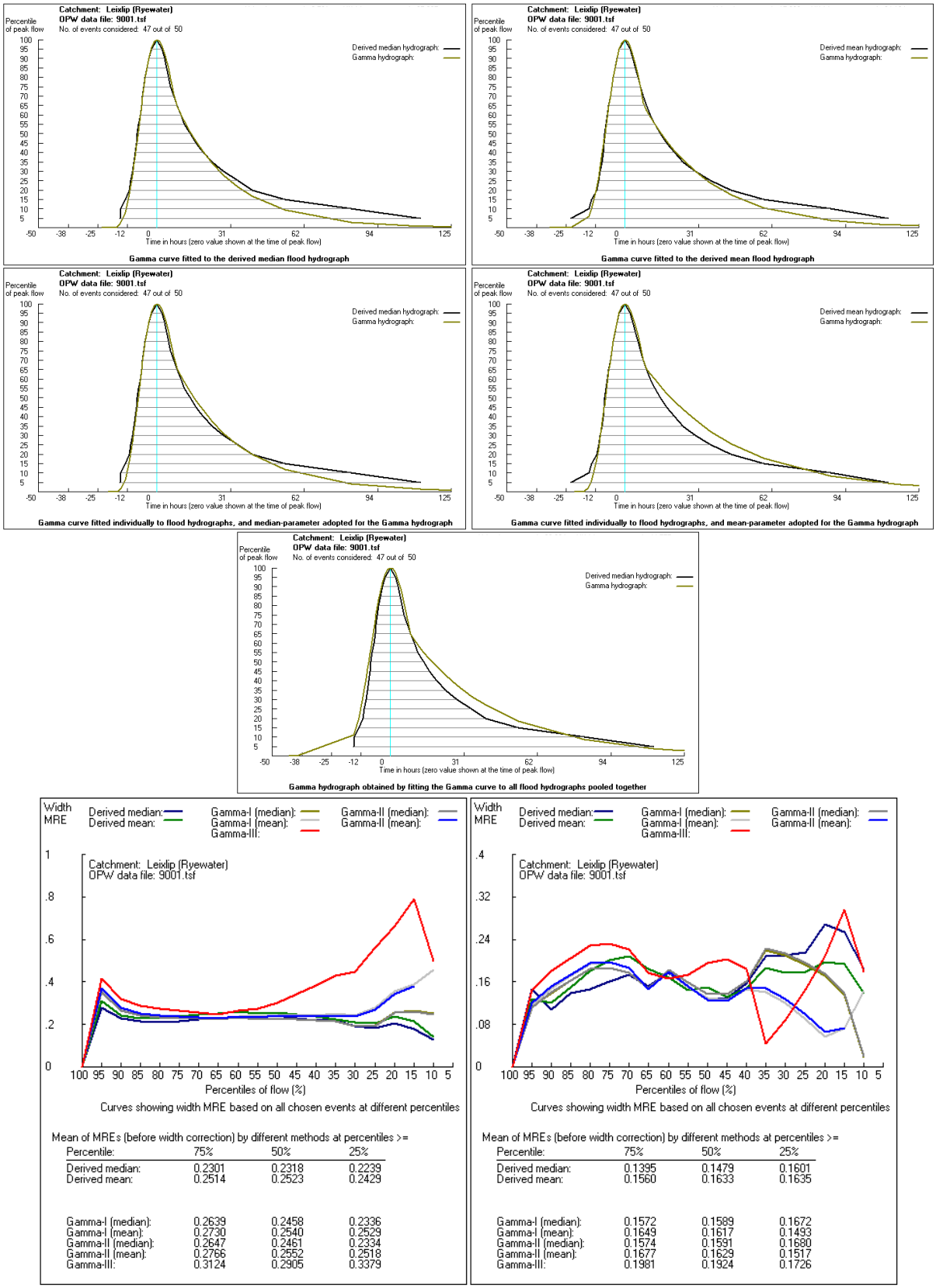

Fig. D.1.10 Calibration results for Station No. 9001

Parametric hydrographs, i.e. the modified Gamma curve coupled with an exponential replacement recession curve, as calibrated for the five alternative methods, are shown in the top five figures together with the derived median and mean hydrographs The bottom two figures display the variation of the Mean Relative Error (MRE) with percentiles of the peak flow and the values of the MRE at and above the 75, 50 and 25 percentiles of the peak flow in calibration (left) and verification (right)

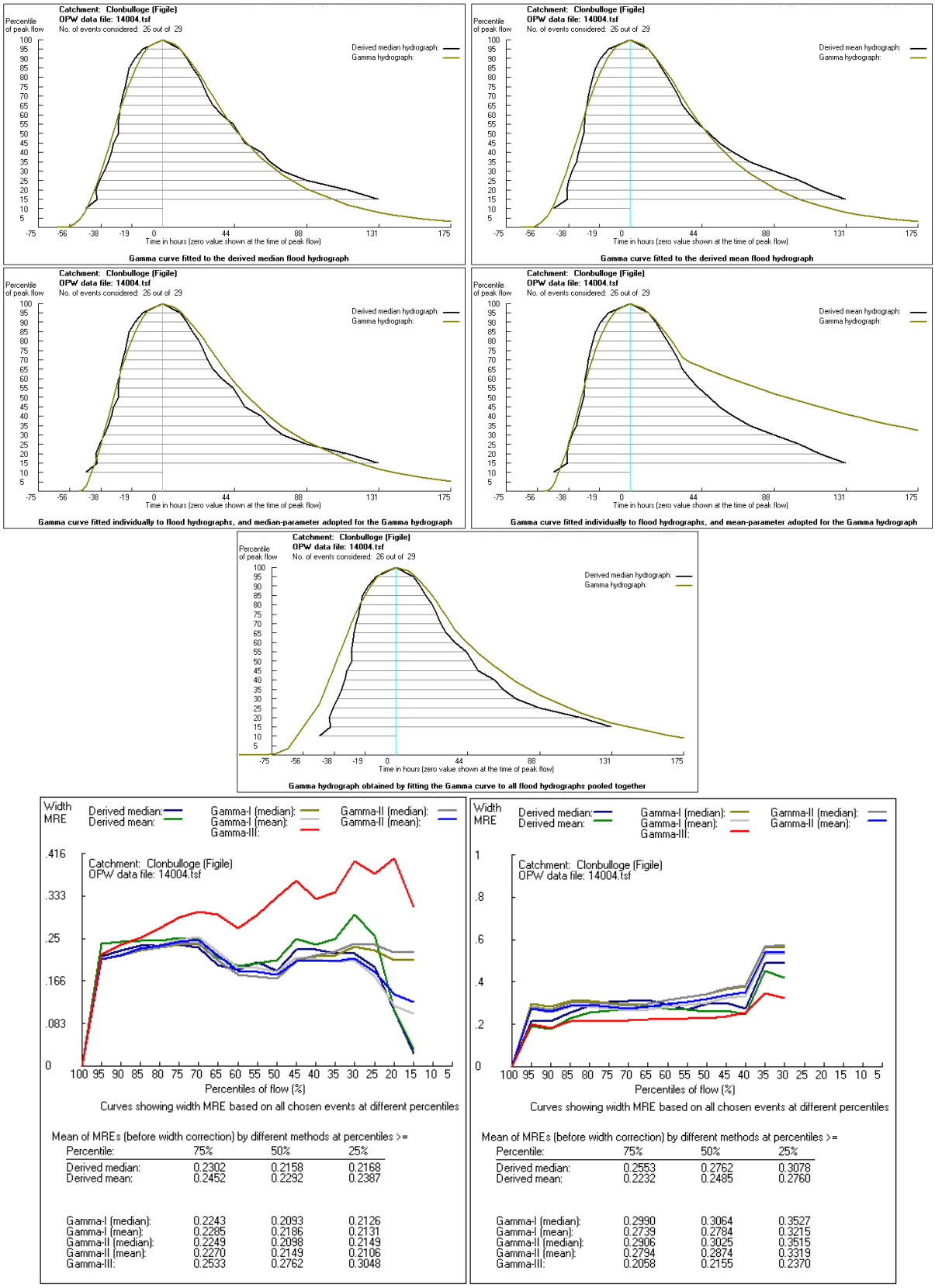

Fig. D.1.11 Calibration results for Station No. 14004

Parametric hydrographs, i.e. the modified Gamma curve coupled with an exponential replacement recession curve, as calibrated for the five alternative methods, are shown in the top five figures together with the derived median and mean hydrographs The bottom two figures display the variation of the Mean Relative Error (MRE) with percentiles of the peak flow and the values of the MRE at and above the 75, 50 and 25 percentiles of the peak flow in calibration (left) and verification (right)

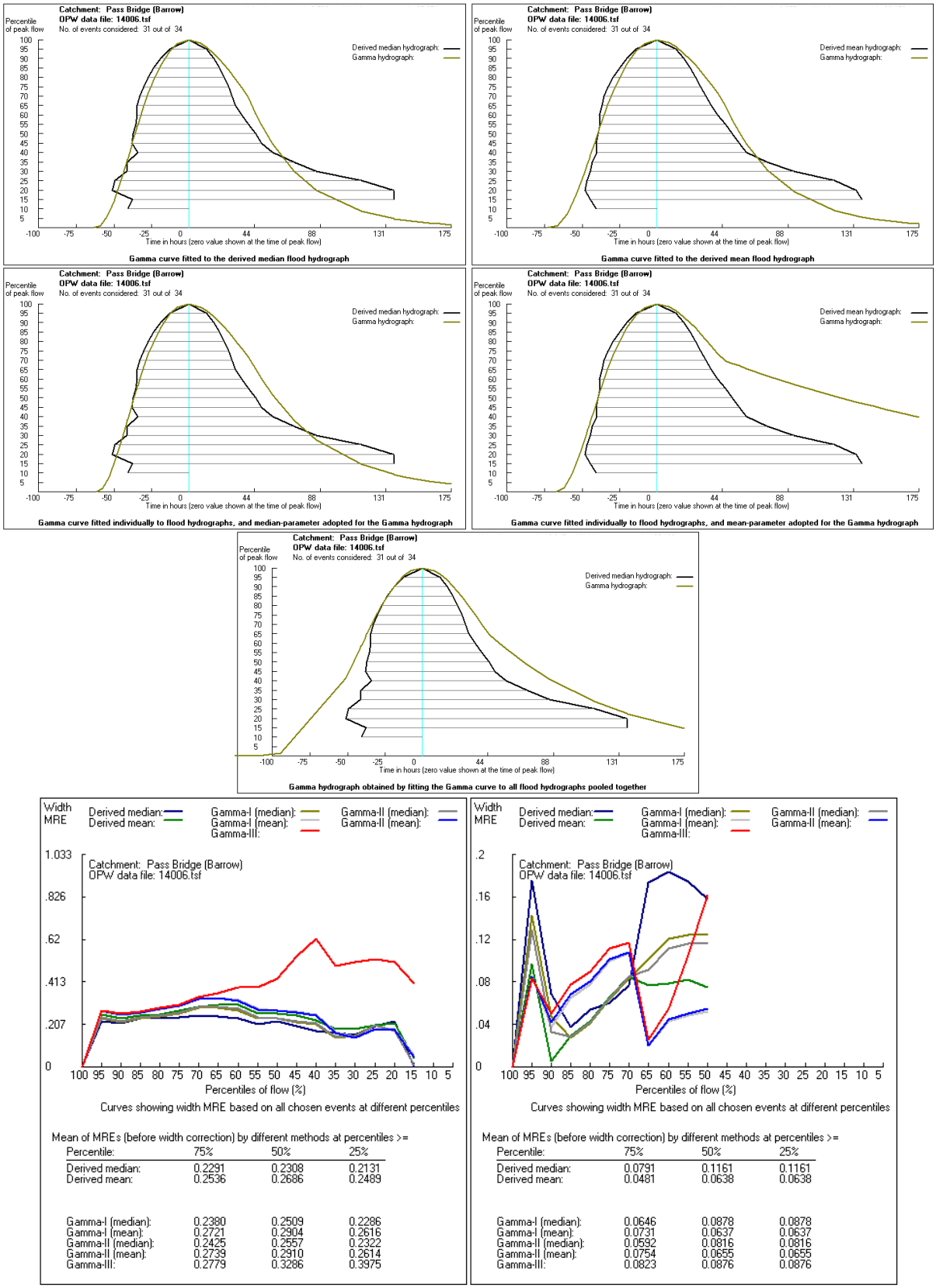

Fig. D.1.12 Calibration results for Station No. 14006

Parametric hydrographs, i.e. the modified Gamma curve coupled with an exponential replacement recession curve, as calibrated for the five alternative methods, are shown in the top five figures together with the derived median and mean hydrographs The bottom two figures display the variation of the Mean Relative Error (MRE) with percentiles of the peak flow and the values of the MRE at and above the 75, 50 and 25 percentiles of the peak flow in calibration (left) and verification (right)

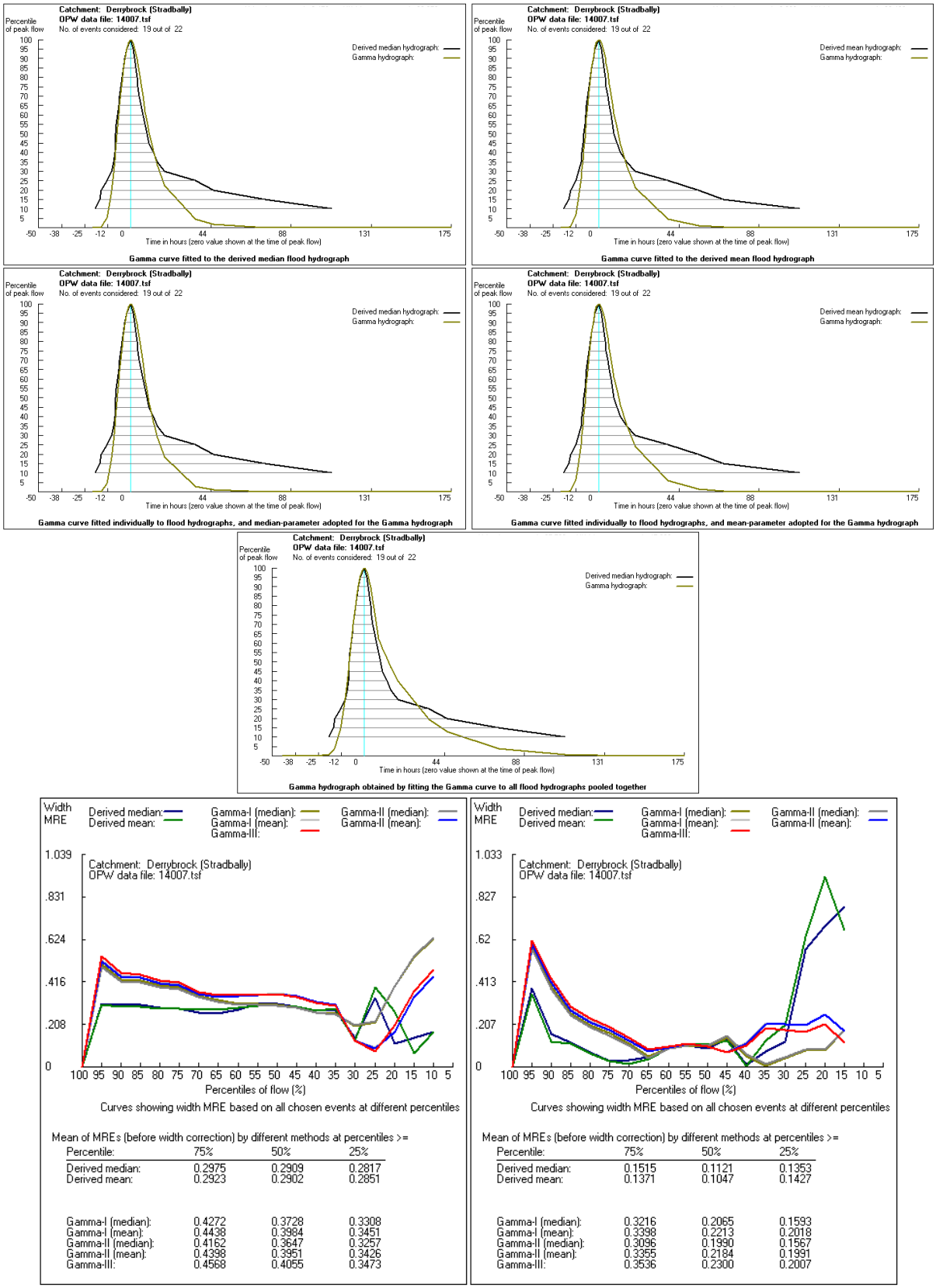

Fig. D.1.13 Calibration results for Station No. 14007

Parametric hydrographs, i.e. the modified Gamma curve coupled with an exponential replacement recession curve, as calibrated for the five alternative methods, are shown in the top five figures together with the derived median and mean hydrographs The bottom two figures display the variation of the Mean Relative Error (MRE) with percentiles of the peak flow and the values of the MRE at and above the 75, 50 and 25 percentiles of the peak flow in calibration (left) and verification (right)

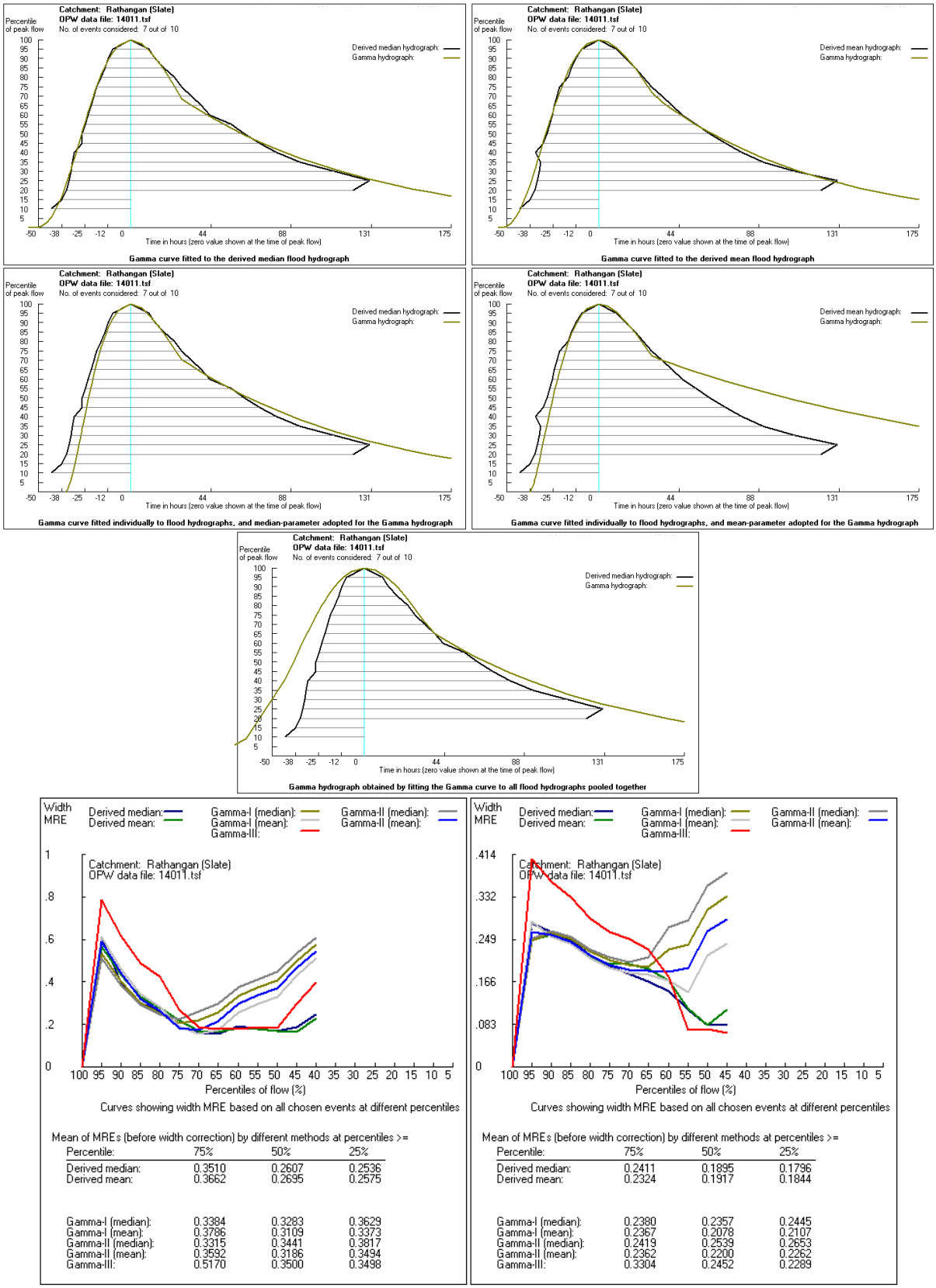

Fig. D.1.14 Calibration results for Station No. 14011

Parametric hydrographs, i.e. the modified Gamma curve coupled with an exponential replacement recession curve, as calibrated for the five alternative methods, are shown in the top five figures together with the derived median and mean hydrographs The bottom two figures display the variation of the Mean Relative Error (MRE) with percentiles of the peak flow and the values of the MRE at and above the 75, 50 and 25 percentiles of the peak flow in calibration (left) and verification (right)

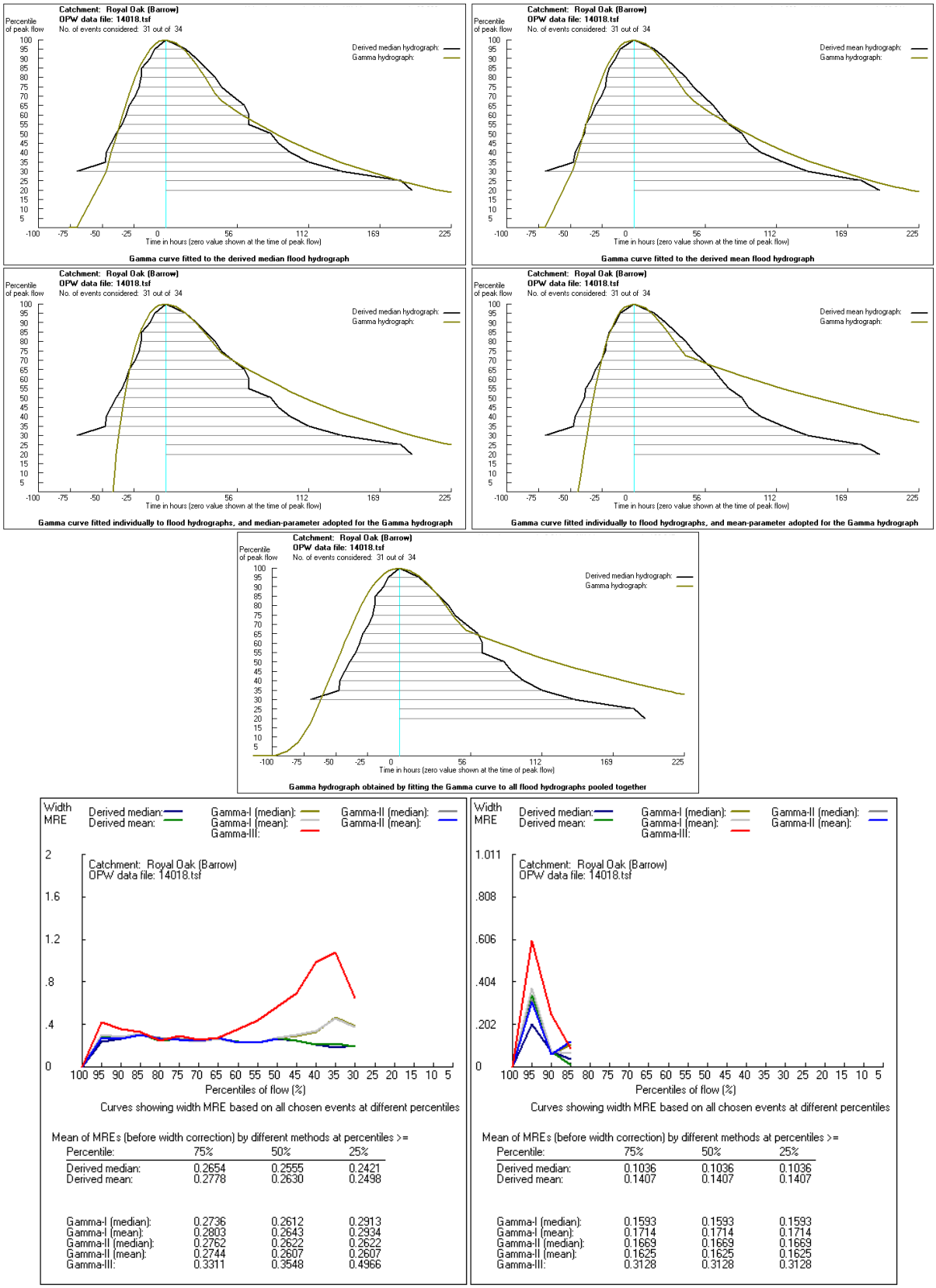

Fig. D.1.15 Calibration results for Station No. 14018

Parametric hydrographs, i.e. the modified Gamma curve coupled with an exponential replacement recession curve, as calibrated for the five alternative methods, are shown in the top five figures together with the derived median and mean hydrographs The bottom two figures display the variation of the Mean Relative Error (MRE) with percentiles of the peak flow and the values of the MRE at and above the 75, 50 and 25 percentiles of the peak flow in calibration (left) and verification (right)

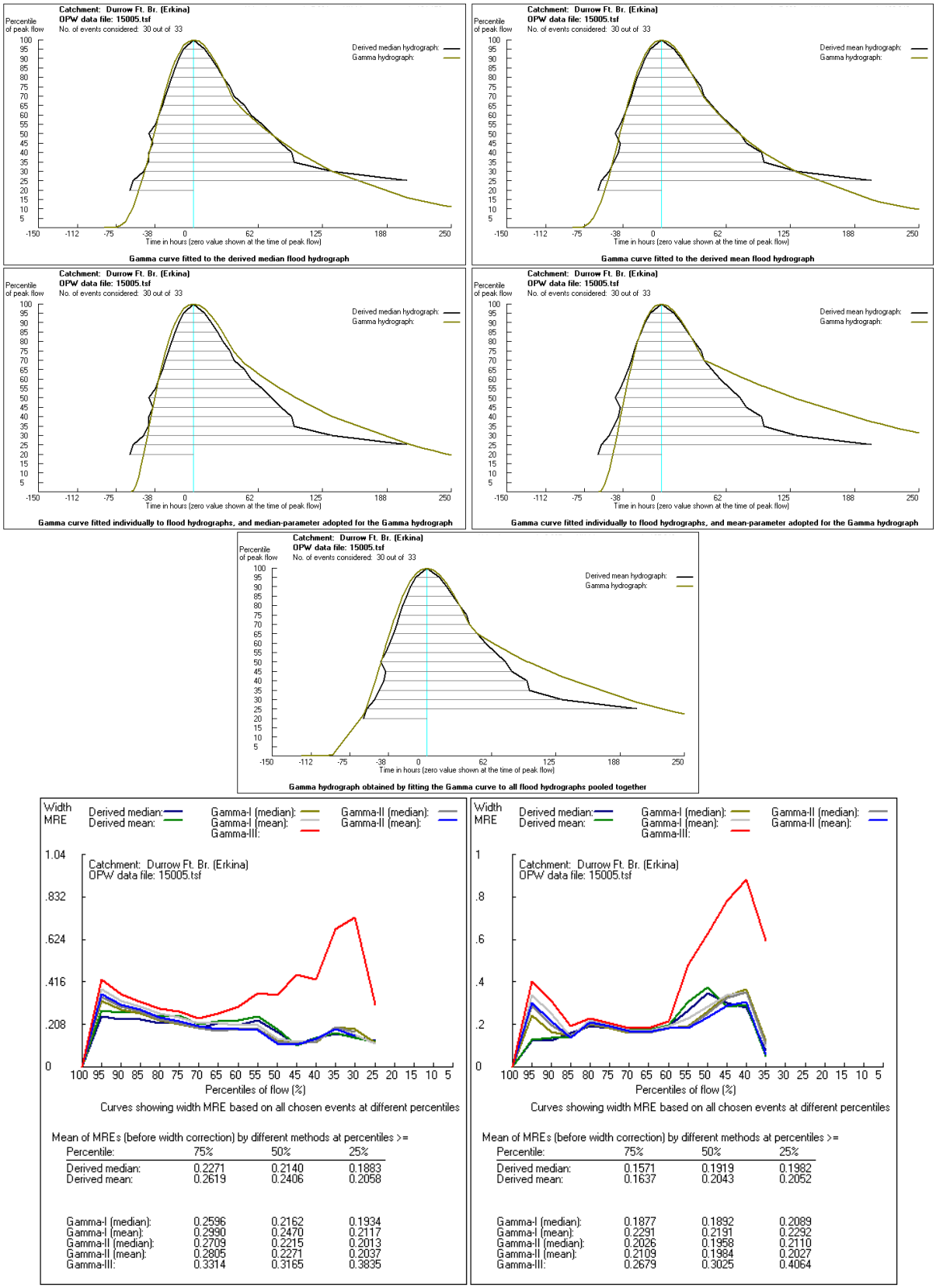

Fig. D.1.16 Calibration results for Station No. 15005

Parametric hydrographs, i.e. the modified Gamma curve coupled with an exponential replacement recession curve, as calibrated for the five alternative methods, are shown in the top five figures together with the derived median and mean hydrographs The bottom two figures display the variation of the Mean Relative Error (MRE) with percentiles of the peak flow and the values of the MRE at and above the 75, 50 and 25 percentiles of the peak flow in calibration (left) and verification (right)

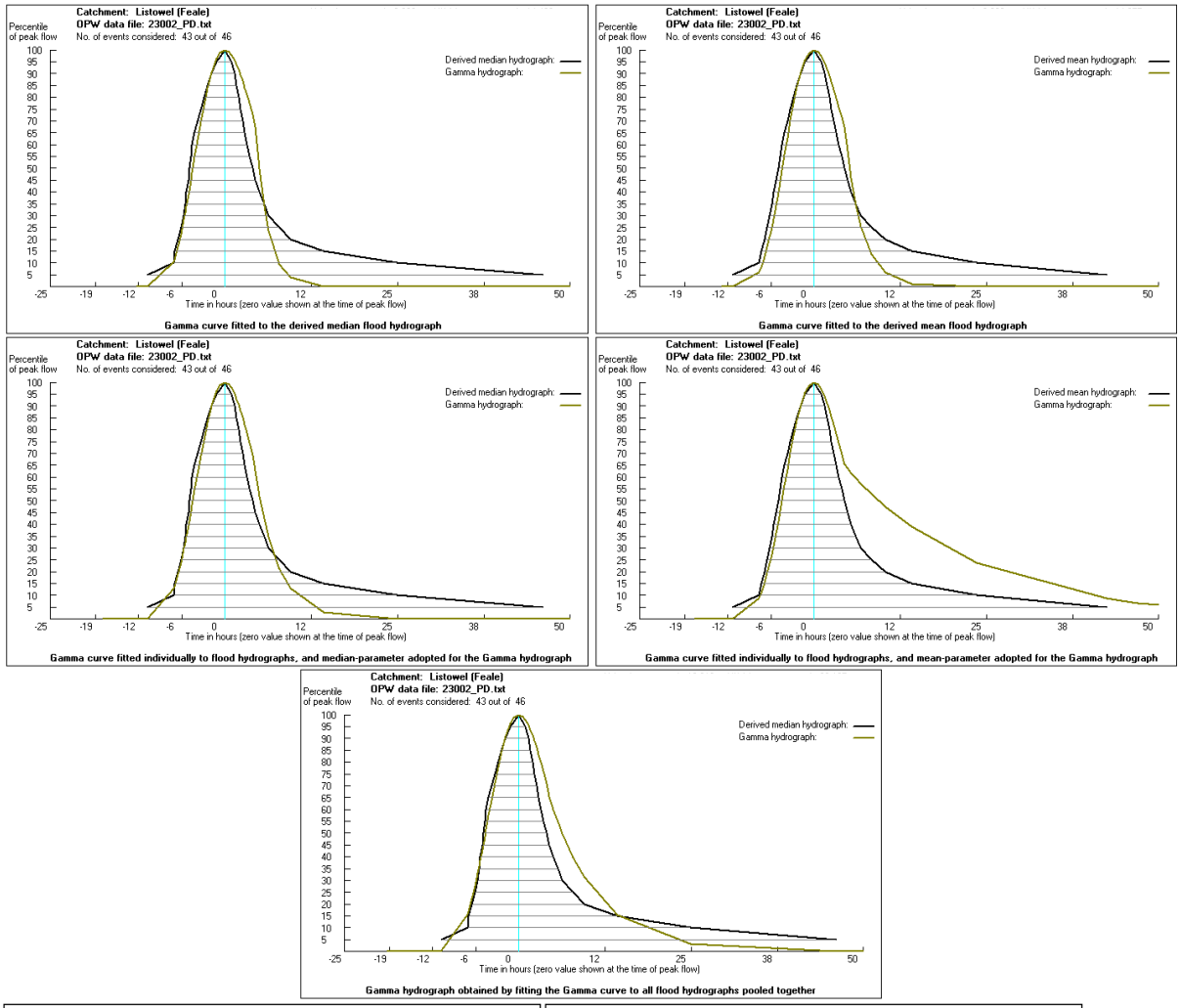

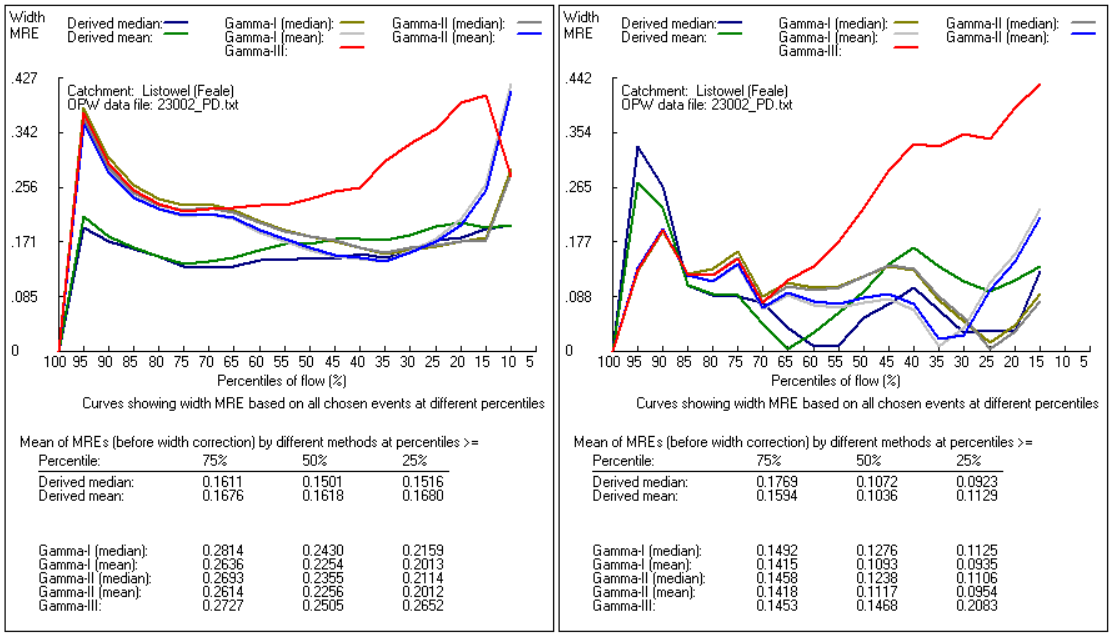

Fig. D.1.17 Calibration results for Station No. 23002 (post-drainage period)

Parametric hydrographs, i.e. the modified Gamma curve coupled with an exponential replacement recession curve, as calibrated for the five alternative methods, are shown in the top five figures together with the derived median and mean hydrographs The bottom two figures display the variation of the Mean Relative Error (MRE) with percentiles of the peak flow and the values of the MRE at and above the 75, 50 and 25 percentiles of the peak flow in calibration (left) and verification (right)

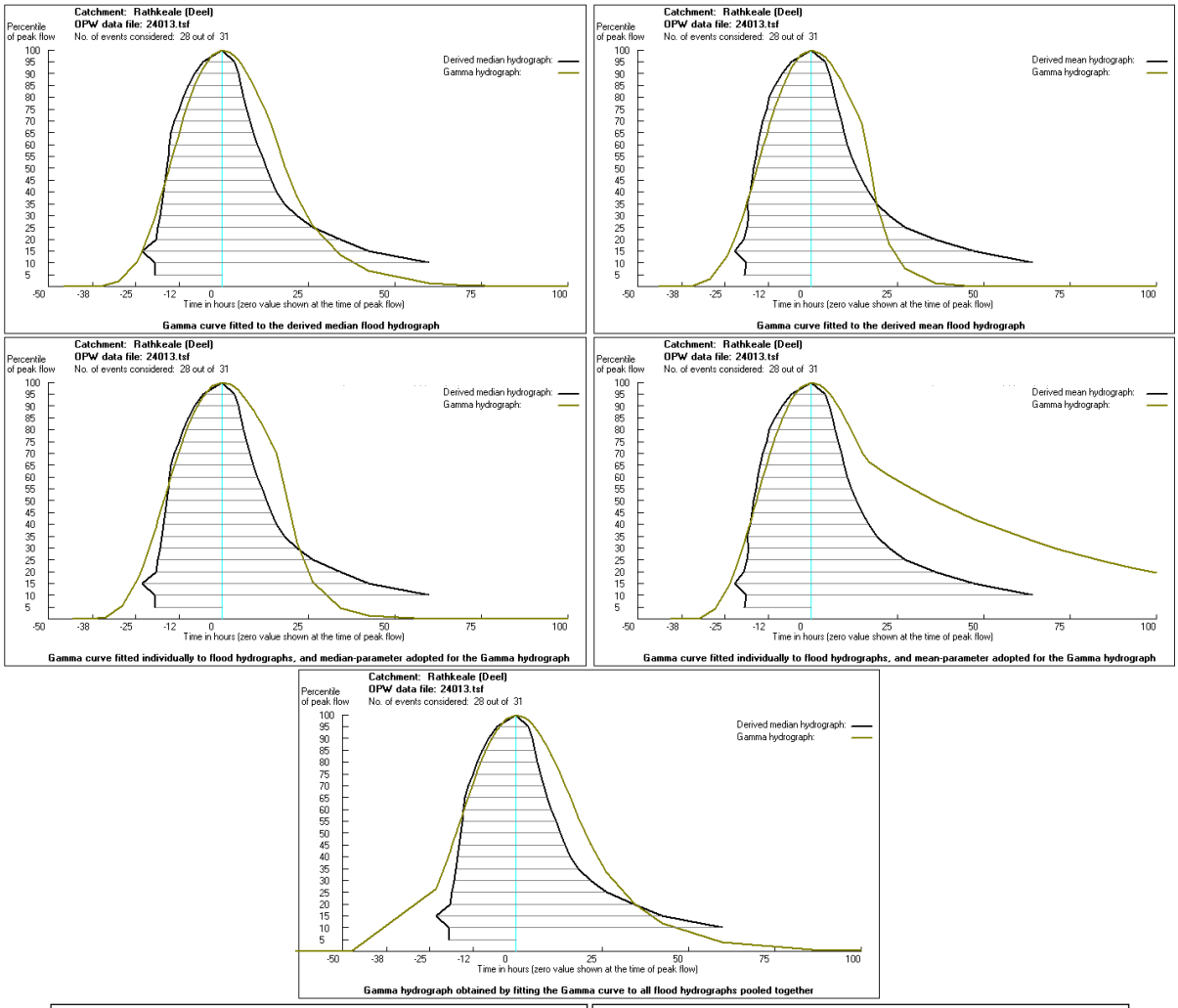

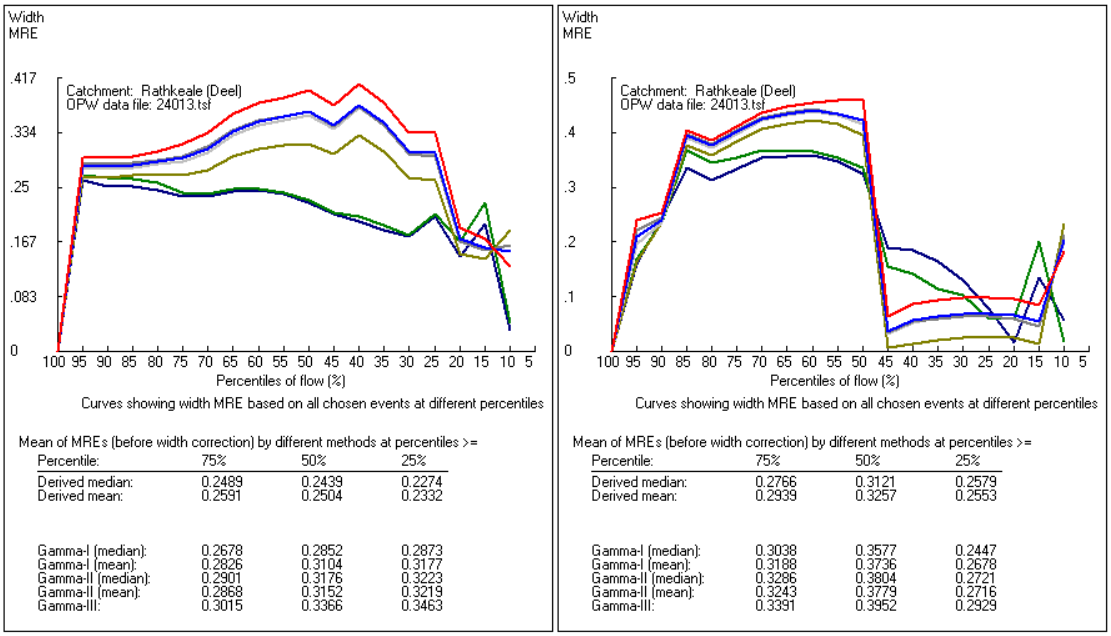

Fig. D.1.18 Calibration results for Station No. 24013

Parametric hydrographs, i.e. the modified Gamma curve coupled with an exponential replacement recession curve, as calibrated for the five alternative methods, are shown in the top five figures together with the derived median and mean hydrographs The bottom two figures display the variation of the Mean Relative Error (MRE) with percentiles of the peak flow and the values of the MRE at and above the 75, 50 and 25 percentiles of the peak flow in calibration (left) and verification (right)

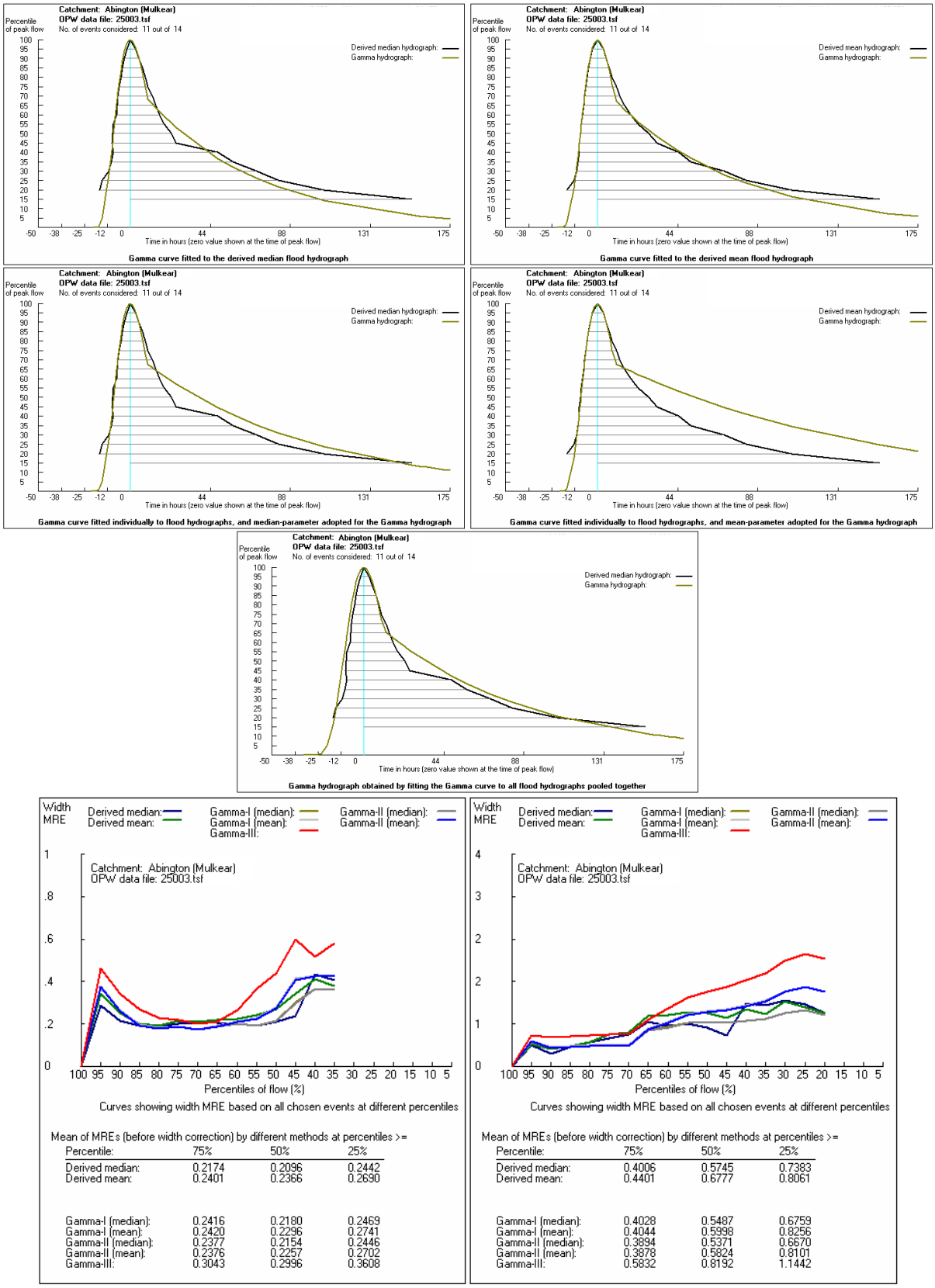

Fig. D.1.19 Calibration results for Station No. 25003

Parametric hydrographs, i.e. the modified Gamma curve coupled with an exponential replacement recession curve, as calibrated for the five alternative methods, are shown in the top five figures together with the derived median and mean hydrographs The bottom two figures display the variation of the Mean Relative Error (MRE) with percentiles of the peak flow and the values of the MRE at and above the 75, 50 and 25 percentiles of the peak flow in calibration (left) and verification (right)

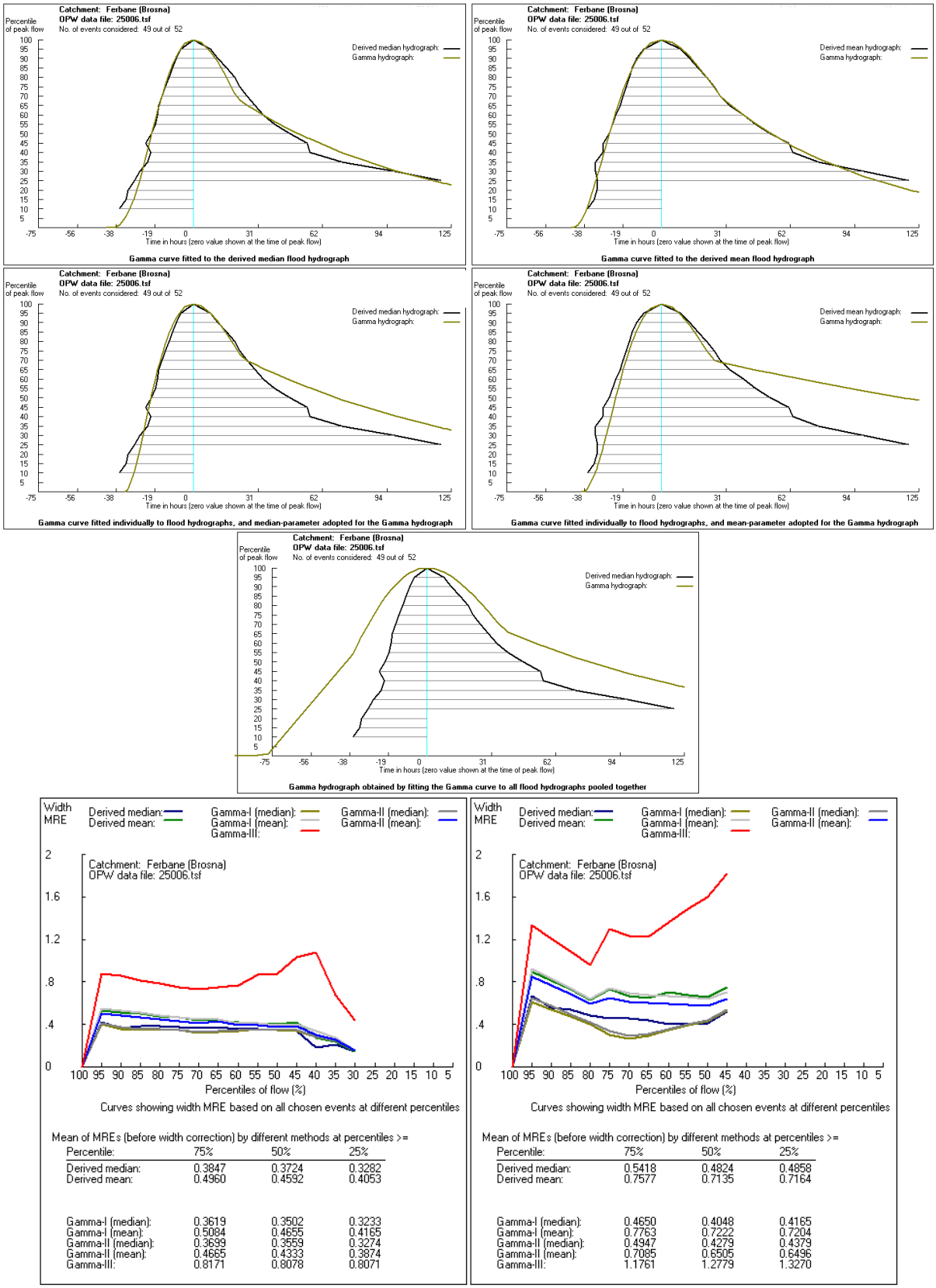

Fig. D.1.20 Calibration results for Station No. 25006

Parametric hydrographs, i.e. the modified Gamma curve coupled with an exponential replacement recession curve, as calibrated for the five alternative methods, are shown in the top five figures together with the derived median and mean hydrographs The bottom two figures display the variation of the Mean Relative Error (MRE) with percentiles of the peak flow and the values of the MRE at and above the 75, 50 and 25 percentiles of the peak flow in calibration (left) and verification (right)

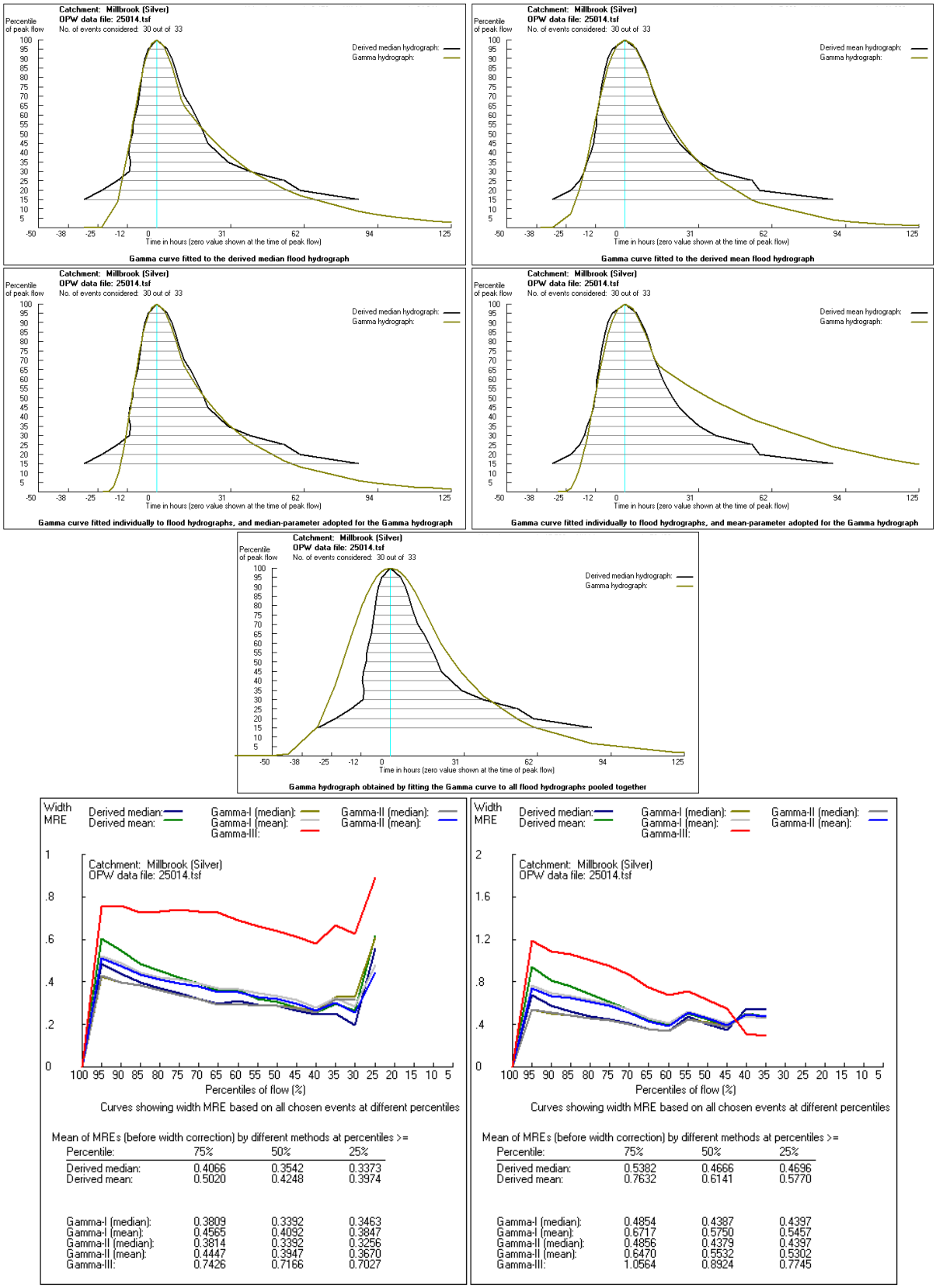

Fig. D.1.21 Calibration results for Station No. 25014

Parametric hydrographs, i.e. the modified Gamma curve coupled with an exponential replacement recession curve, as calibrated for the five alternative methods, are shown in the top five figures together with the derived median and mean hydrographs The bottom two figures display the variation of the Mean Relative Error (MRE) with percentiles of the peak flow and the values of the MRE at and above the 75, 50 and 25 percentiles of the peak flow in calibration (left) and verification (right)

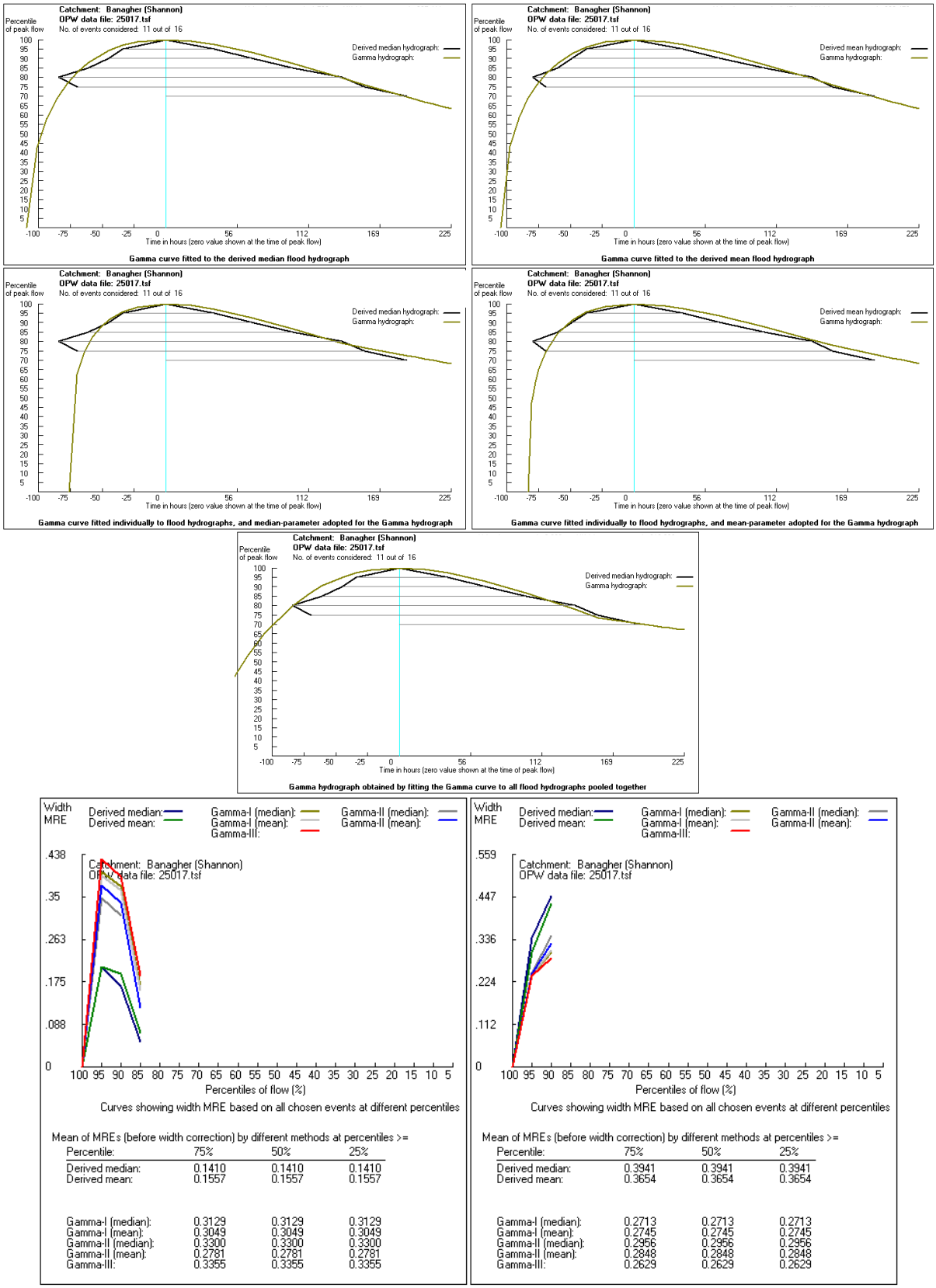

Fig. D.1.22 Calibration results for Station No. 25017

Parametric hydrographs, i.e. the modified Gamma curve coupled with an exponential replacement recession curve, as calibrated for the five alternative methods, are shown in the top five figures together with the derived median and mean hydrographs The bottom two figures display the variation of the Mean Relative Error (MRE) with percentiles of the peak flow and the values of the MRE at and above the 75, 50 and 25 percentiles of the peak flow in calibration (left) and verification (right)

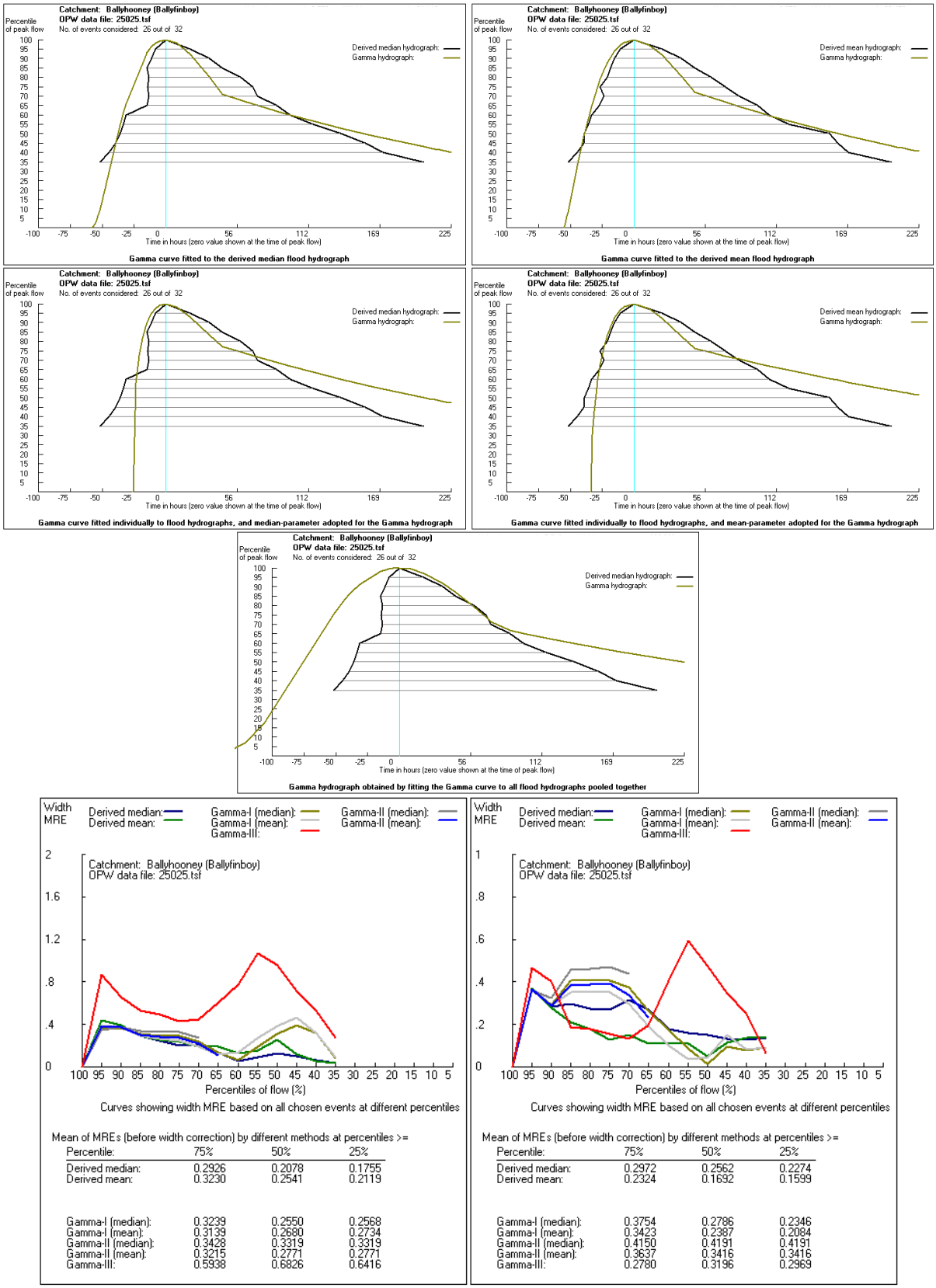

Fig. D.1.23 Calibration results for Station No. 25025

Parametric hydrographs, i.e. the modified Gamma curve coupled with an exponential replacement recession curve, as calibrated for the five alternative methods, are shown in the top five figures together with the derived median and mean hydrographs The bottom two figures display the variation of the Mean Relative Error (MRE) with percentiles of the peak flow and the values of the MRE at and above the 75, 50 and 25 percentiles of the peak flow in calibration (left) and verification (right)

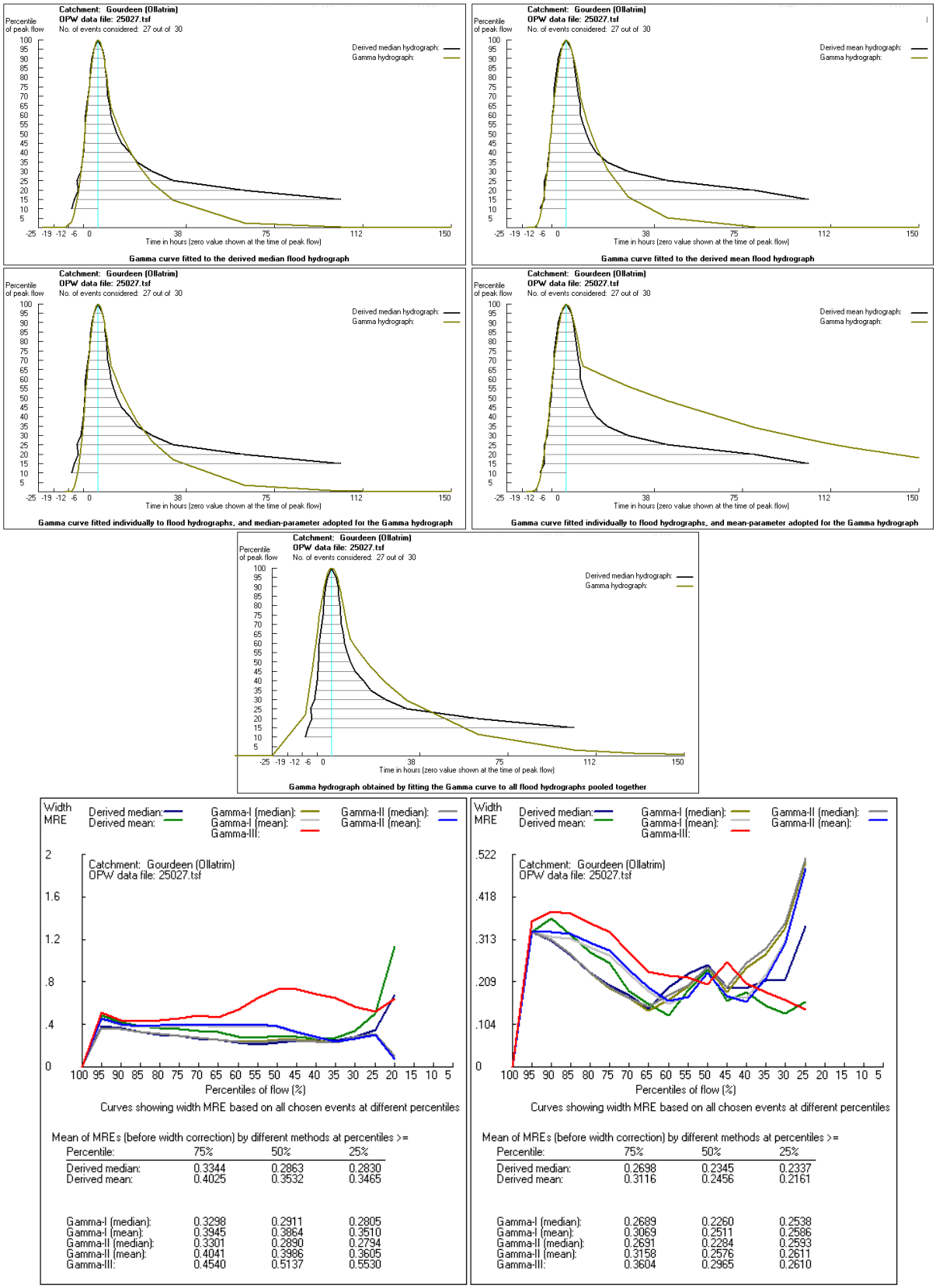

Fig. D.1.24 Calibration results for Station No. 25027

Parametric hydrographs, i.e. the modified Gamma curve coupled with an exponential replacement recession curve, as calibrated for the five alternative methods, are shown in the top five figures together with the derived median and mean hydrographs The bottom two figures display the variation of the Mean Relative Error (MRE) with percentiles of the peak flow and the values of the MRE at and above the 75, 50 and 25 percentiles of the peak flow in calibration (left) and verification (right)

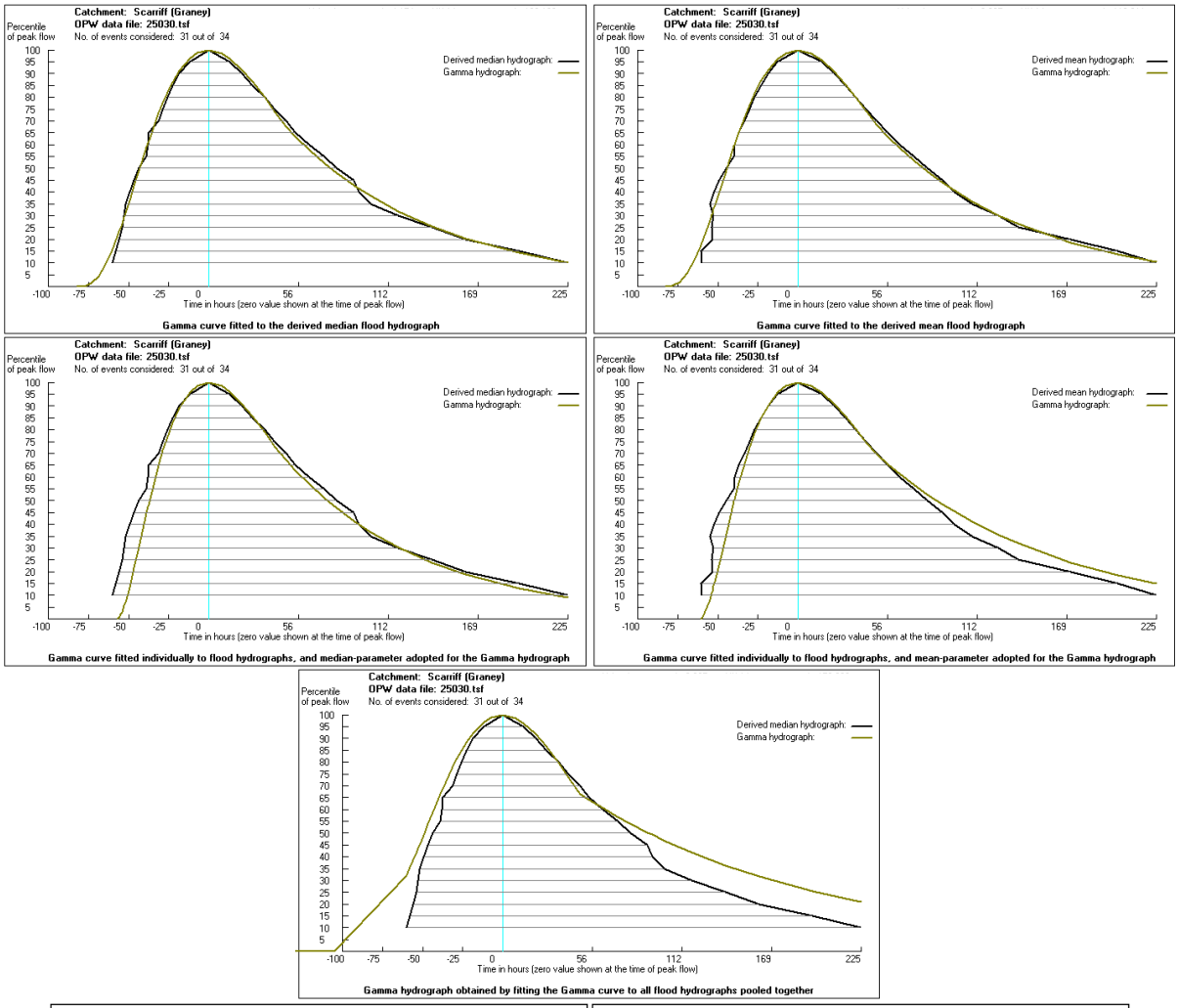

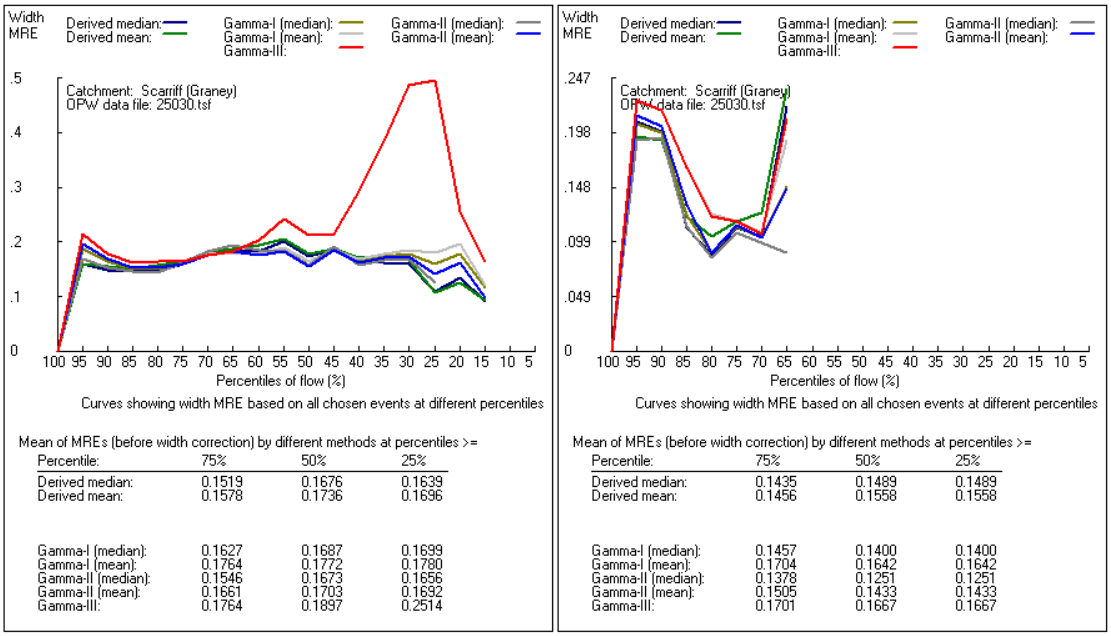

Percentile:	75%	50%	25%
Derived median:	0.1519	0.1676	0.1639
Derived mean:	0.1578	0.1736	0.1696
Gamma-I (median):	0.1627	0.1687	0.1699
Gamma-I (mean):	0.1764	0.1772	0.1780
Gamma-II (median):	0.1546	0.1673	0.1656
Gamma-II (mean):	0.1661	0.1703	0.1692
Gamma-III:	0.1764	0.1897	0.2514

Percentile:	75%	50%	25%
Derived median:	0.1435	0.1489	0.1489
Derived mean:	0.1456	0.1558	0.1558
Gamma-I (median):	0.1457	0.1400	0.1400
Gamma-I (mean):	0.1704	0.1642	0.1642
Gamma-II (median):	0.1378	0.1251	0.1251
Gamma-II (mean):	0.1505	0.1433	0.1433
Gamma-III:	0.1701	0.1667	0.1667

Fig. D.1.25 Calibration results for Station No. 25030

Parametric hydrographs, i.e. the modified Gamma curve coupled with an exponential replacement recession curve, as calibrated for the five alternative methods, are shown in the top five figures together with the derived median and mean hydrographs The bottom two figures display the variation of the Mean Relative Error (MRE) with percentiles of the peak flow and the values of the MRE at and above the 75, 50 and 25 percentiles of the peak flow in calibration (left) and verification (right)

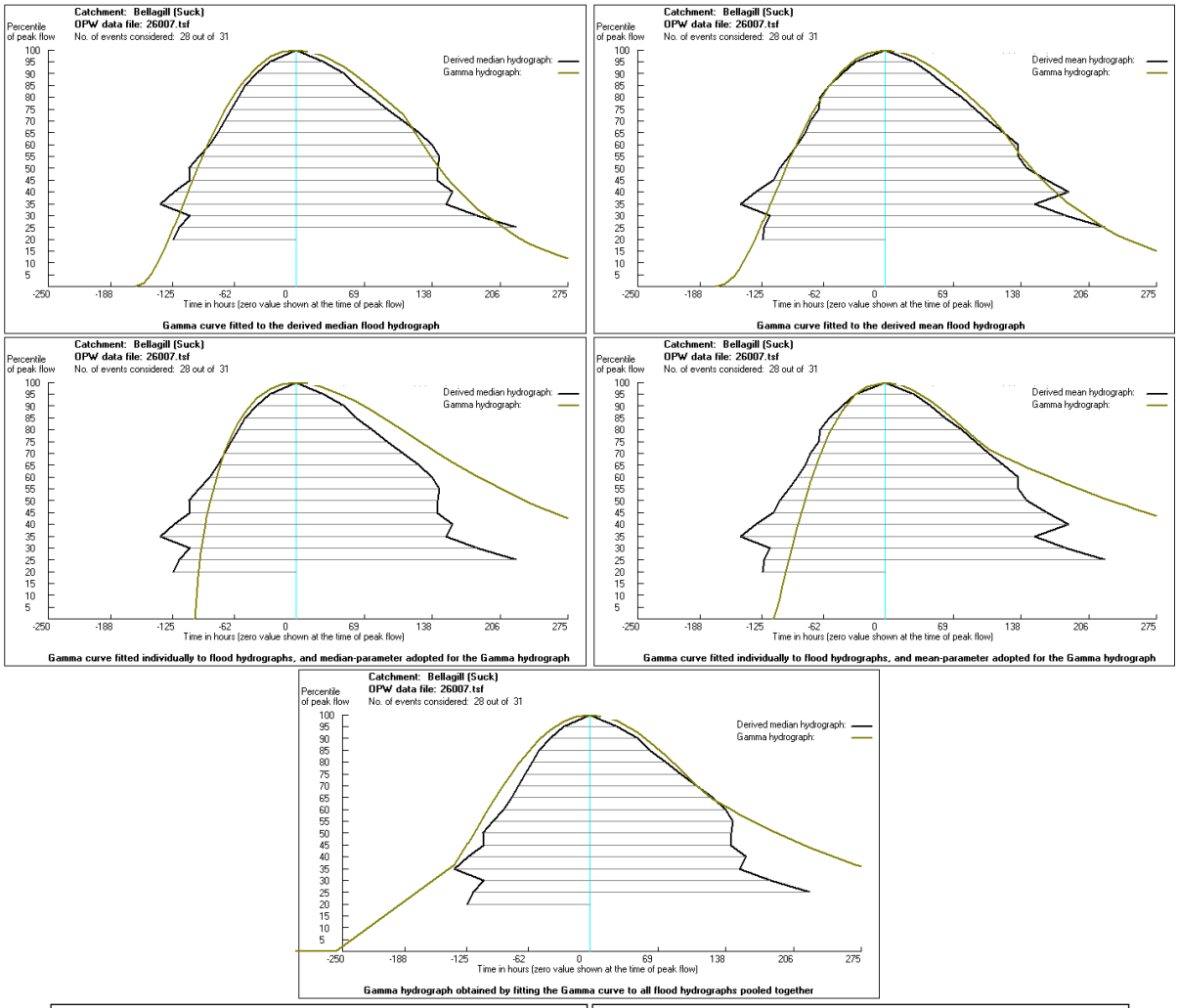

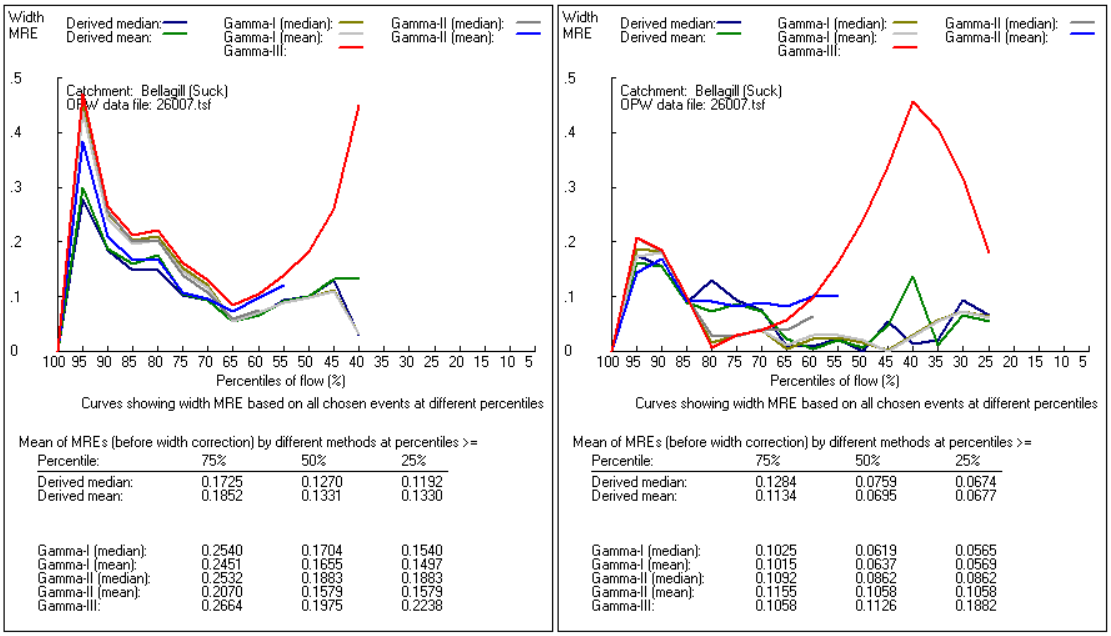

Fig. D.1.26 Calibration results for Station No. 26007

Parametric hydrographs, i.e. the modified Gamma curve coupled with an exponential replacement recession curve, as calibrated for the five alternative methods, are shown in the top five figures together with the derived median and mean hydrographs The bottom two figures display the variation of the Mean Relative Error (MRE) with percentiles of the peak flow and the values of the MRE at and above the 75, 50 and 25 percentiles of the peak flow in calibration (left) and verification (right)

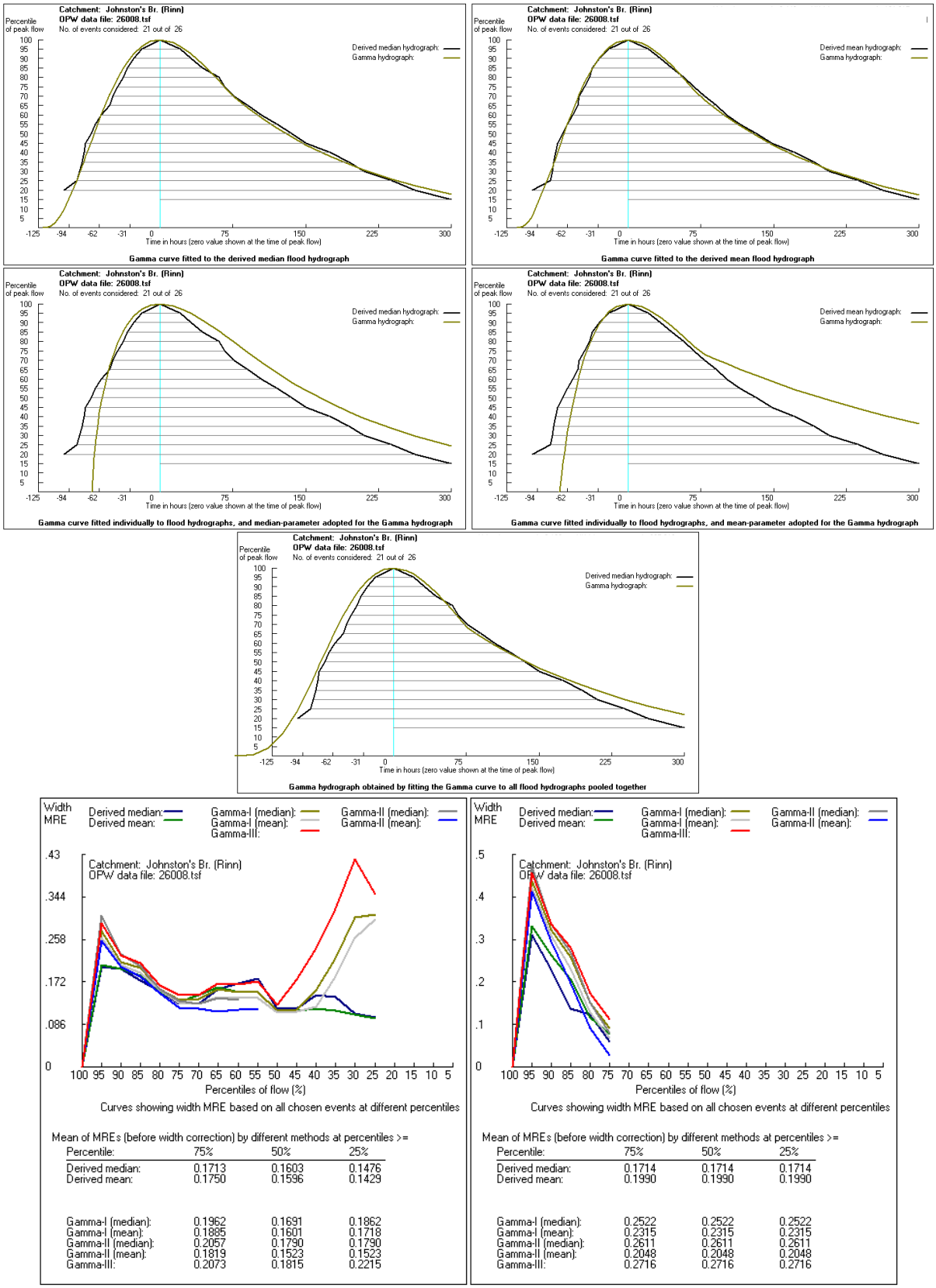

Fig. D.1.27 Calibration results for Station No. 26008

Parametric hydrographs, i.e. the modified Gamma curve coupled with an exponential replacement recession curve, as calibrated for the five alternative methods, are shown in the top five figures together with the derived median and mean hydrographs The bottom two figures display the variation of the Mean Relative Error (MRE) with percentiles of the peak flow and the values of the MRE at and above the 75, 50 and 25 percentiles of the peak flow in calibration (left) and verification (right)

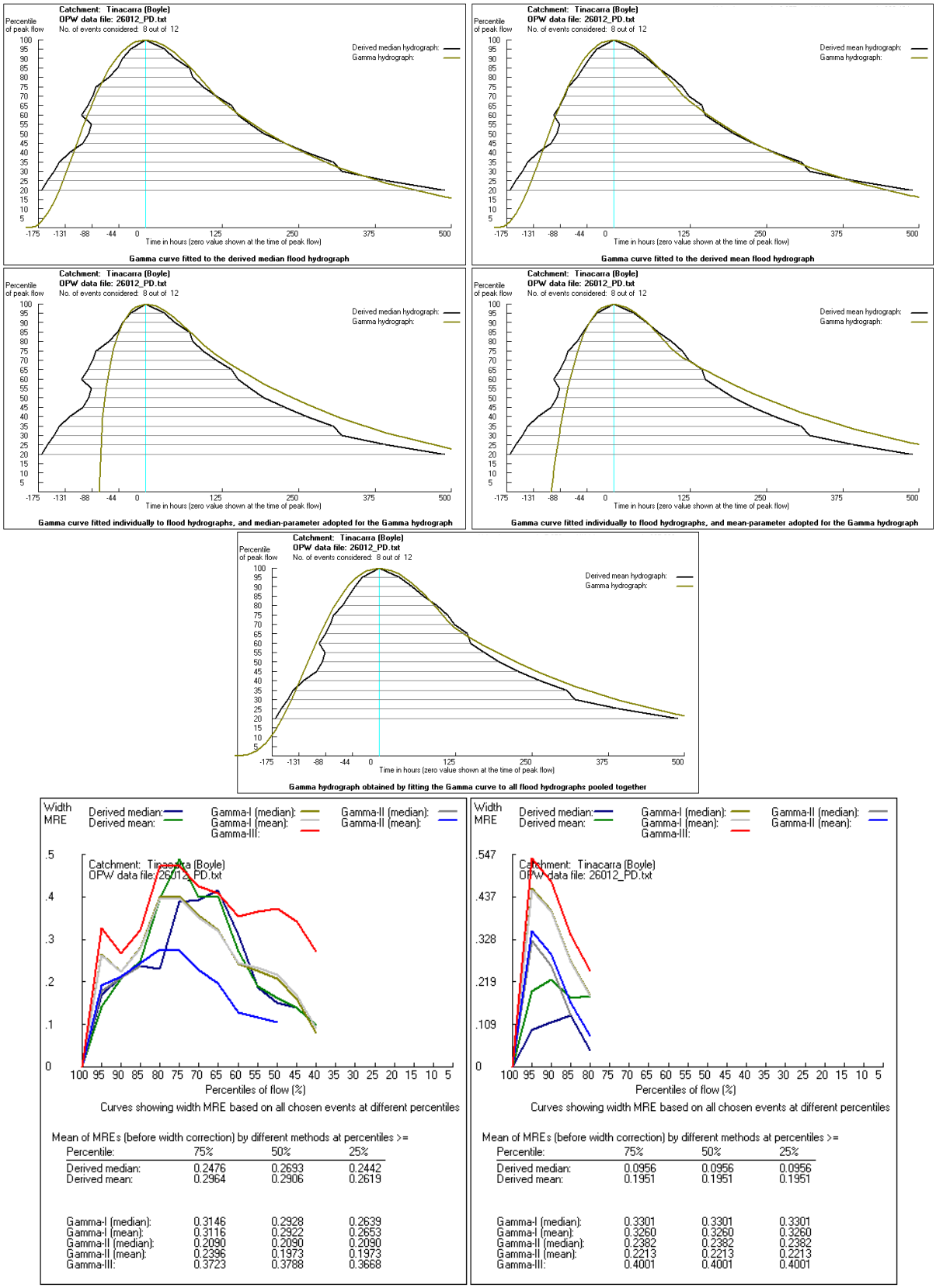

Fig. D.1.28 Calibration results for Station No. 26012 (post-drainage period)

Parametric hydrographs, i.e. the modified Gamma curve coupled with an exponential replacement recession curve, as calibrated for the five alternative methods, are shown in the top five figures together with the derived median and mean hydrographs The bottom two figures display the variation of the Mean Relative Error (MRE) with percentiles of the peak flow and the values of the MRE at and above the 75, 50 and 25 percentiles of the peak flow in calibration (left) and verification (right)

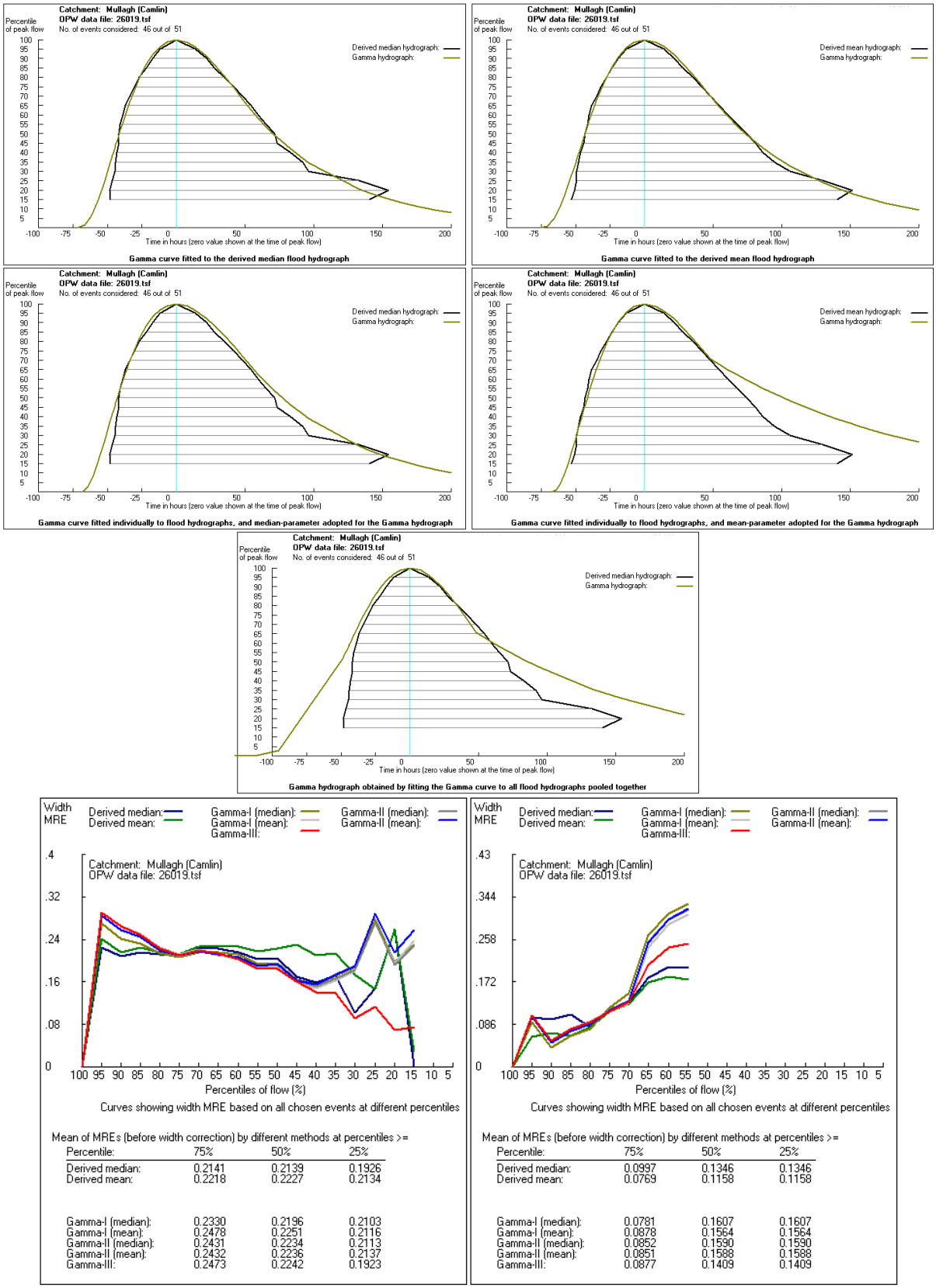

Fig. D.1.29 Calibration results for Station No. 26019

Parametric hydrographs, i.e. the modified Gamma curve coupled with an exponential replacement recession curve, as calibrated for the five alternative methods, are shown in the top five figures together with the derived median and mean hydrographs The bottom two figures display the variation of the Mean Relative Error (MRE) with percentiles of the peak flow and the values of the MRE at and above the 75, 50 and 25 percentiles of the peak flow in calibration (left) and verification (right)

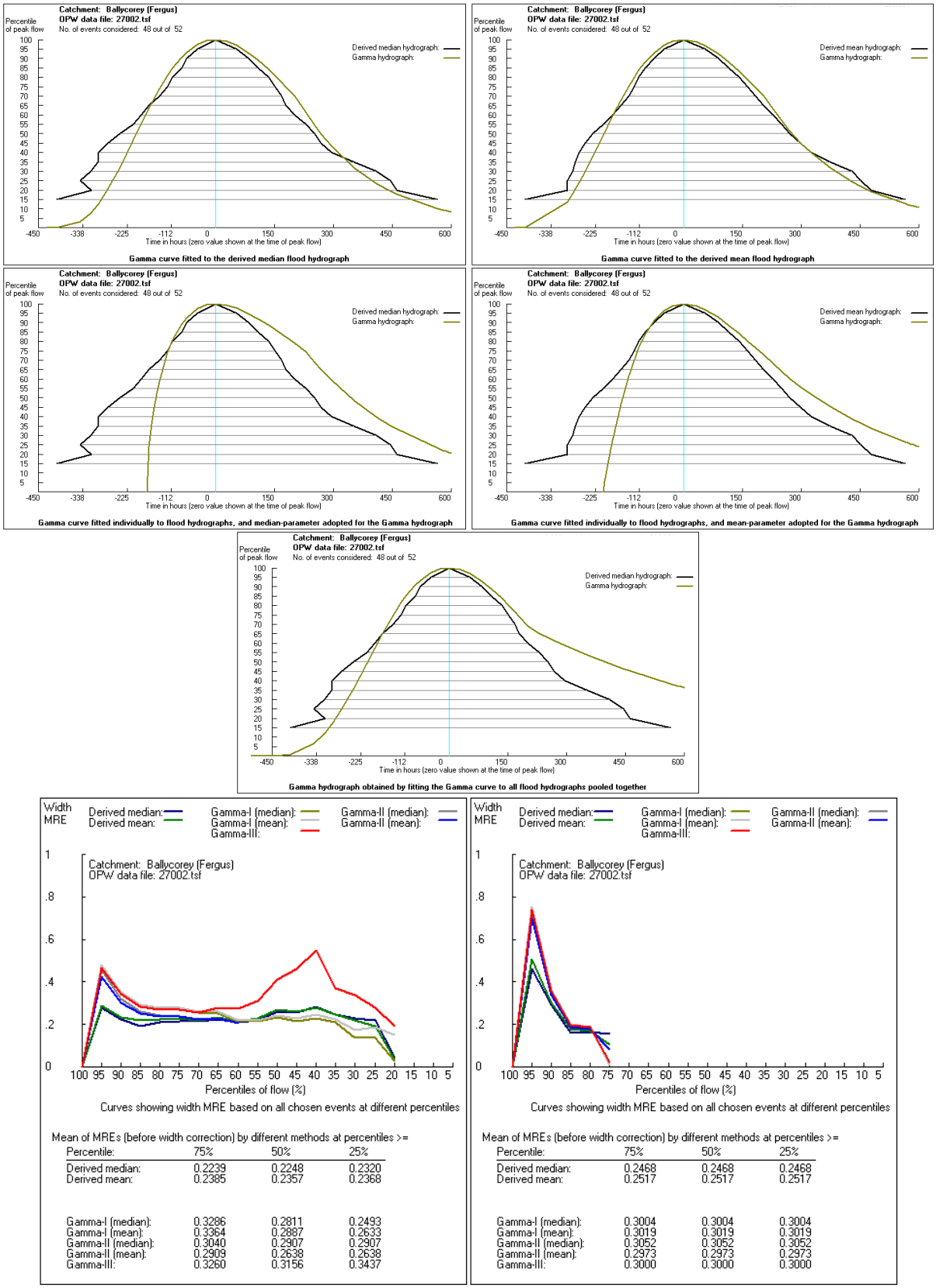

Fig. D.1.30 Calibration results for Station No. 27002

Parametric hydrographs, i.e. the modified Gamma curve coupled with an exponential replacement recession curve, as calibrated for the five alternative methods, are shown in the top five figures together with the derived median and mean hydrographs The bottom two figures display the variation of the Mean Relative Error (MRE) with percentiles of the peak flow and the values of the MRE at and above the 75, 50 and 25 percentiles of the peak flow in calibration (left) and verification (right)

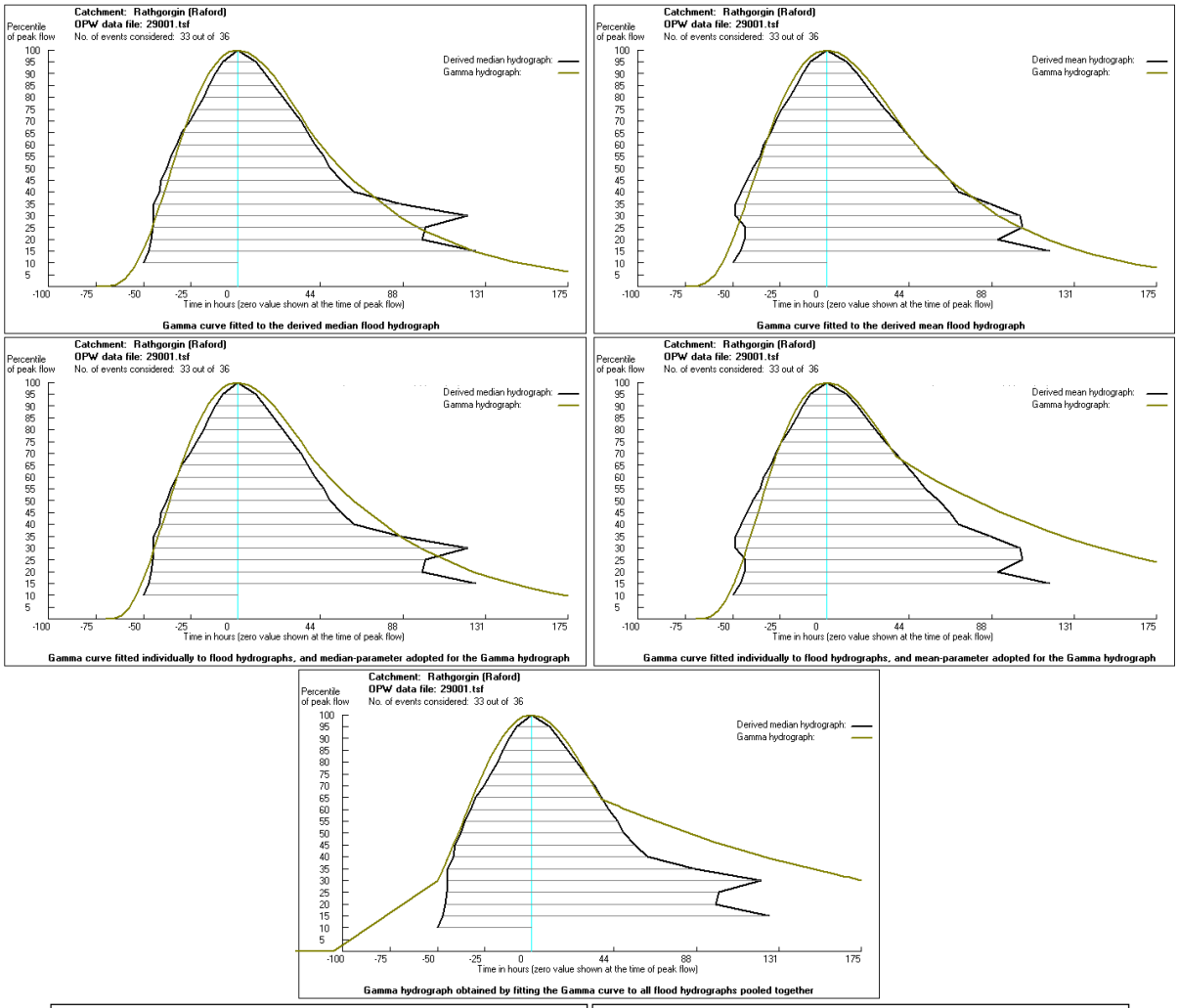

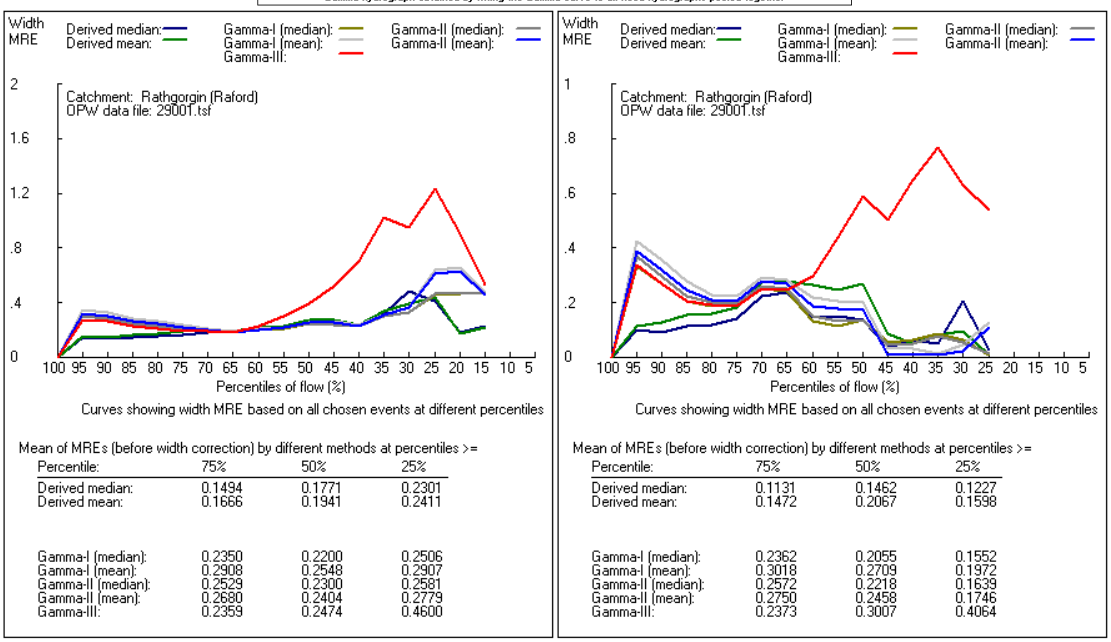

Fig. D.1.31 Calibration results for Station No. 29001

Parametric hydrographs, i.e. the modified Gamma curve coupled with an exponential replacement recession curve, as calibrated for the five alternative methods, are shown in the top five figures together with the derived median and mean hydrographs The bottom two figures display the variation of the Mean Relative Error (MRE) with percentiles of the peak flow and the values of the MRE at and above the 75, 50 and 25 percentiles of the peak flow in calibration (left) and verification (right)

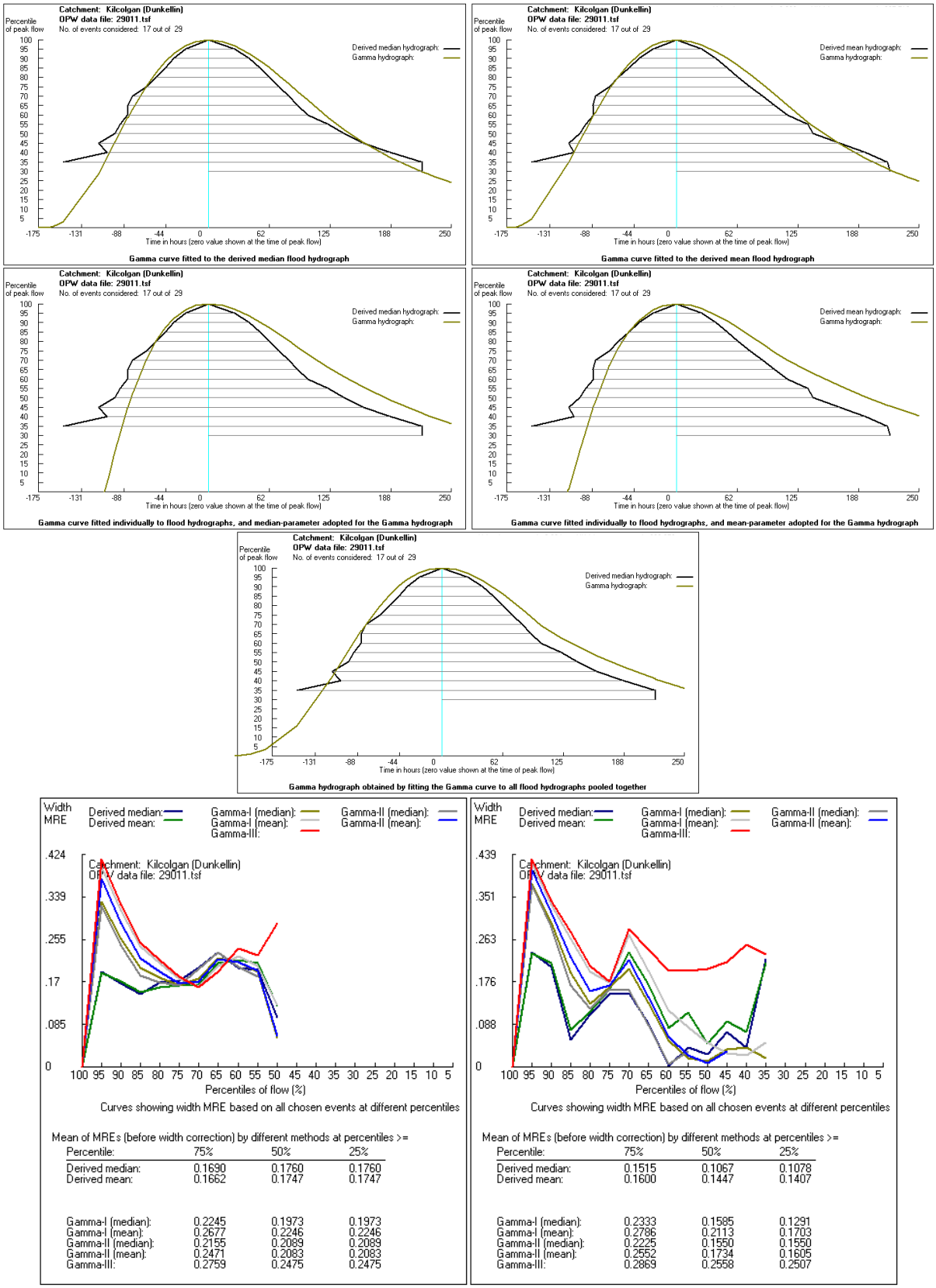

Fig. D.1.32 Calibration results for Station No. 29011

Parametric hydrographs, i.e. the modified Gamma curve coupled with an exponential replacement recession curve, as calibrated for the five alternative methods, are shown in the top five figures together with the derived median and mean hydrographs The bottom two figures display the variation of the Mean Relative Error (MRE) with percentiles of the peak flow and the values of the MRE at and above the 75, 50 and 25 percentiles of the peak flow in calibration (left) and verification (right)

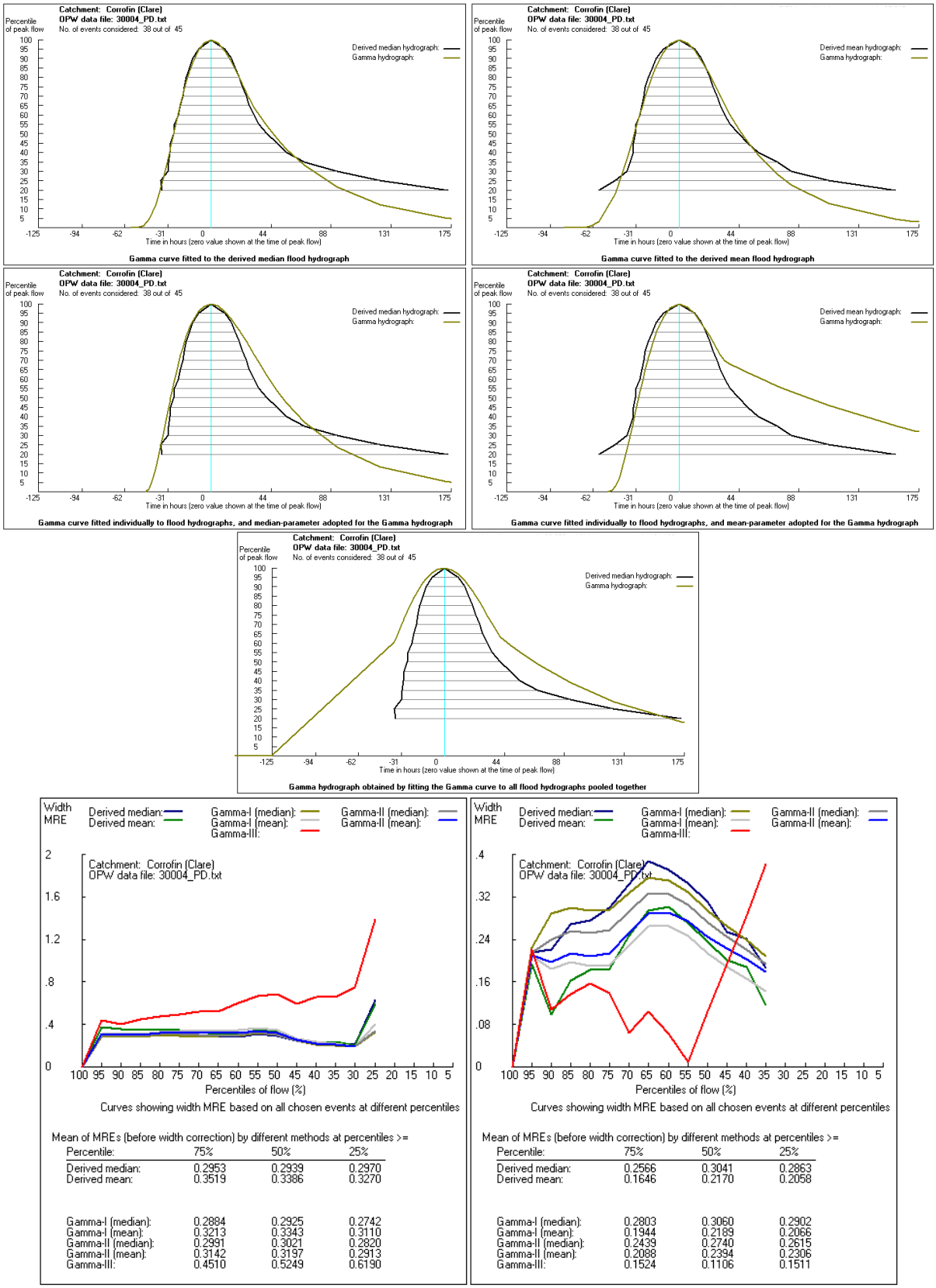

Fig. D.1.33 Calibration results for Station No. 30004 (post-drainage period)

Parametric hydrographs, i.e. the modified Gamma curve coupled with an exponential replacement recession curve, as calibrated for the five alternative methods, are shown in the top five figures together with the derived median and mean hydrographs The bottom two figures display the variation of the Mean Relative Error (MRE) with percentiles of the peak flow and the values of the MRE at and above the 75, 50 and 25 percentiles of the peak flow in calibration (left) and verification (right)

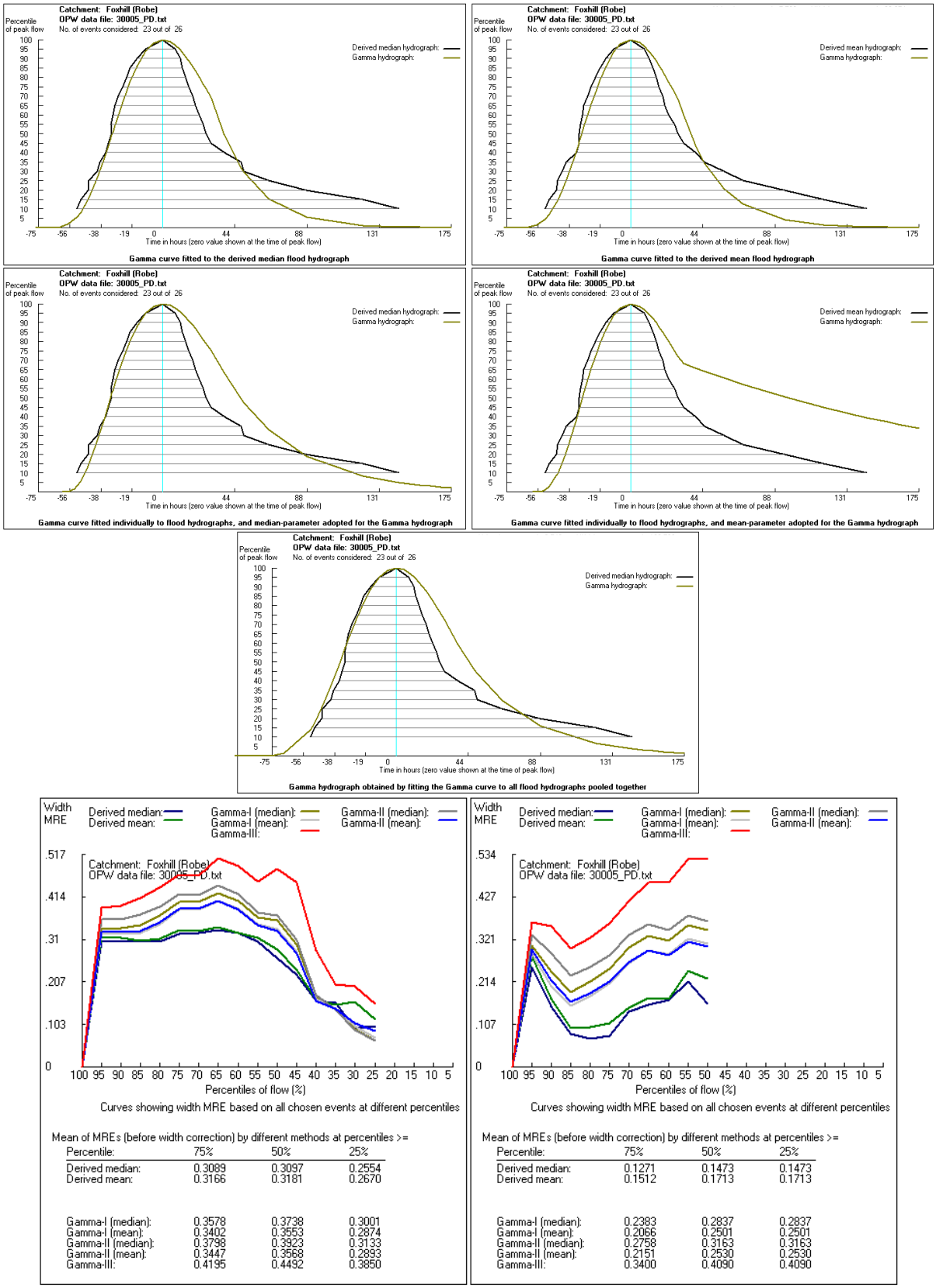

Fig. D.1.34 Calibration results for Station No. 30005 (post-drainage period)

Parametric hydrographs, i.e. the modified Gamma curve coupled with an exponential replacement recession curve, as calibrated for the five alternative methods, are shown in the top five figures together with the derived median and mean hydrographs The bottom two figures display the variation of the Mean Relative Error (MRE) with percentiles of the peak flow and the values of the MRE at and above the 75, 50 and 25 percentiles of the peak flow in calibration (left) and verification (right)

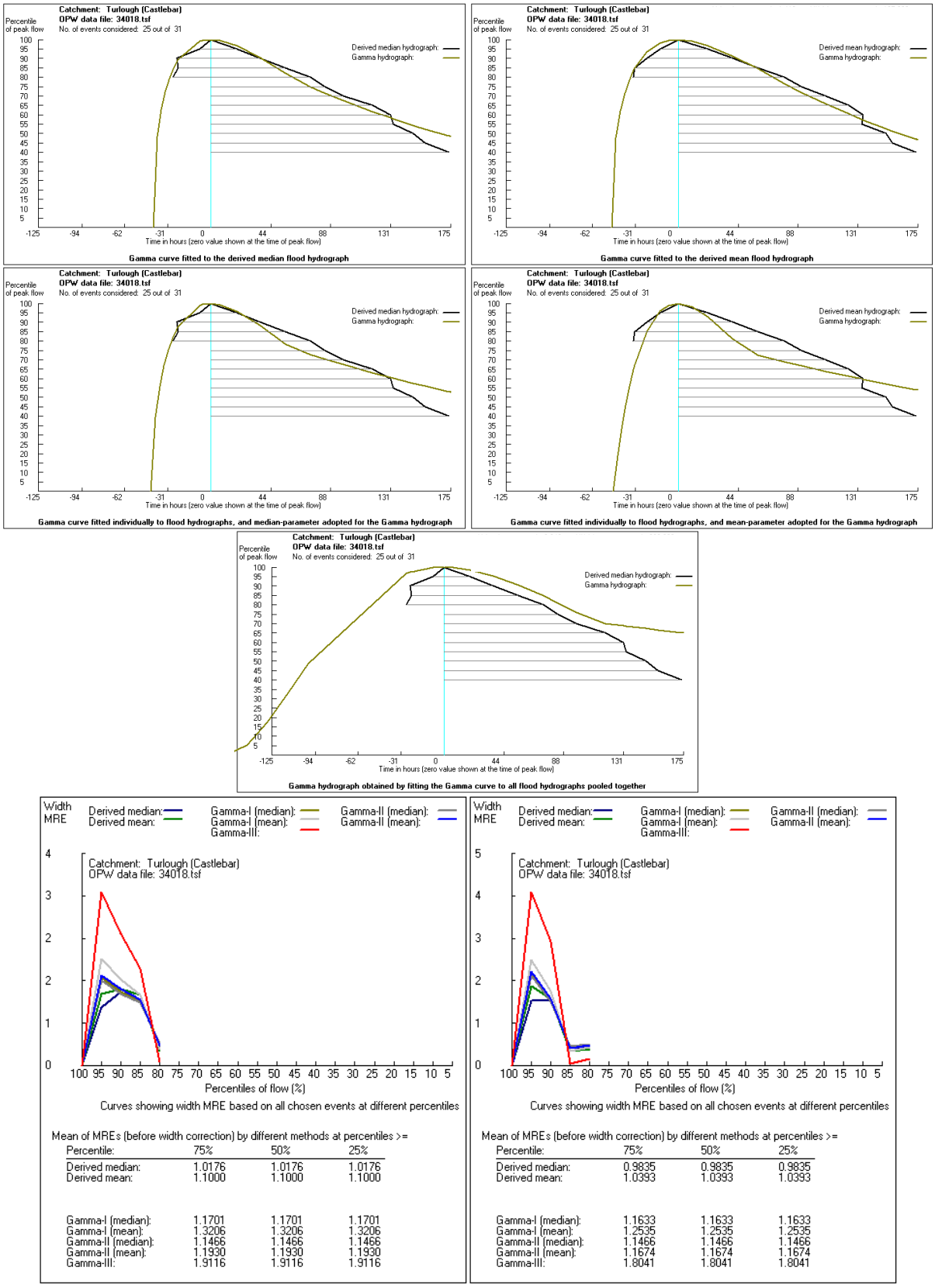

Fig. D.1.35 Calibration results for Station No. 34018

Parametric hydrographs, i.e. the modified Gamma curve coupled with an exponential replacement recession curve, as calibrated for the five alternative methods, are shown in the top five figures together with the derived median and mean hydrographs The bottom two figures display the variation of the Mean Relative Error (MRE) with percentiles of the peak flow and the values of the MRE at and above the 75, 50 and 25 percentiles of the peak flow in calibration (left) and verification (right)

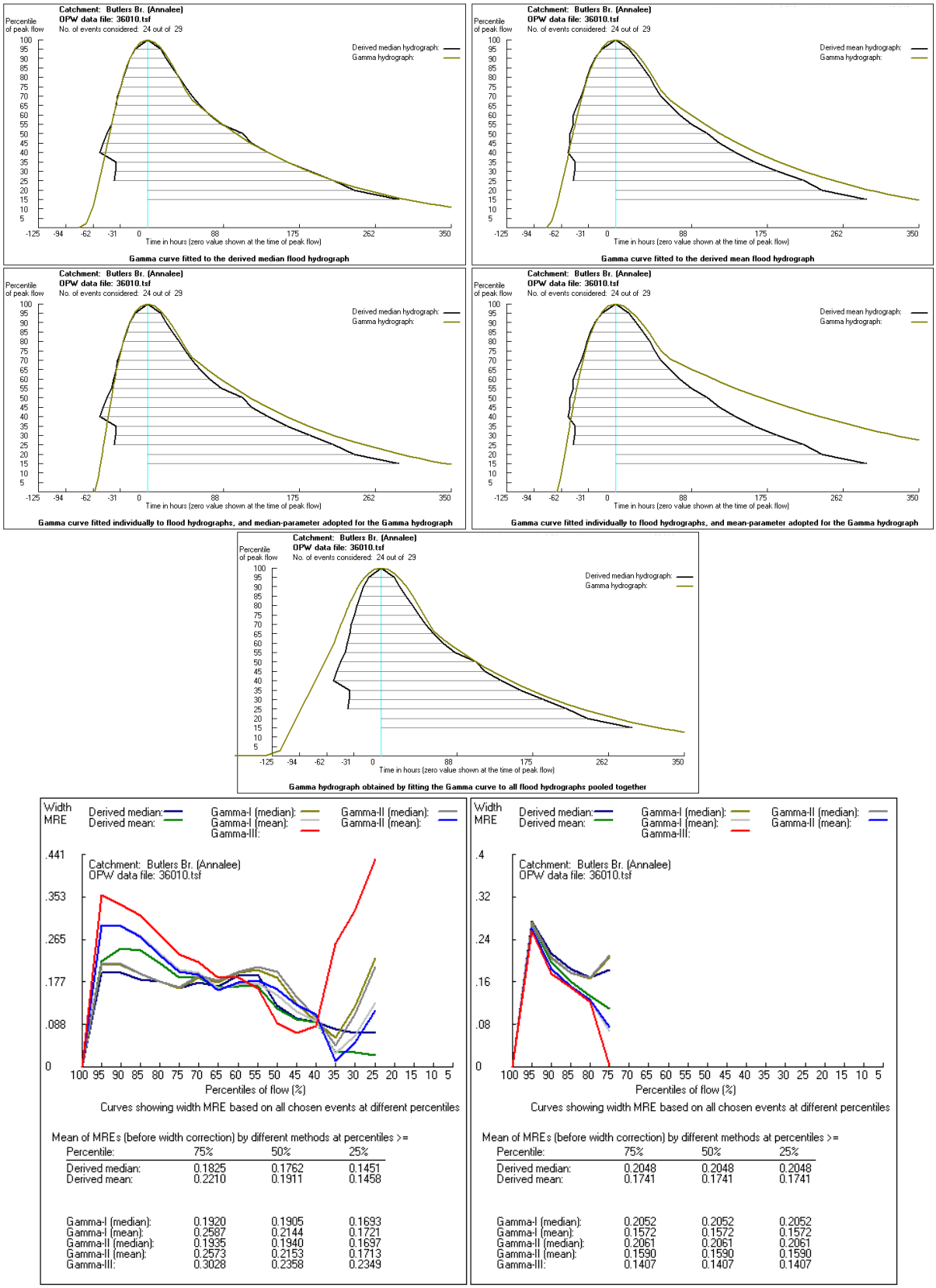

Fig. D.1.36 Calibration results for Station No. 36010

Parametric hydrographs, i.e. the modified Gamma curve coupled with an exponential replacement recession curve, as calibrated for the five alternative methods, are shown in the top five figures together with the derived median and mean hydrographs The bottom two figures display the variation of the Mean Relative Error (MRE) with percentiles of the peak flow and the values of the MRE at and above the 75, 50 and 25 percentiles of the peak flow in calibration (left) and verification (right)

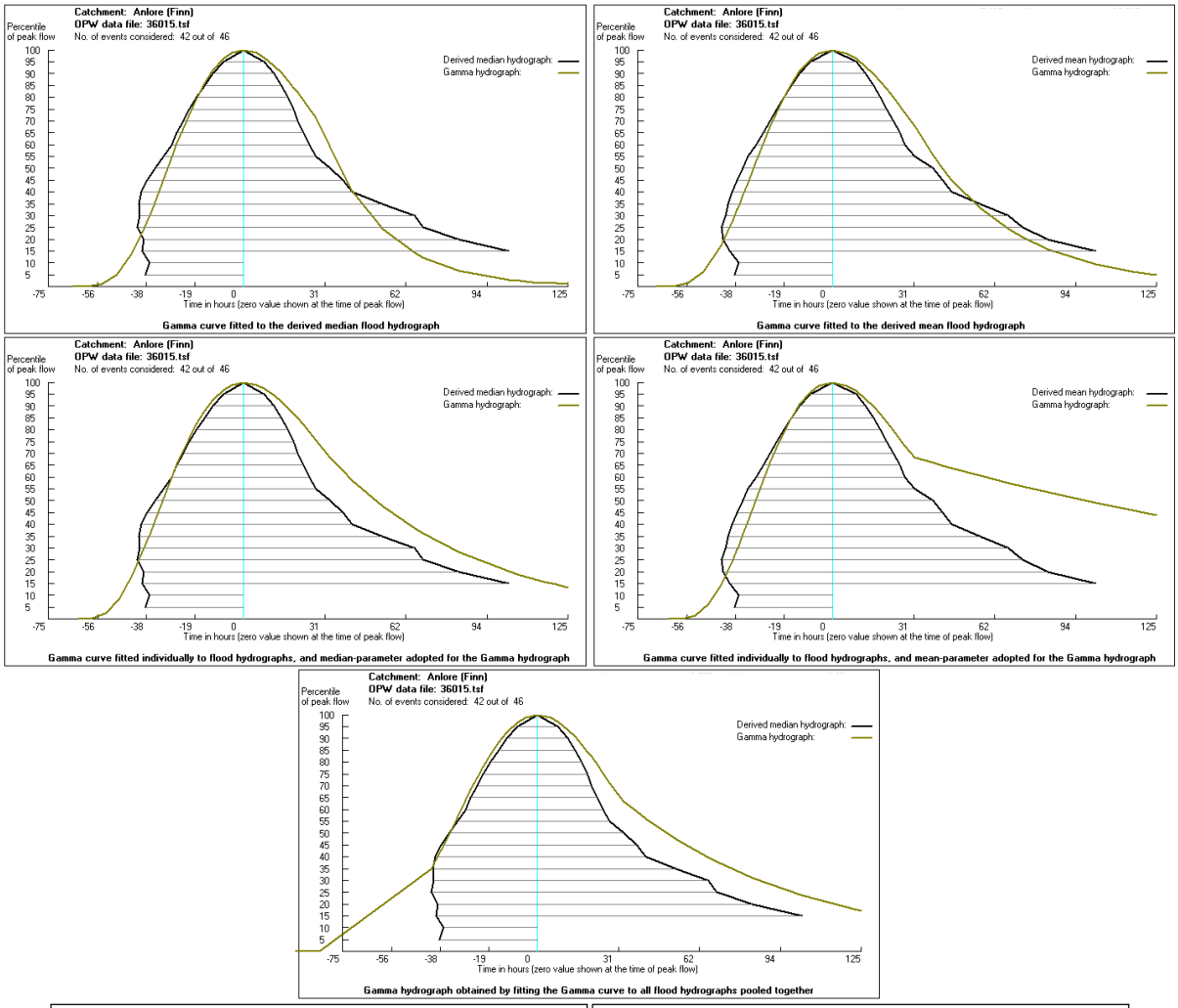

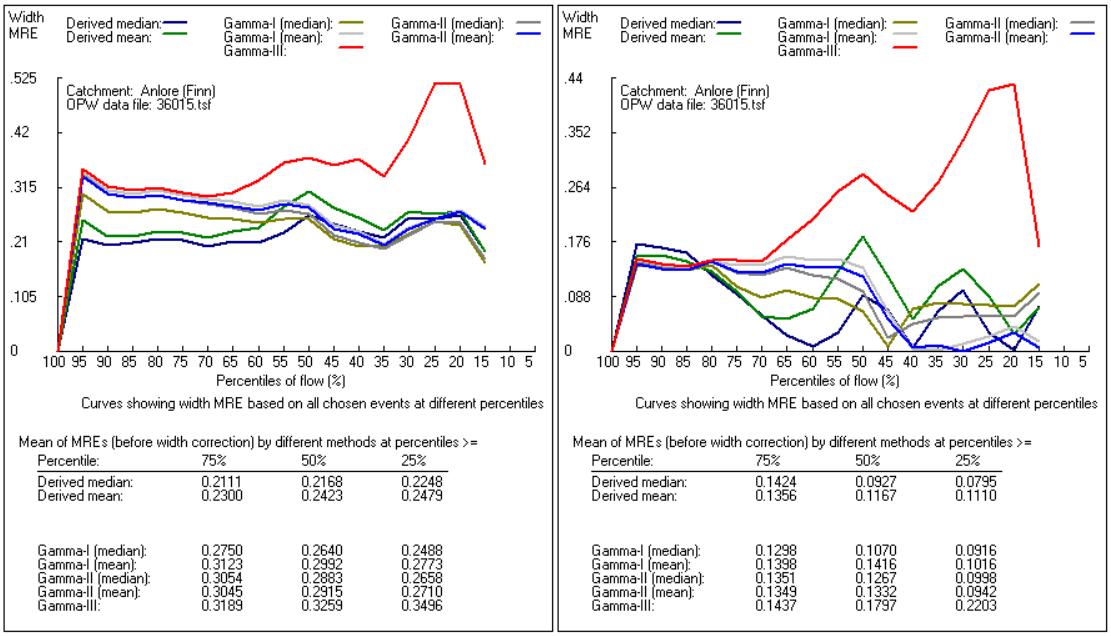

Fig. D.1.37 Calibration results for Station No. 36015

Parametric hydrographs, i.e. the modified Gamma curve coupled with an exponential replacement recession curve, as calibrated for the five alternative methods, are shown in the top five figures together with the derived median and mean hydrographs The bottom two figures display the variation of the Mean Relative Error (MRE) with percentiles of the peak flow and the values of the MRE at and above the 75, 50 and 25 percentiles of the peak flow in calibration (left) and verification (right)

Table D.1 Results of 'Hydrograph Width Analysis' in calibration and verification considering A1 category stations only

Station number	Total number of events selected (i.e., the number of the available AM events)	No. of the events chosen for verification	No. of the events rejected	Best method in calibration, evaluated by the mean of MRE of width for percentiles at and above 50		Best method in verification, evaluated by the mean of MRE of width for percentiles at and above 50		If MRE in verification is lower than that in calibration in the case of	
				Non-parametric	Parametric	Non-parametric	Parametric	Derived median	Gamma I median
6011	29	5,16,26	9,24(2)	Median	Gamma II median	Mean	Gamma II median	Yes	Yes
6012	32	5,16,27	---	Median	Gamma I median	Mean	Gamma III	Yes	Yes
6013	30	6,16,27	1,26(2)	Median	Gamma I median	Median	Gamma II median	Yes	Yes
6014	28	5,14,23	---	Median	Gamma II median	Median	Gamma II median	No	No
6026	29	5,15,24	---	Median	Gamma II median	Mean	Gamma III	Yes	No
7007	25	4,13,21	---	Median	Gamma I median	Mean	Gamma II mean	Yes	Yes
7009	30	5,15,24	---	Median	Gamma II mean	Median	Gamma III	Yes	Yes
7010	17	3,9,14	---	Median	Gamma I median	Mean	Gamma II mean	Yes	No
7012	20	3,10,17	---	Median	Gamma I median	Mean	Gamma III	No	No
9001	50	8,25,42	---	Median	Gamma I median	Median	Gamma I median	Yes	Yes
14004	29	5,15,24	---	Median	Gamma I median	Mean	Gamma III	No	No
14006	34	6,17,28	---	Median	Gamma I median	Mean	Gamma I mean	Yes	Yes
14007	22	4,11,18	---	Mean	Gamma II median	Mean	Gamma II median	Yes	Yes
14011	5	2,5,8	---	Median	Gamma I mean	Median	Gamma I mean	Yes	Yes
14018	34	6,16,28	---	Median	Gamma II mean	Median	Gamma I median	Yes	Yes

Table D.1 (contd…) Results of 'Hydrograph Width Analysis' in calibration and verification considering A1 category stations only

Station number	Total number of events selected (i.e., the number of the available AM events)	No. of the events chosen for verification	No. of the events rejected	Best method in calibration, evaluated by the mean of MRE of width for percentiles at and above 50		Best method in verification, evaluated by the mean of MRE of width for percentiles at and above 50		If MRE in verification is lower than that in calibration in the case of	
				Non-parametric	Parametric	Non-parametric	Parametric	Derived median	Gamma I median
15005	33	6,17,28	---	Median	Gamma I median	Median	Gamma I median	Yes	Yes
23002	46	8,23,38	---	Median	Gamma I mean	Mean	Gamma I mean	Yes	Yes
24013	31	5,16,26	---	Median	Gamma I median	Median	Gamma I median	No	No
25003	7	2, 7,12	---	Median	Gamma II median	Median	Gamma II median	No	No
25006	52	9,26,43	---	Median	Gamma I median	Median	Gamma I median	No	No
25014	33	6,17,28	---	Median	Gamma I median	Median	Gamma II median	No	No
25017	14	3,8,14	2,12(2)	Median	Gamma II mean	Mean	Gamma III	No	Yes
25025	31	5,17,28	14,18,31 (3)	Median	Gamma I median	Mean	Gamma I mean	Yes	Yes
25027	30	5,15,25	---	Median	Gamma I median	Median	Gamma I median	Yes	Yes
25030	34	6,17,28	---	Median	Gamma II median	Median	Gamma II median	Yes	Yes
26007	31	5,16,26	---	Median	Gamma II mean	Mean	Gamma I median	Yes	Yes
26008	24	4,13,22	7,10(2)	Mean	Gamma II mean	Median	Gamma II mean	No	No
26012	11	2,6,9	10(1)	Median	Gamma II mean	Median	Gamma II mean	Yes	No
26019	49	8,26,43	11,35 (2)	Median	Gamma I median	Mean	Gamma III	Yes	Yes

Table D.1 (contd…) Results of 'Hydrograph Width Analysis' in calibration and verification considering A1 category stations only

Station number	Total number of events selected (i.e., the number of the available AM events)	No. of the events chosen for verification	No. of the events rejected	Best method in calibration, evaluated by the mean of MRE of width for percentiles at and above 50		Best method in verification, evaluated by the mean of MRE of width for percentiles at and above 50		If MRE in verification is lower than that in calibration in the case of	
				Non-parametric	Parametric	Non-parametric	Parametric	Derived median	Gamma I median
27002	52	9,26,44	39(1)	Median	Gamma II mean	Median	Gamma II mean	No	No
29001	36	6,18,30	---	Median	Gamma I median	Median	Gamma I median	Yes	Yes
29011	20	6,14,26	3,4,5,13, 15, 16,17, 23,24 (9)	Mean	Gamma I median	Median	Gamma II median	Yes	Yes
30004	41	8,22,36	7,31, 37,40 (4)	Median	Gamma I median	Mean	Gamma III	No	No
30005	26	4,13,22	---	Median	Gamma I mean	Median	Gamma II mean	Yes	Yes
34018	28	5,16,26	9,10,24 (3)	Median	Gamma II median	Median	Gamma II median	Yes	Yes
36010	27	6,16,25	2,12(2)	Median	Gamma I median	Mean	Gamma III	No	No
36015	45	8,24,39	12(1)	Median	Gamma I median	Mean	Gamma I median	Yes	Yes

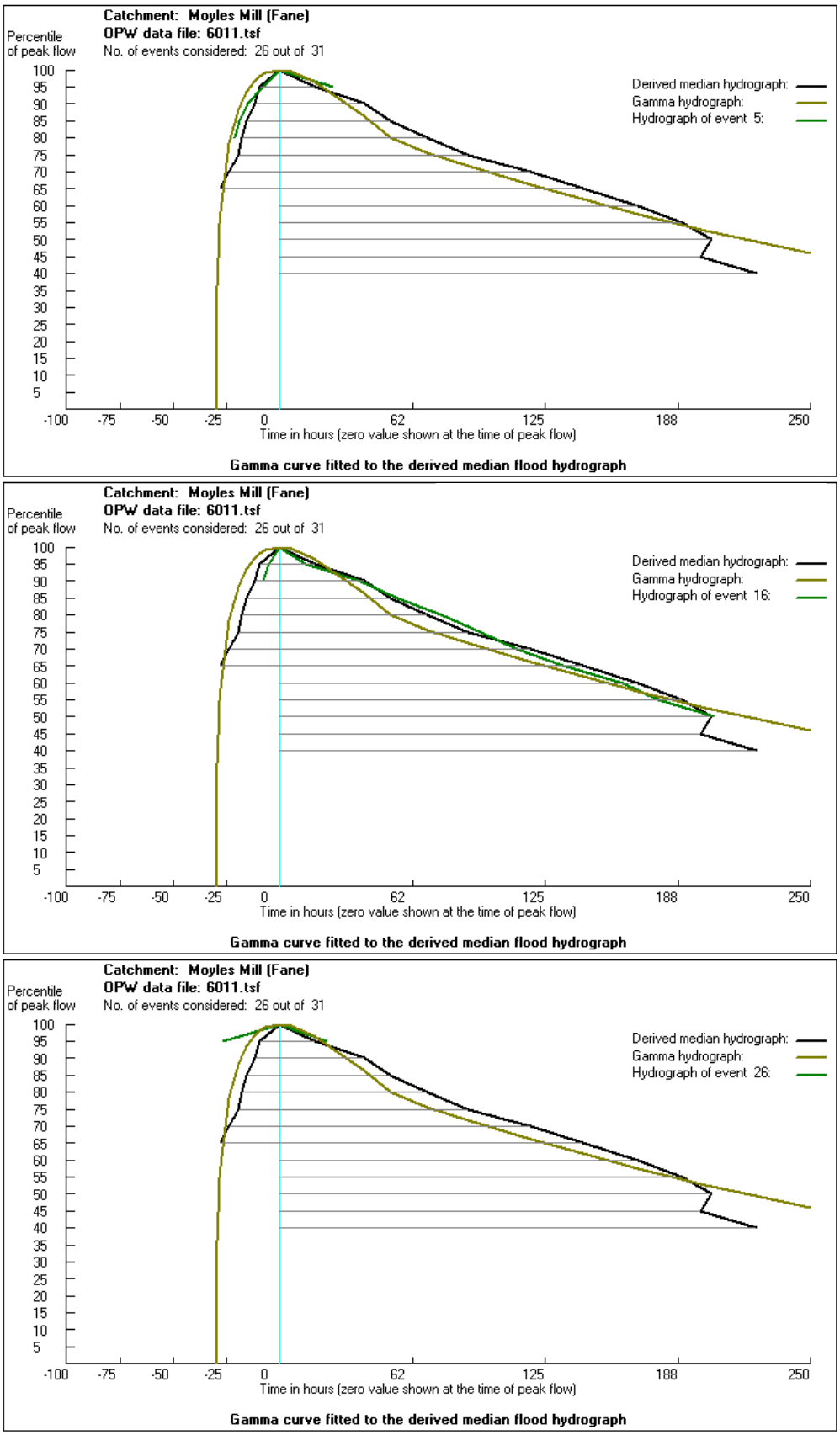

Fig. D.2.1 The derived median (best non-parametric) and Gamma-I median (best parametric) hydrographs, produced using the calibration events, shown superimposed on the observed flood hydrographs of the three verification events at Station No. 6011

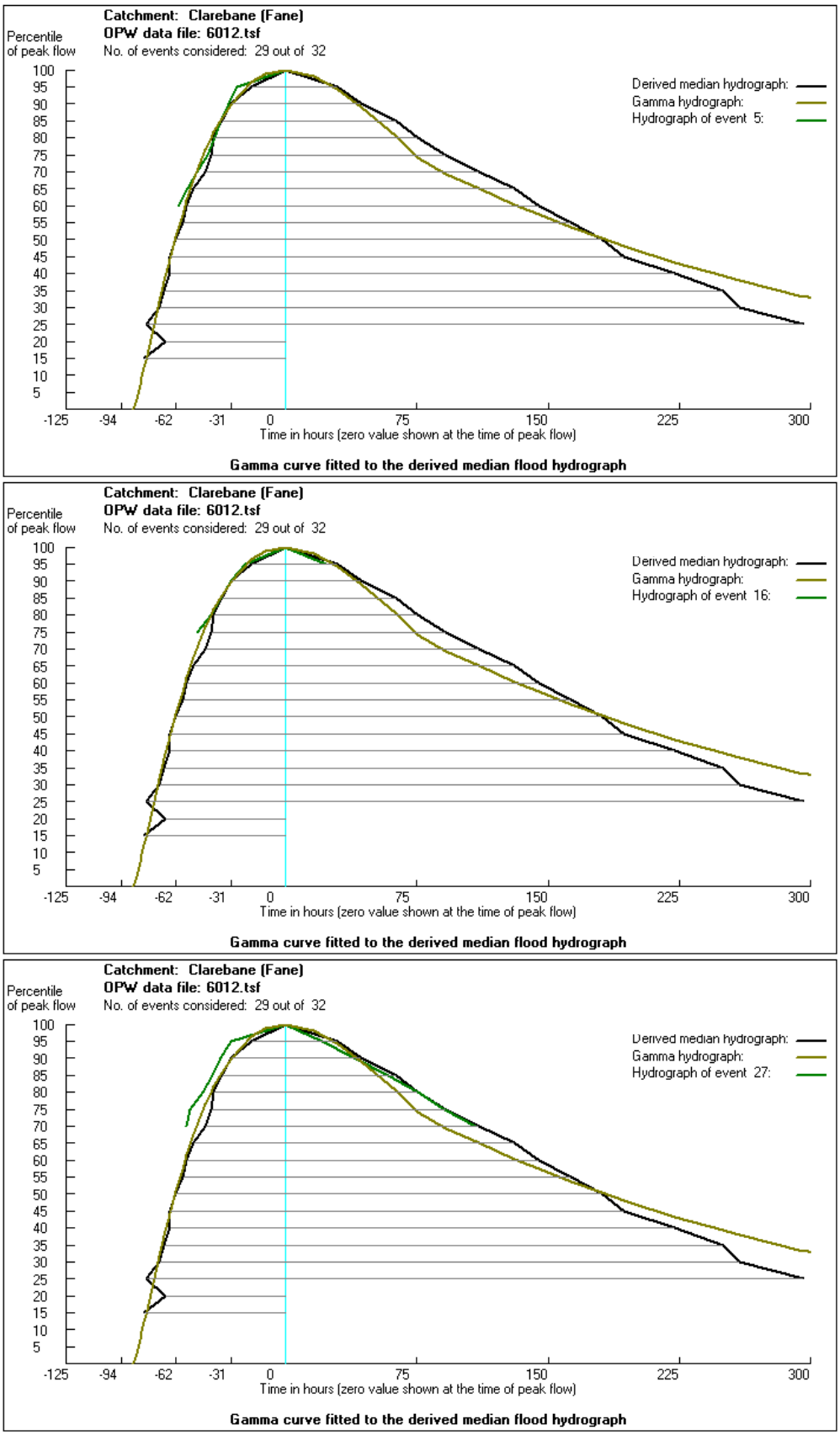

Fig. D.2.2 The derived median (best non-parametric) and Gamma-I median (best parametric) hydrographs, produced using the calibration events, shown superimposed on the observed flood hydrographs of the three verification events at Station No. 6012 (Clarebane on the Fane)

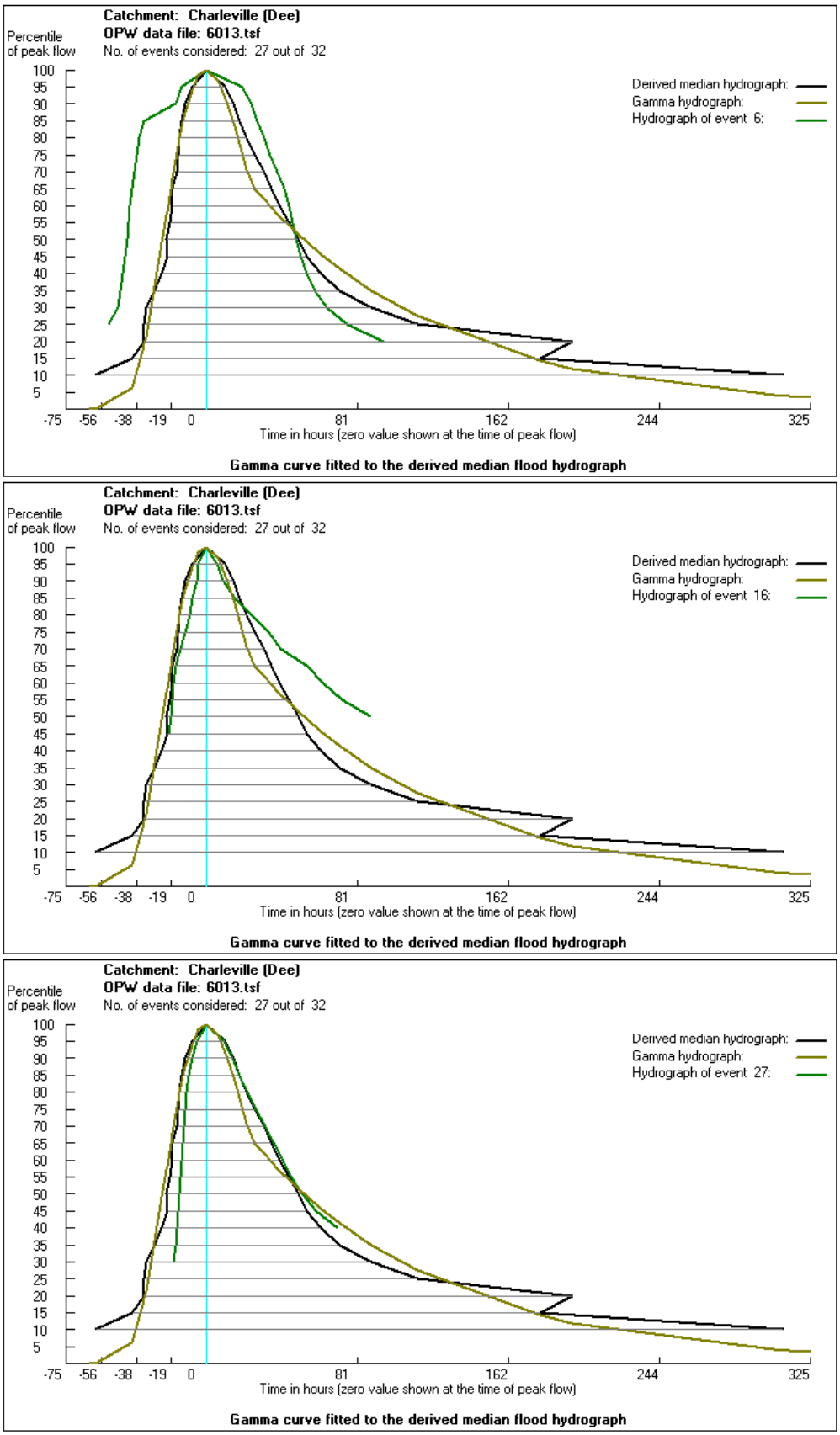

Fig. D.2.3 The derived median (best non-parametric) and Gamma-I median (best parametric) hydrographs, produced using the calibration events, shown superimposed on the observed flood hydrographs of the three verification events at Station No. 6013 (Charleville on the Dee)

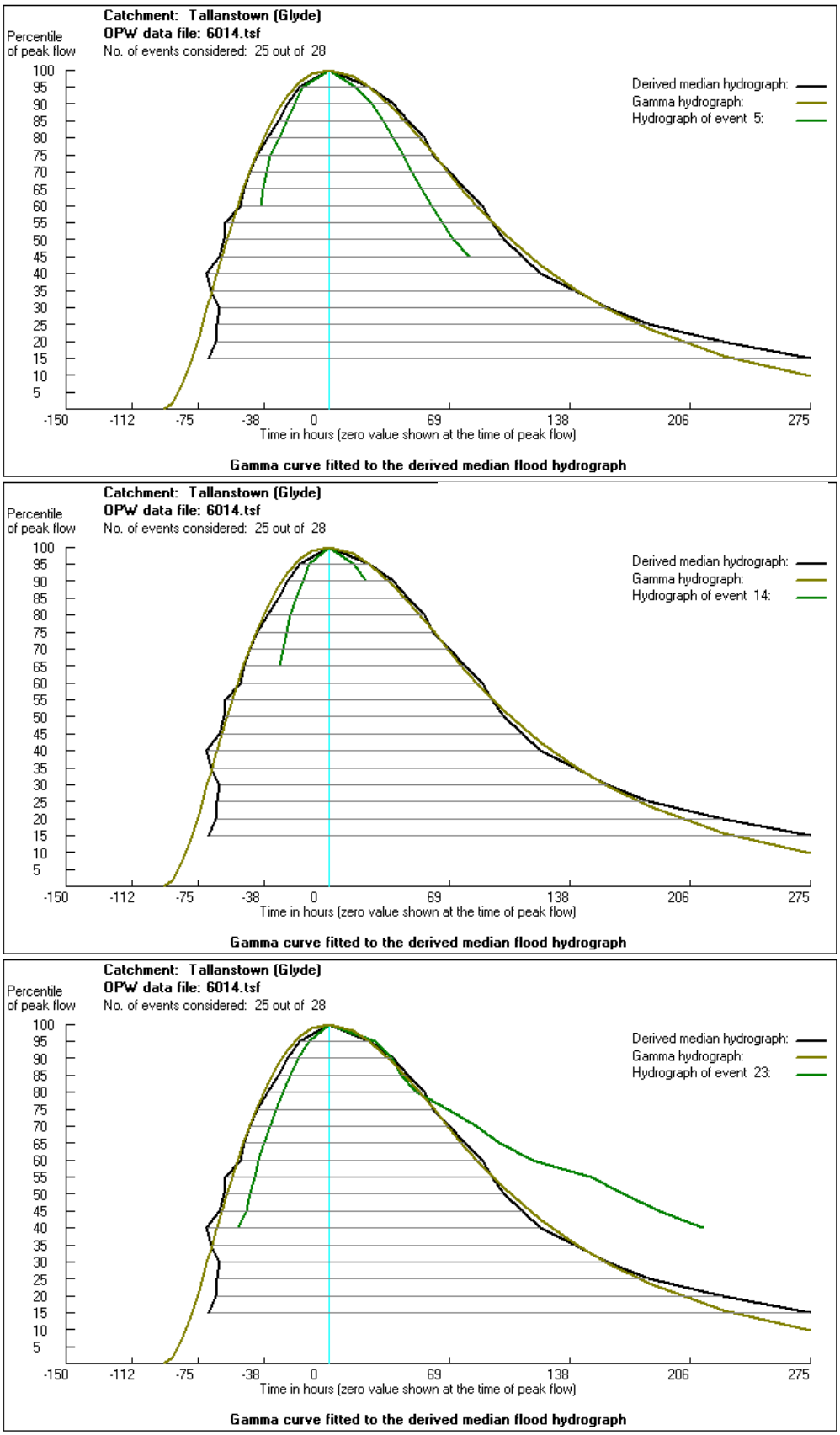

Fig. D.2.4 The derived median (best non-parametric) and Gamma-I median (best parametric) hydrographs, produced using the calibration events, shown superimposed on the observed flood hydrographs of the three verification events at Station No. 6014 (Tallanstown on the Glyde)

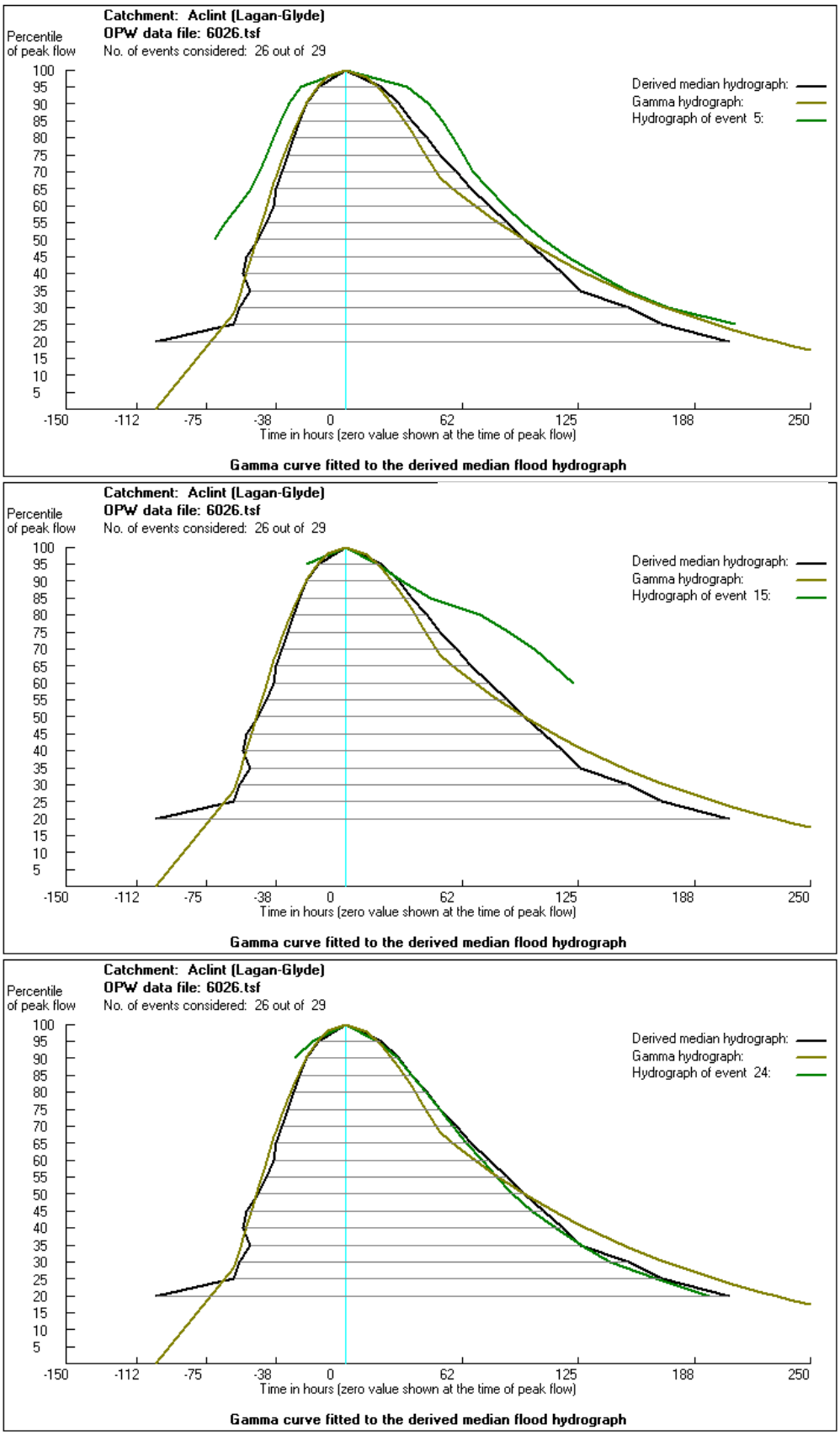

Fig. D.2.5 The derived median (best non-parametric) and Gamma-I median (best parametric) hydrographs, produced using the calibration events, shown superimposed on the observed flood hydrographs of the three verification events at Station No. 6026 (Lagan on the Glyde)

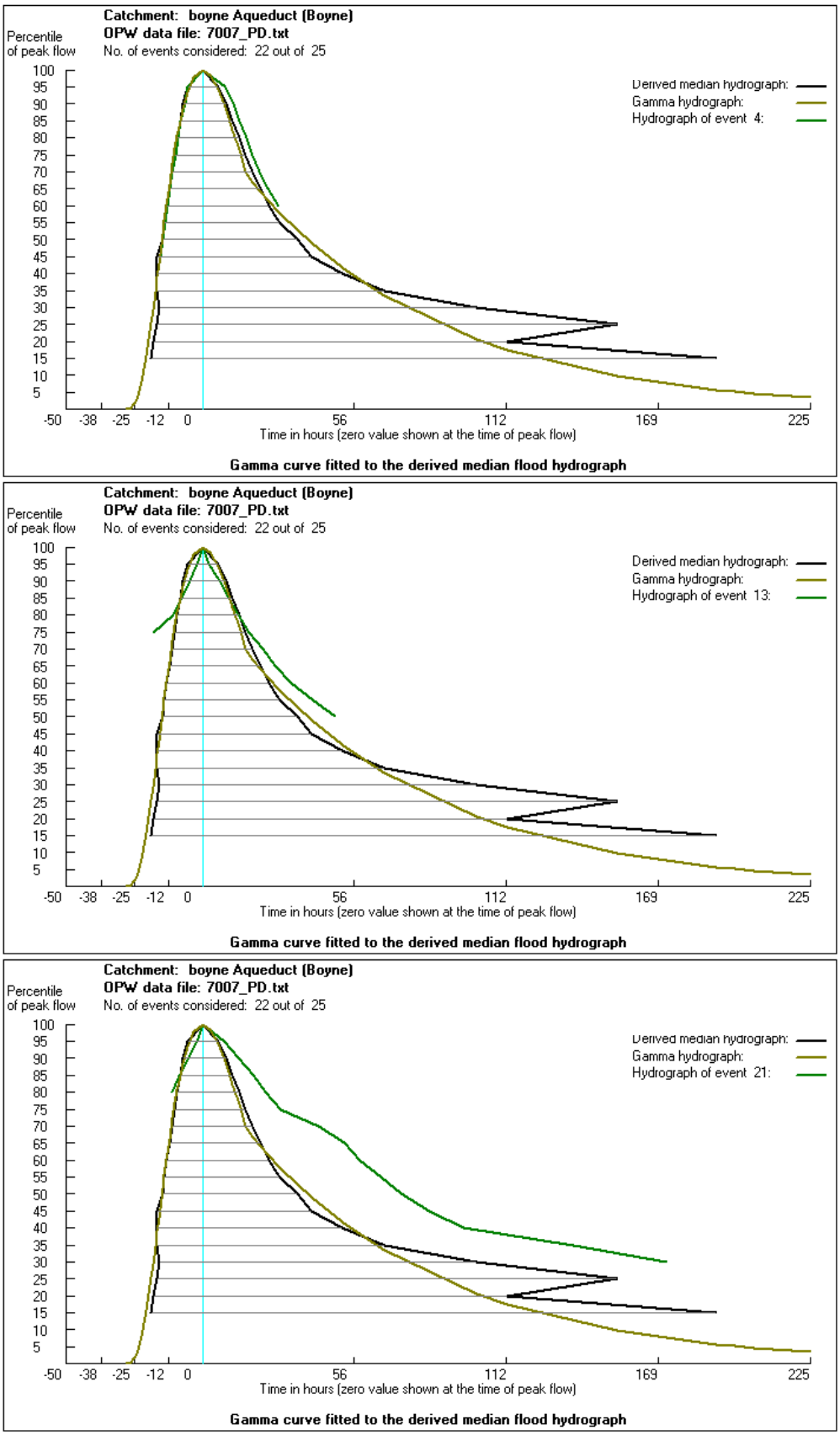

Fig. D.2.6 The derived median (best non-parametric) and Gamma-I median (best parametric) hydrographs, produced using the calibration events, shown superimposed on the observed flood hydrographs of the three verification events at Station No. 7007 (Boyne on the Boyne)

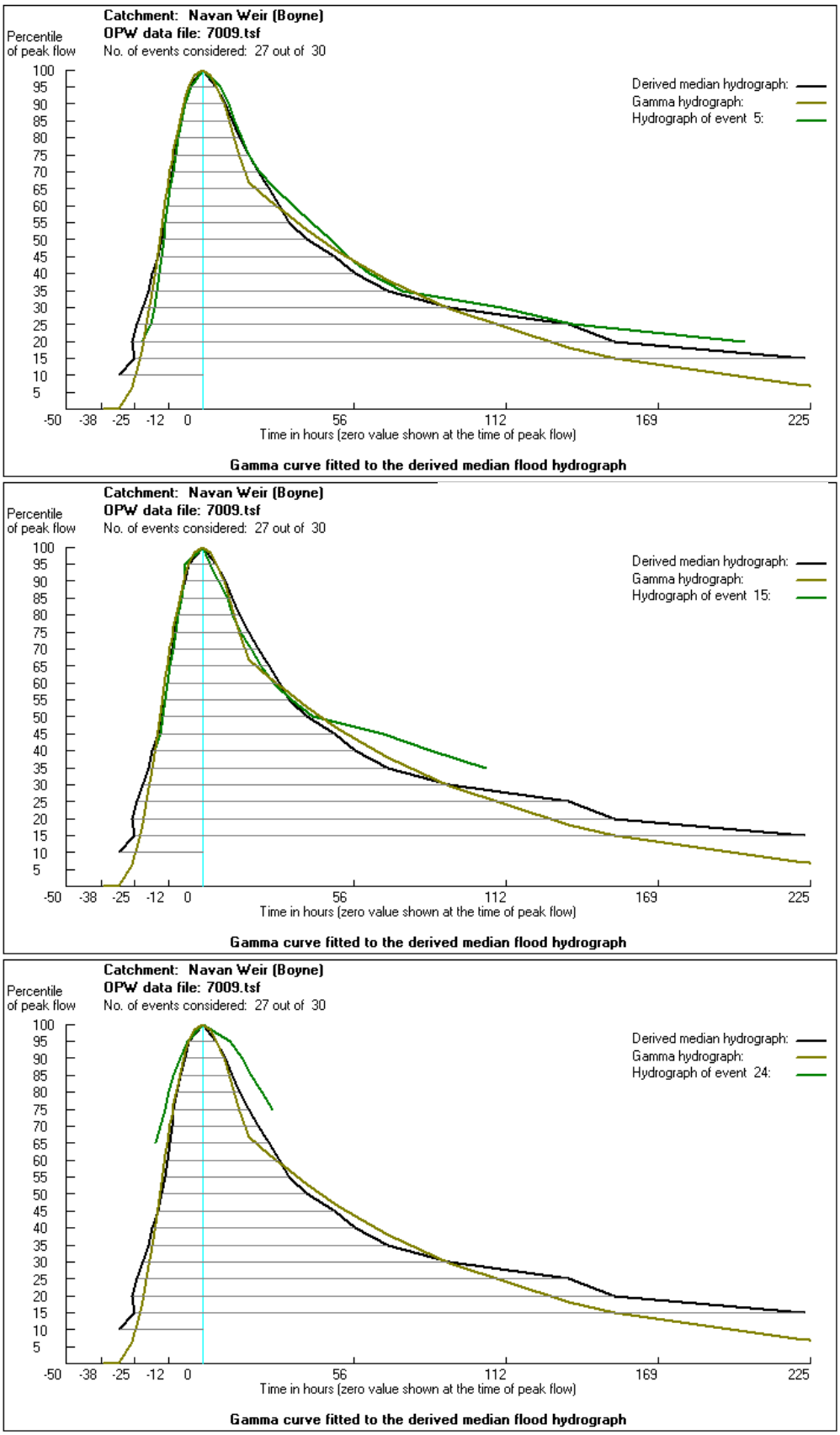

Fig. D.2.7 The derived median (best non-parametric) and Gamma-I median (best parametric) hydrographs, produced using the calibration events, shown superimposed on the observed flood hydrographs of the three verification events at Station No. 7009 (Navan Weir on the Boyne)

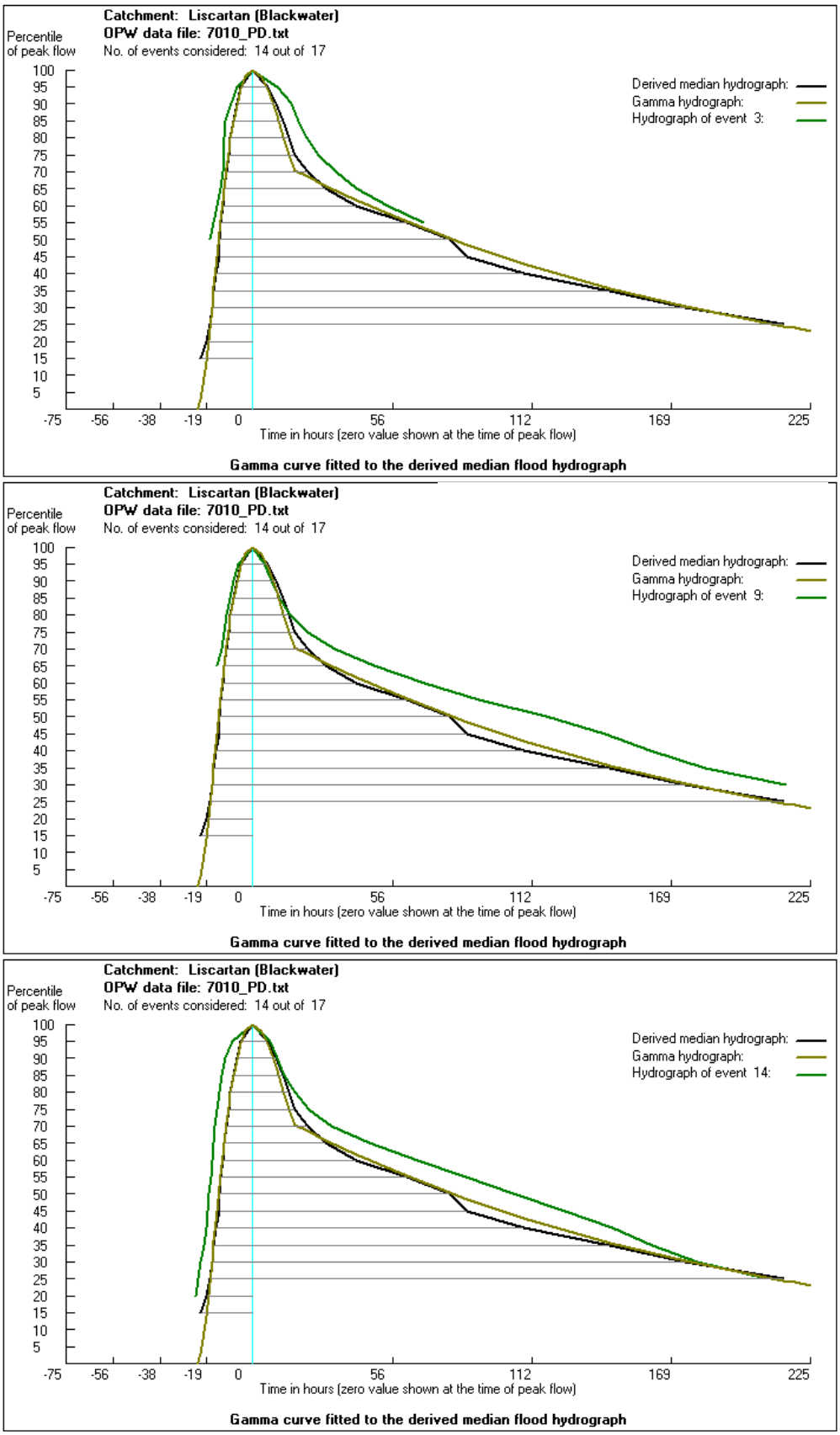

Fig. D.2.8 The derived median (best non-parametric) and Gamma-I median (best parametric) hydrographs, produced using the calibration events, shown superimposed on the observed flood hydrographs of the three verification events at Station No. 7010 (Liscartan on the Blackwater)

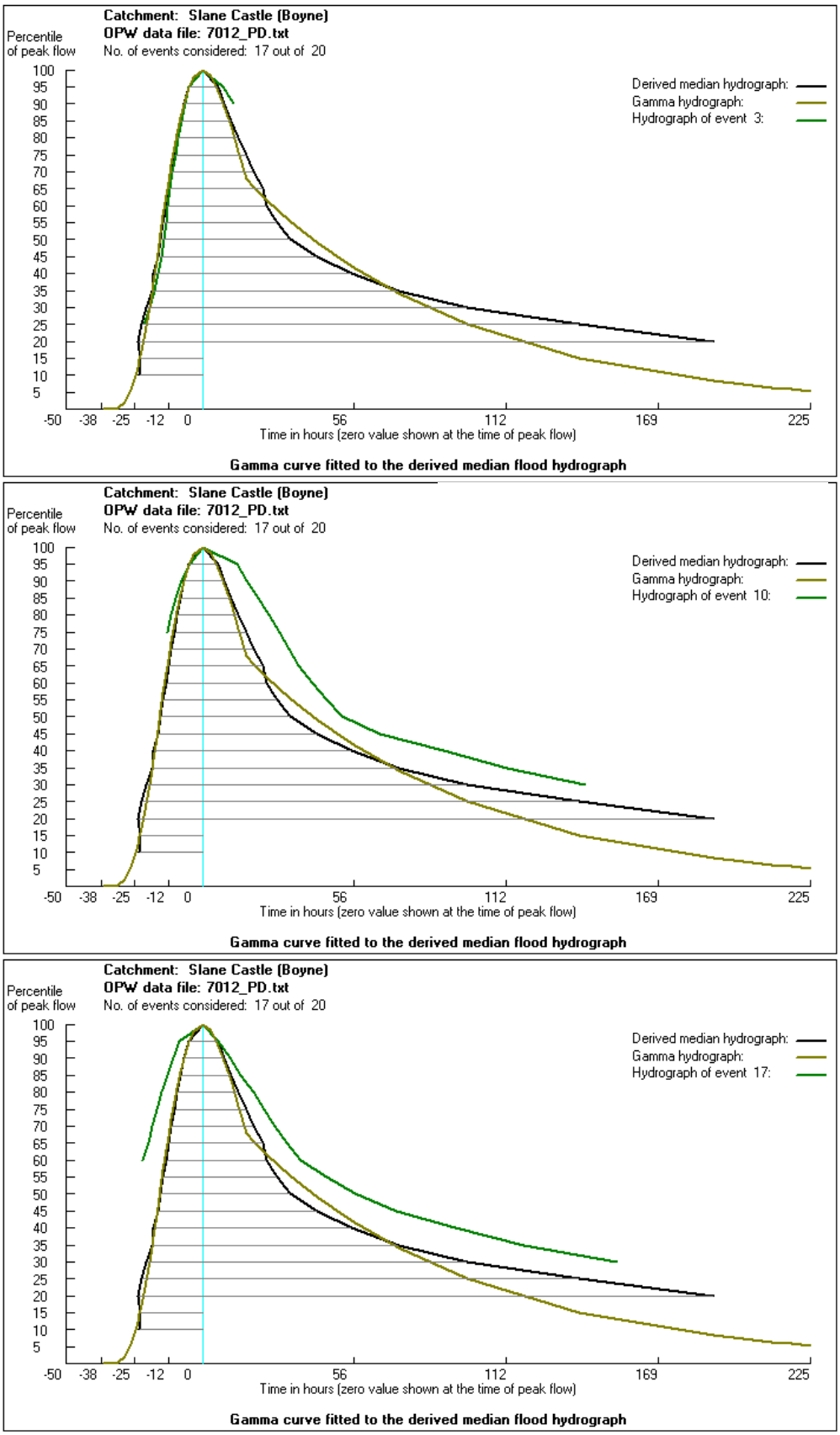

Fig. D.2.9 The derived median (best non-parametric) and Gamma-I median (best parametric) hydrographs, produced using the calibration events, shown superimposed on the observed flood hydrographs of the three verification events at Station No. 7012 (Slane on the Boyne)

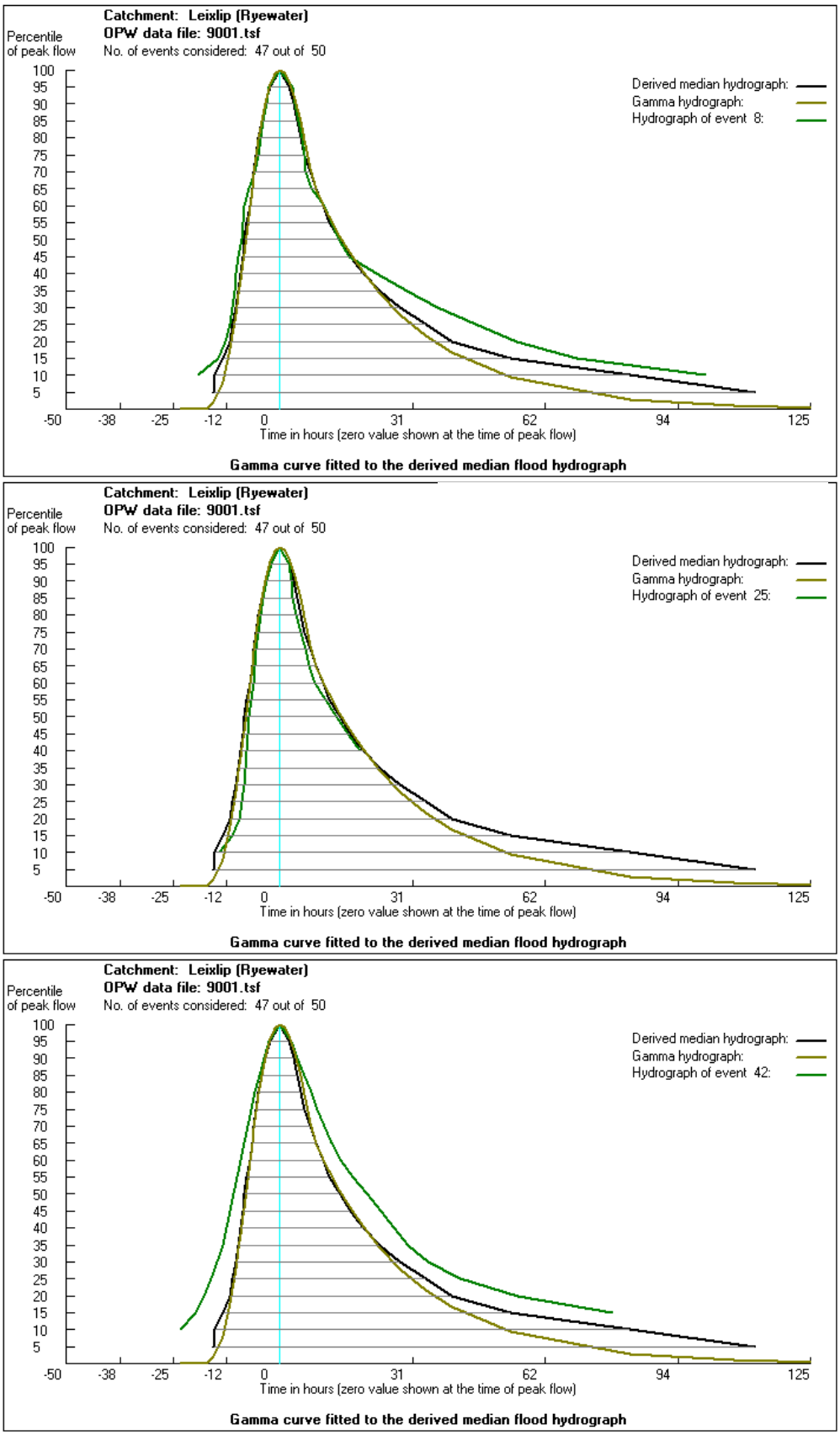

Fig. D.2.10 The derived median (best non-parametric) and Gamma-I median (best parametric) hydrographs, produced using the calibration events, shown superimposed on the observed flood hydrographs of the three verification events at Station No. 9001 (Leixlip on the Ryewater)

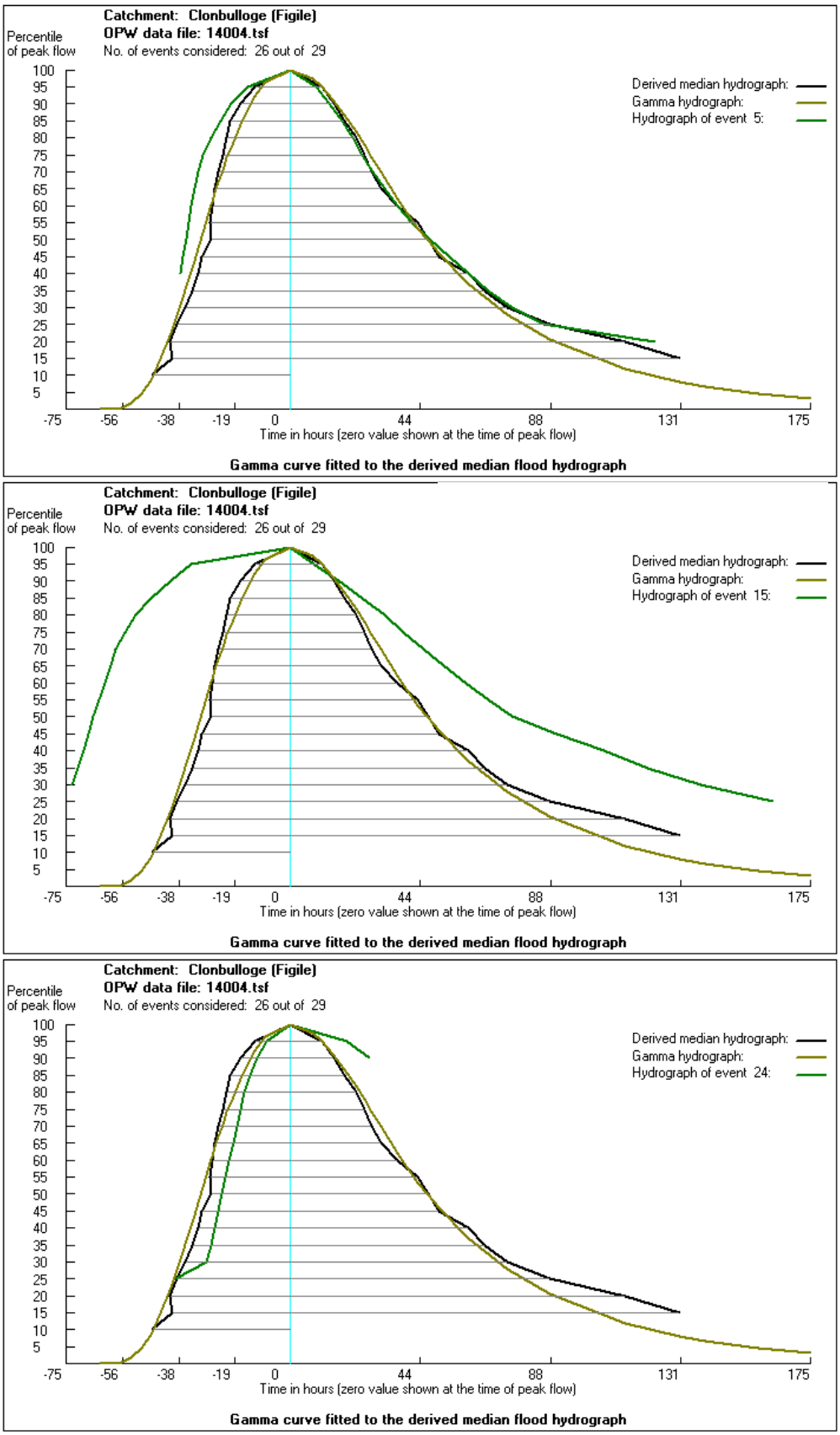

Fig. D.2.11 The derived median (best non-parametric) and Gamma-I median (best parametric) hydrographs, produced using the calibration events, shown superimposed on the observed flood hydrographs of the three verification events at Station No. 14004 (Clonbulloge on the Figile)

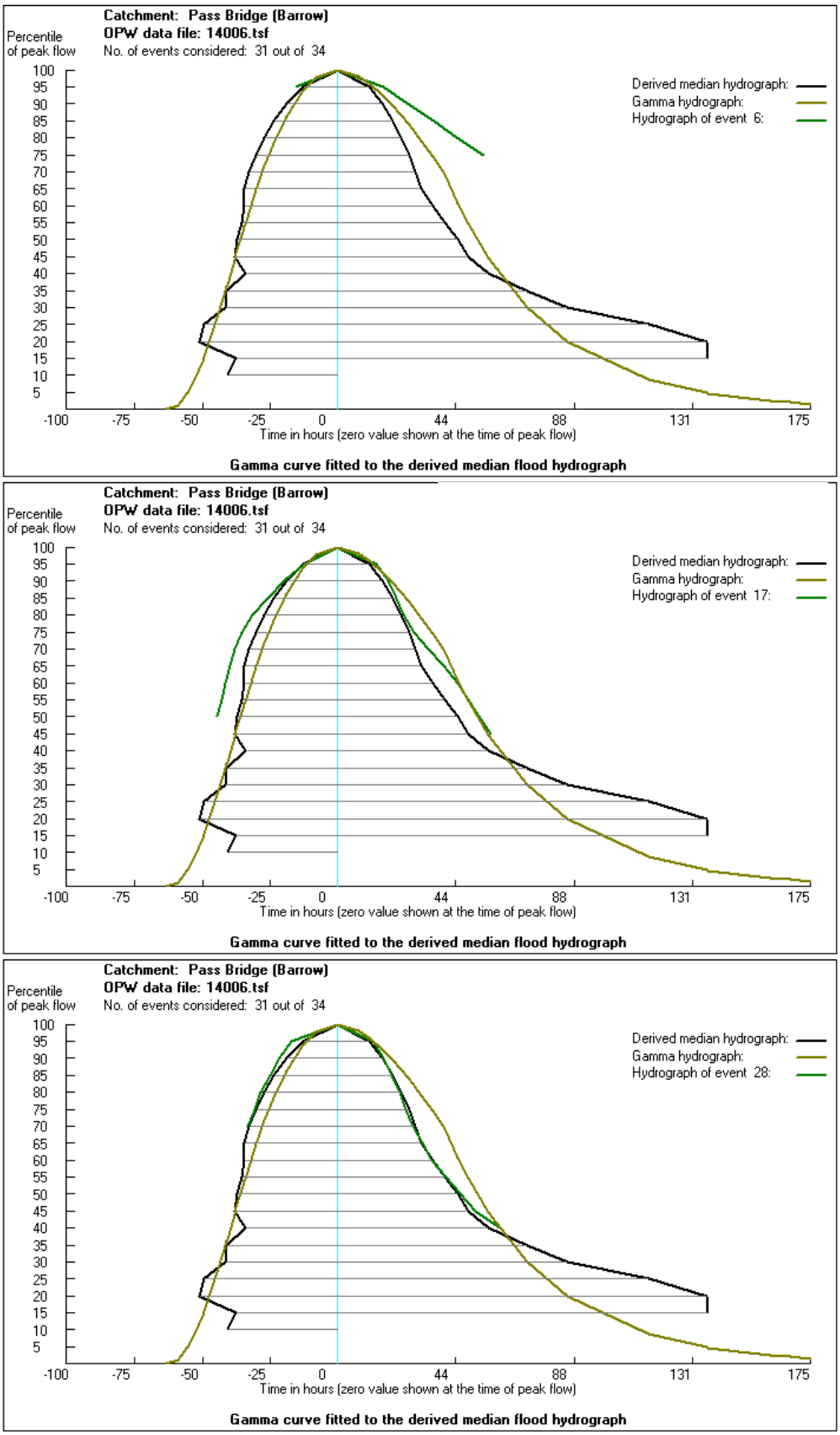

Fig. D.2.12 The derived median (best non-parametric) and Gamma-I median (best parametric) hydrographs, produced using the calibration events, shown superimposed on the observed flood hydrographs of the three verification events at Station No. 14006 (Pass on the Barrow)

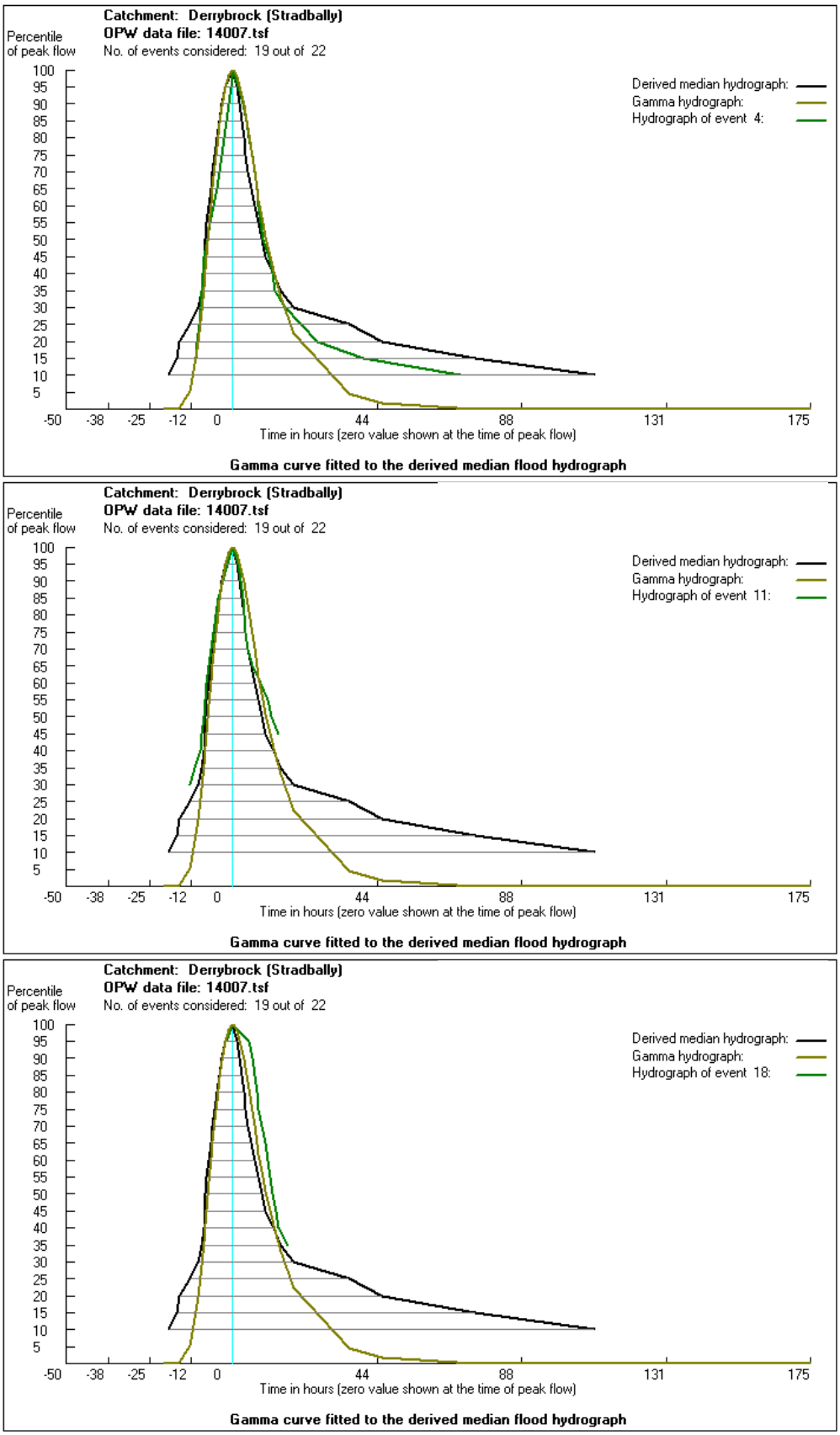

Fig. D.2.13 The derived median (best non-parametric) and Gamma-I median (best parametric) hydrographs, produced using the calibration events, shown superimposed on the observed flood hydrographs of the three verification events at Station No. 14007 (Derrybrock on the Stradbally)

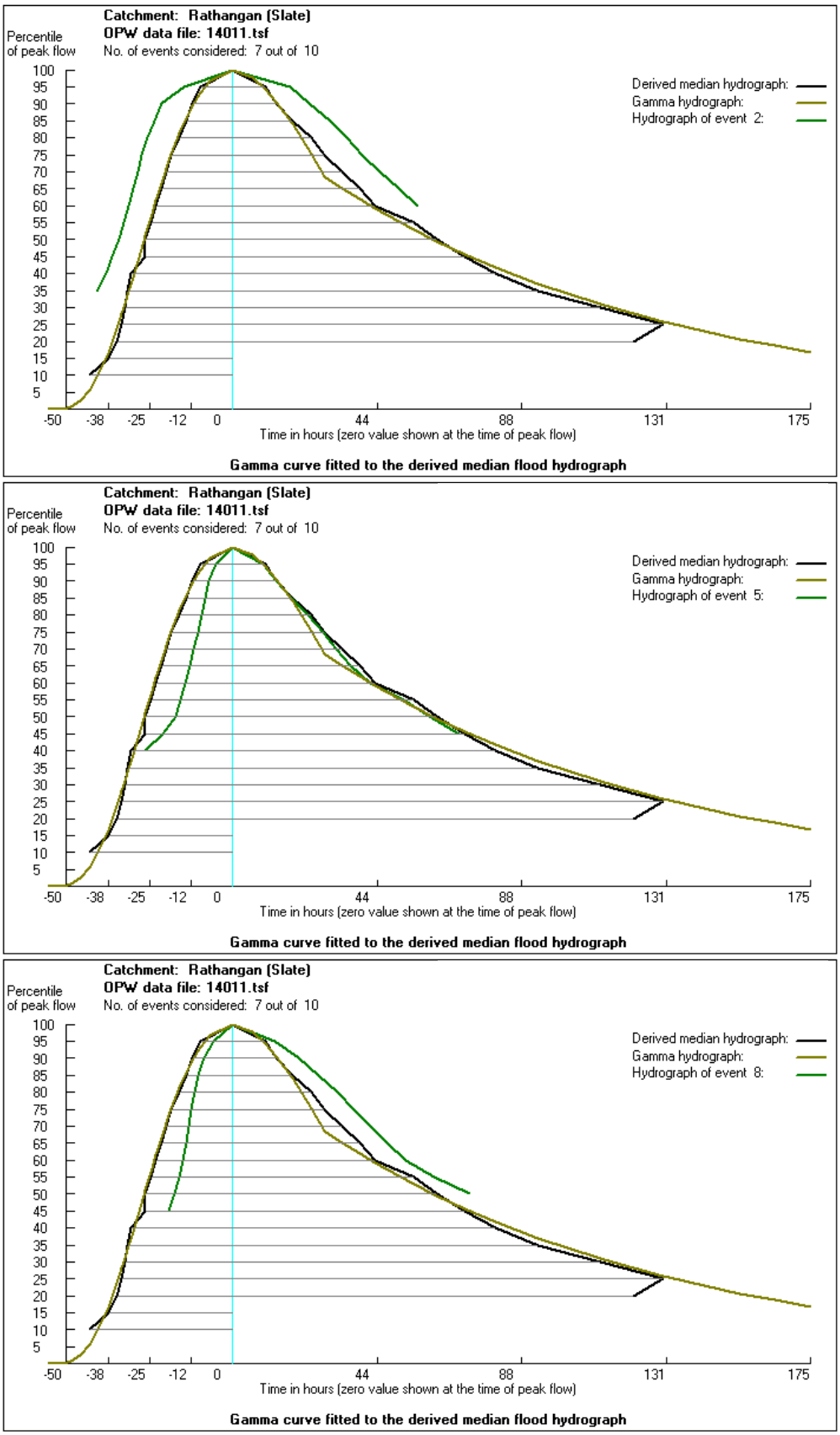

Fig. D.2.14 The derived median (best non-parametric) and Gamma-I median (best parametric) hydrographs, produced using the calibration events, shown superimposed on the observed flood hydrographs of the three verification events at Station No. 14011 (Rathangan on the Slate)

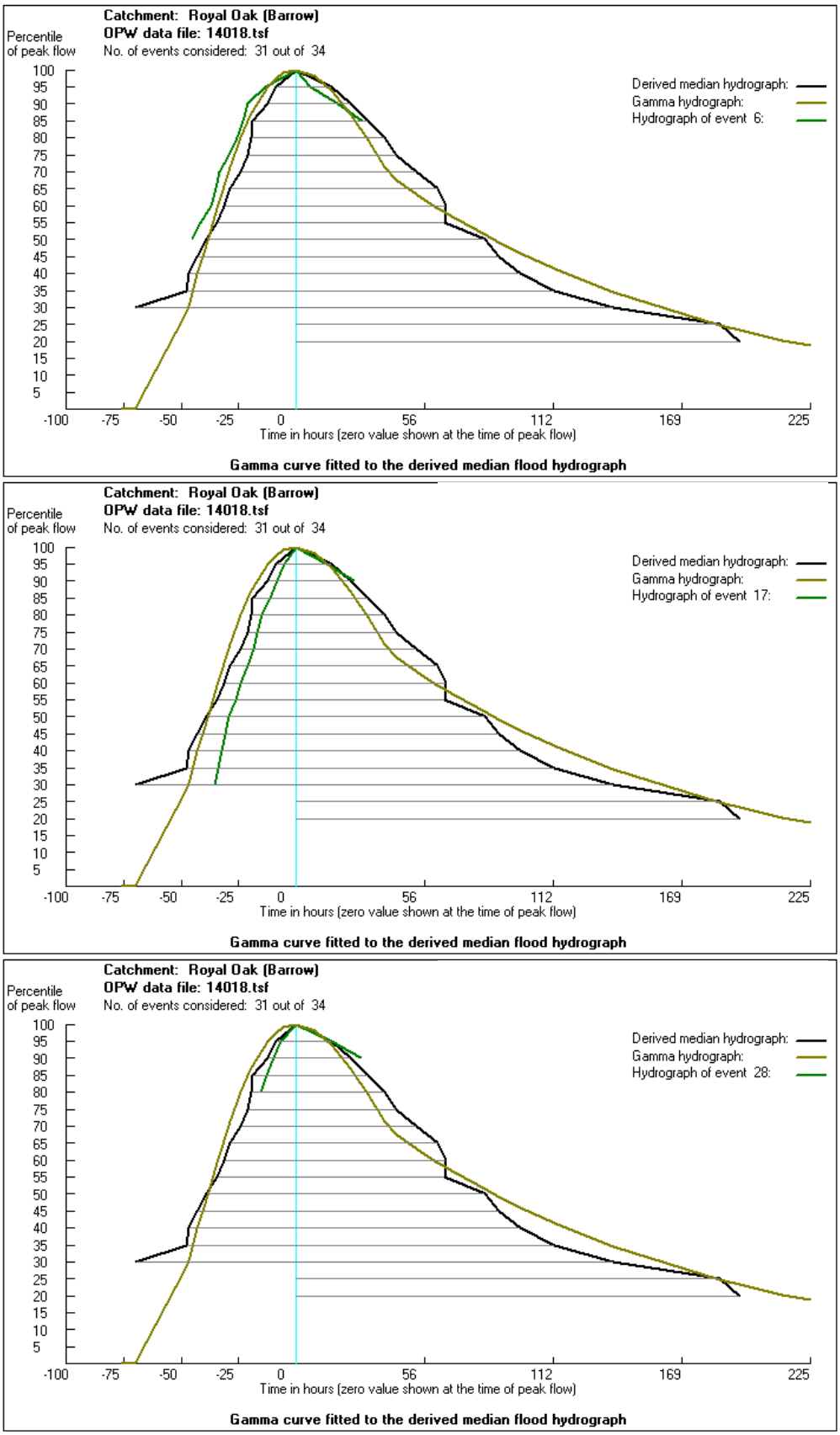

Fig. D.2.15 The derived median (best non-parametric) and Gamma-I median (best parametric) hydrographs, produced using the calibration events, shown superimposed on the observed flood hydrographs of the three verification events at Station No. 14018 (Royal Oak on the Barrow)

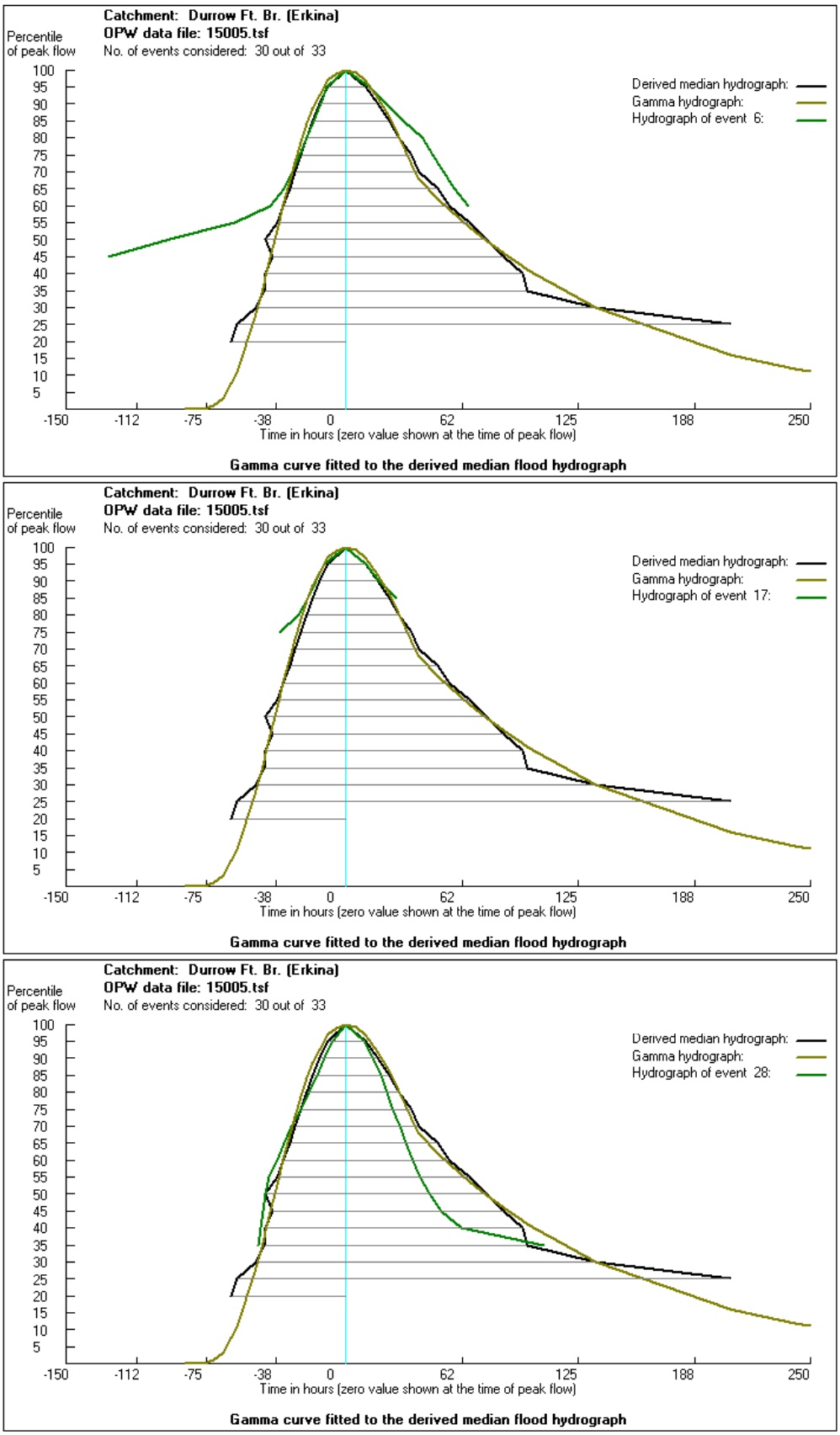

Fig. D.2.16 The derived median (best non-parametric) and Gamma-I median (best parametric) hydrographs, produced using the calibration events, shown superimposed on the observed flood hydrographs of the three verification events at Station No. 15005 (Durrow Ft. Br. on the Erkina)

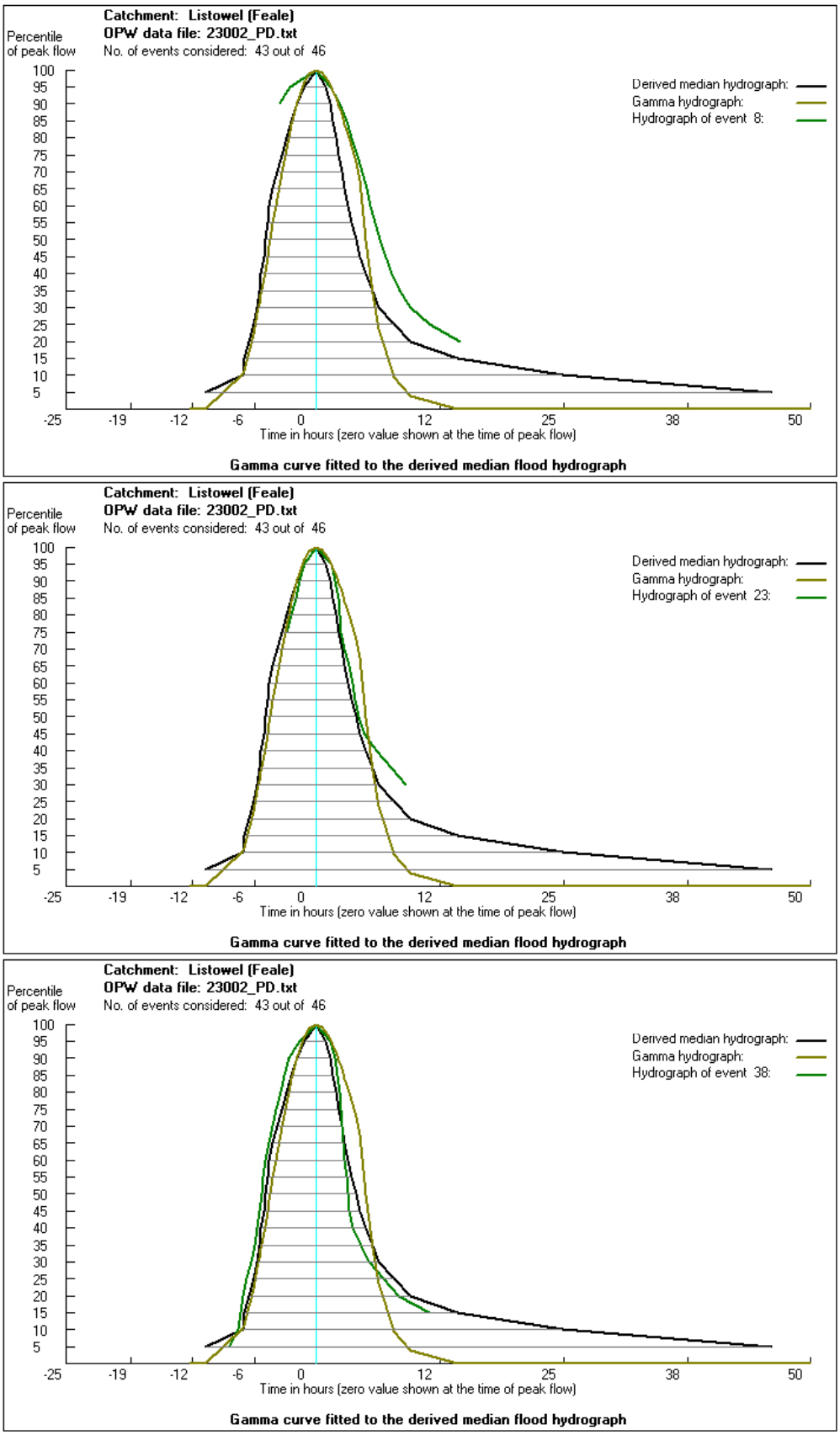

Fig. D.2.17 The derived median (best non-parametric) and Gamma-I median (best parametric) hydrographs, produced using the calibration events, shown superimposed on the observed flood hydrographs of the three verification events at Station No. 23002 (Listowel on the Feale)

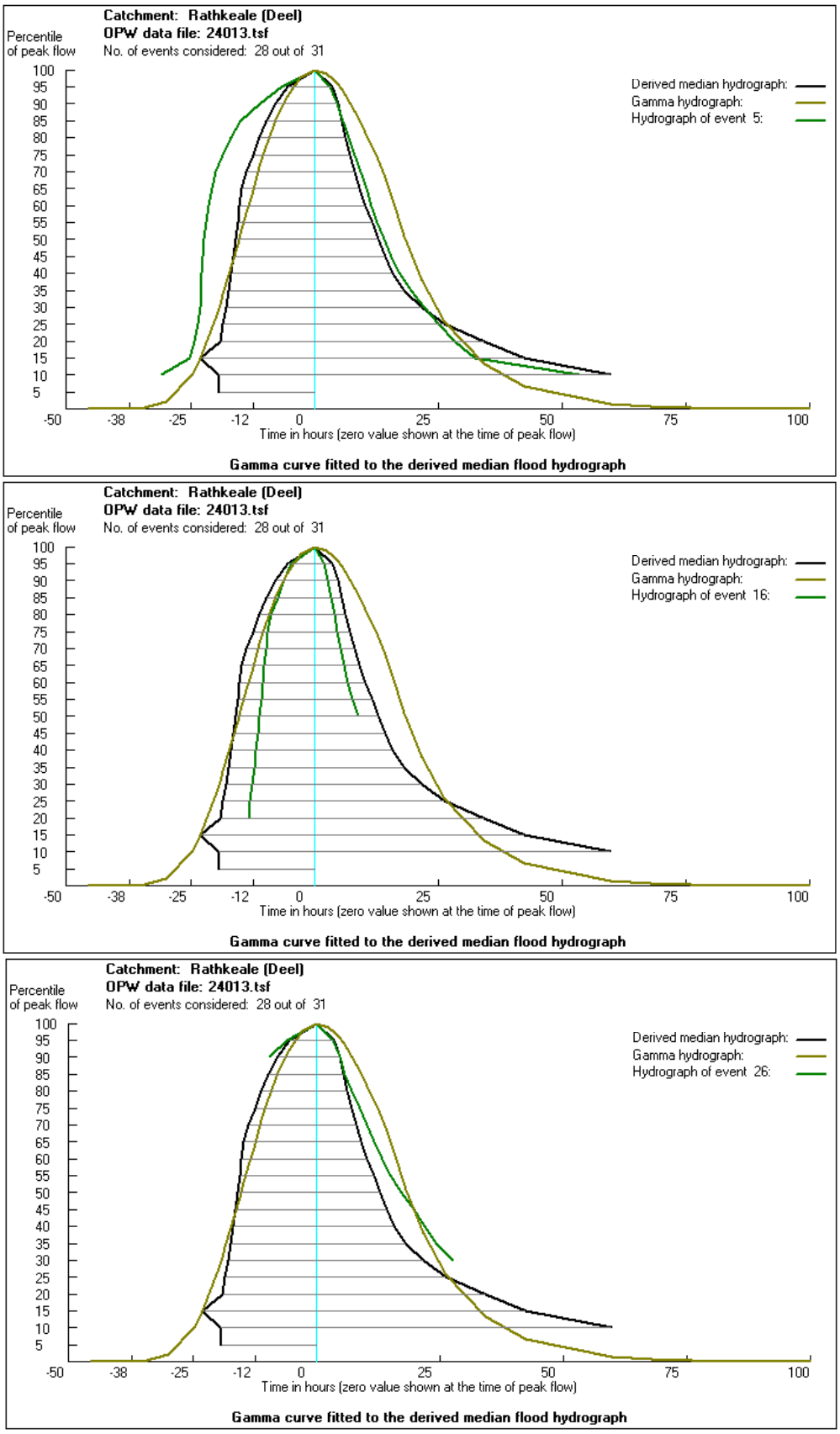

Fig. D.2.18 The derived median (best non-parametric) and Gamma-I median (best parametric) hydrographs, produced using the calibration events, shown superimposed on the observed flood hydrographs of the three verification events at Station No. 24013 (Rathkeale on the Deel)

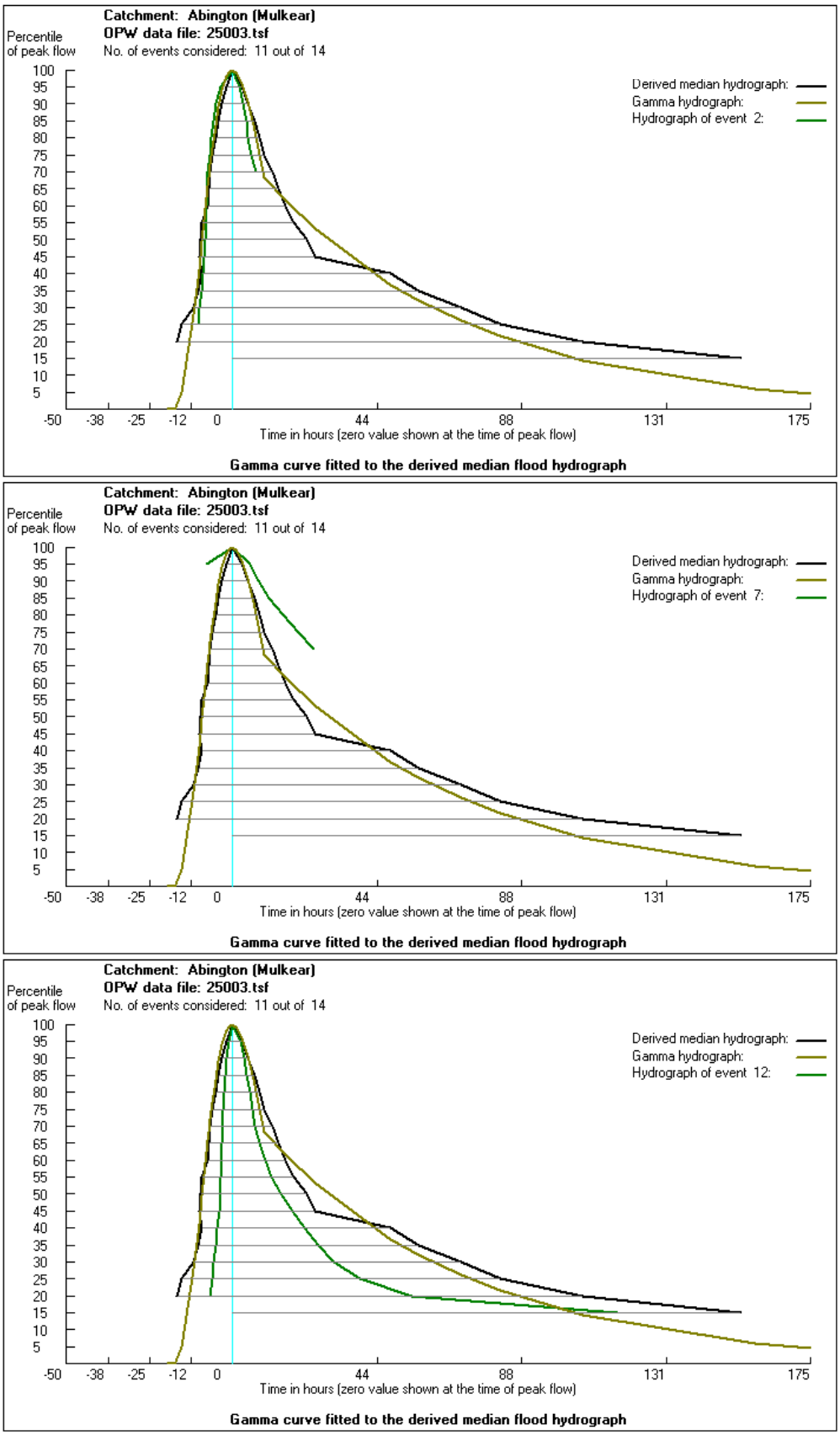

Fig. D.2.19 The derived median (best non-parametric) and Gamma-I median (best parametric) hydrographs, produced using the calibration events, shown superimposed on the observed flood hydrographs of the three verification events at Station No. 25003 (Abington on the Mulkear)

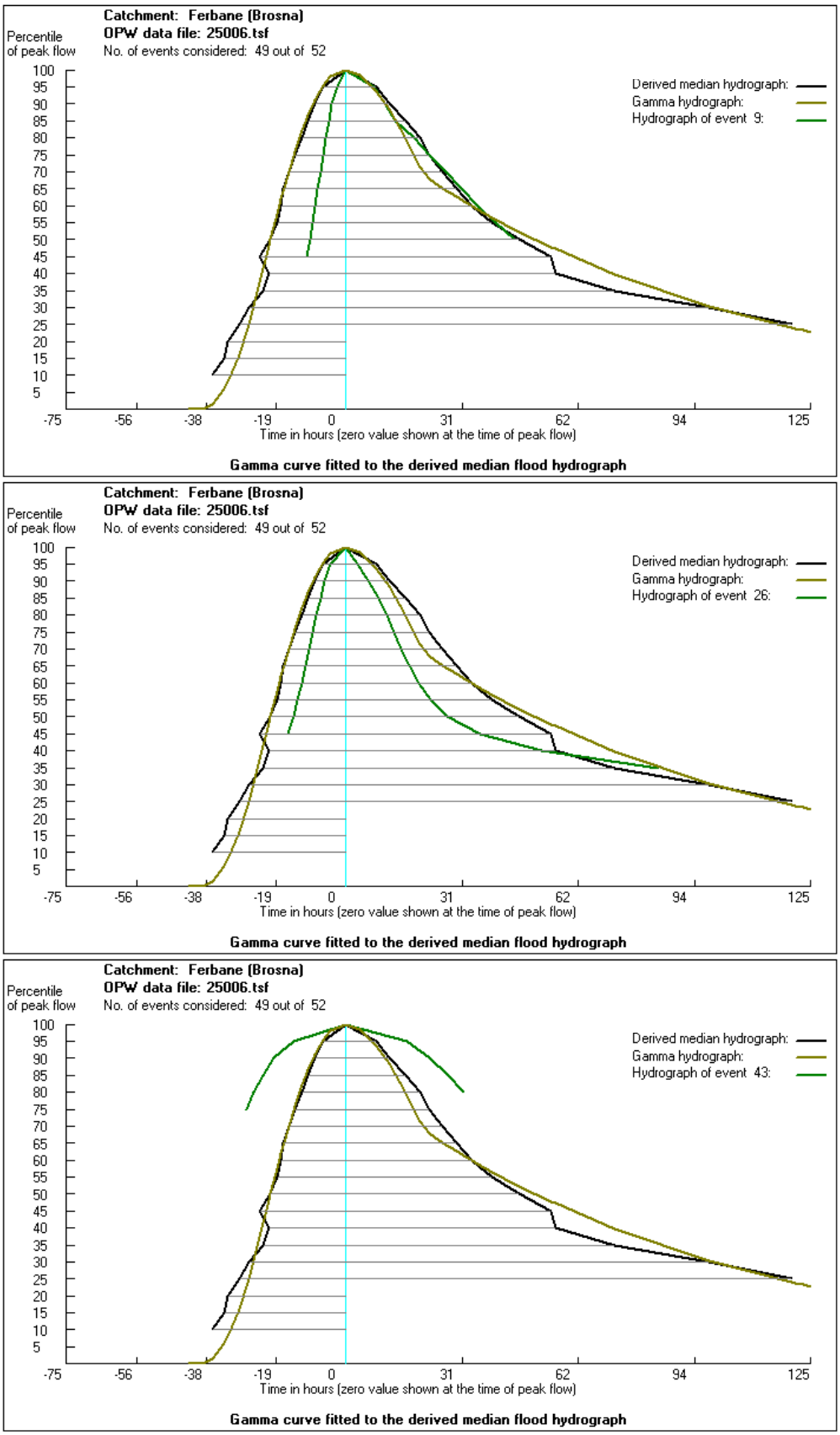

Fig. D.2.20 The derived median (best non-parametric) and Gamma-I median (best parametric) hydrographs, produced using the calibration events, shown superimposed on the observed flood hydrographs of the three verification events at Station No. 25006 (Ferbane on the Brosna)

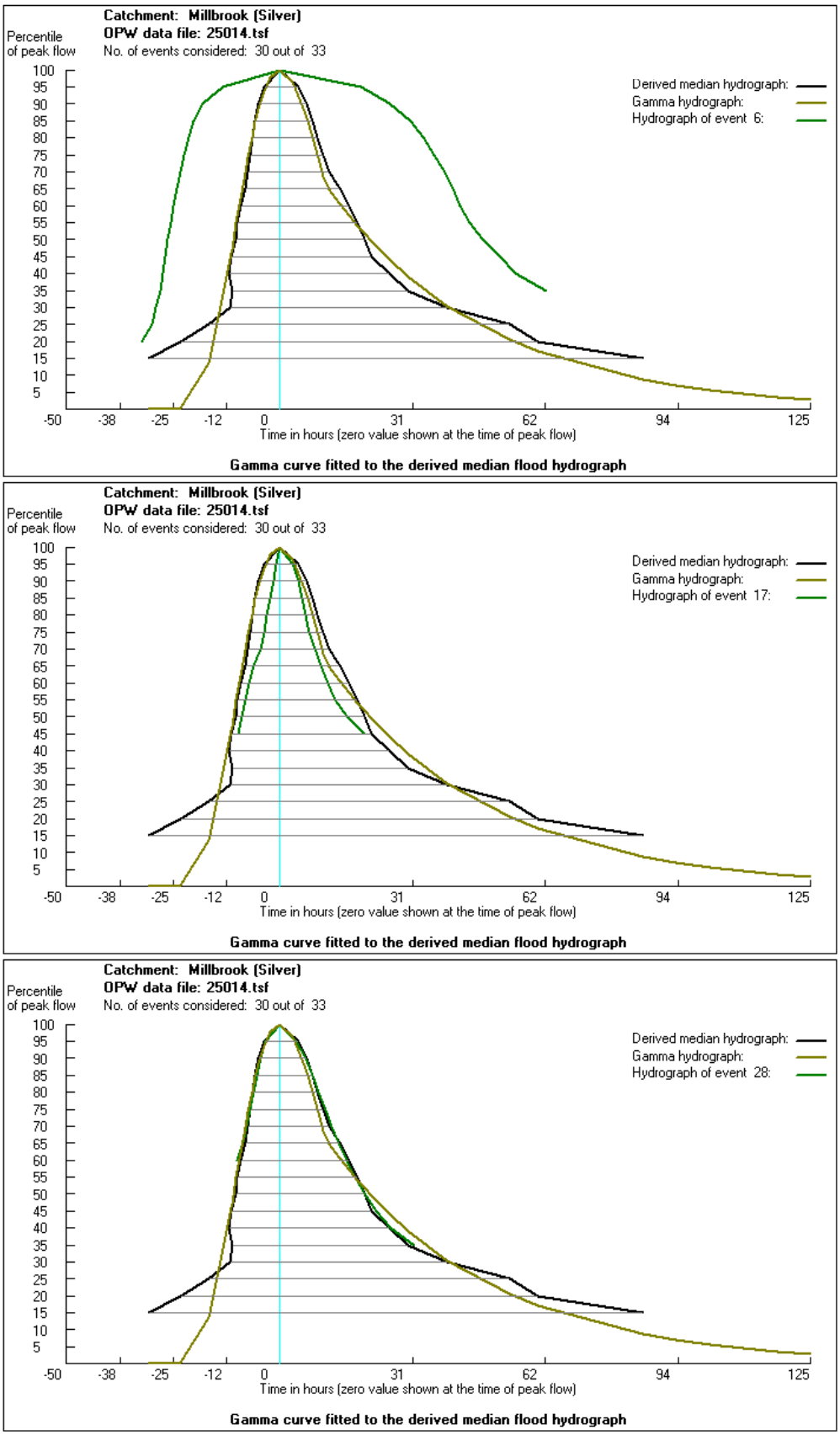

Fig. D.2.21 The derived median (best non-parametric) and Gamma-I median (best parametric) hydrographs, produced using the calibration events, shown superimposed on the observed flood hydrographs of the three verification events at Station No. 25014 (Millbrook on the Silver)

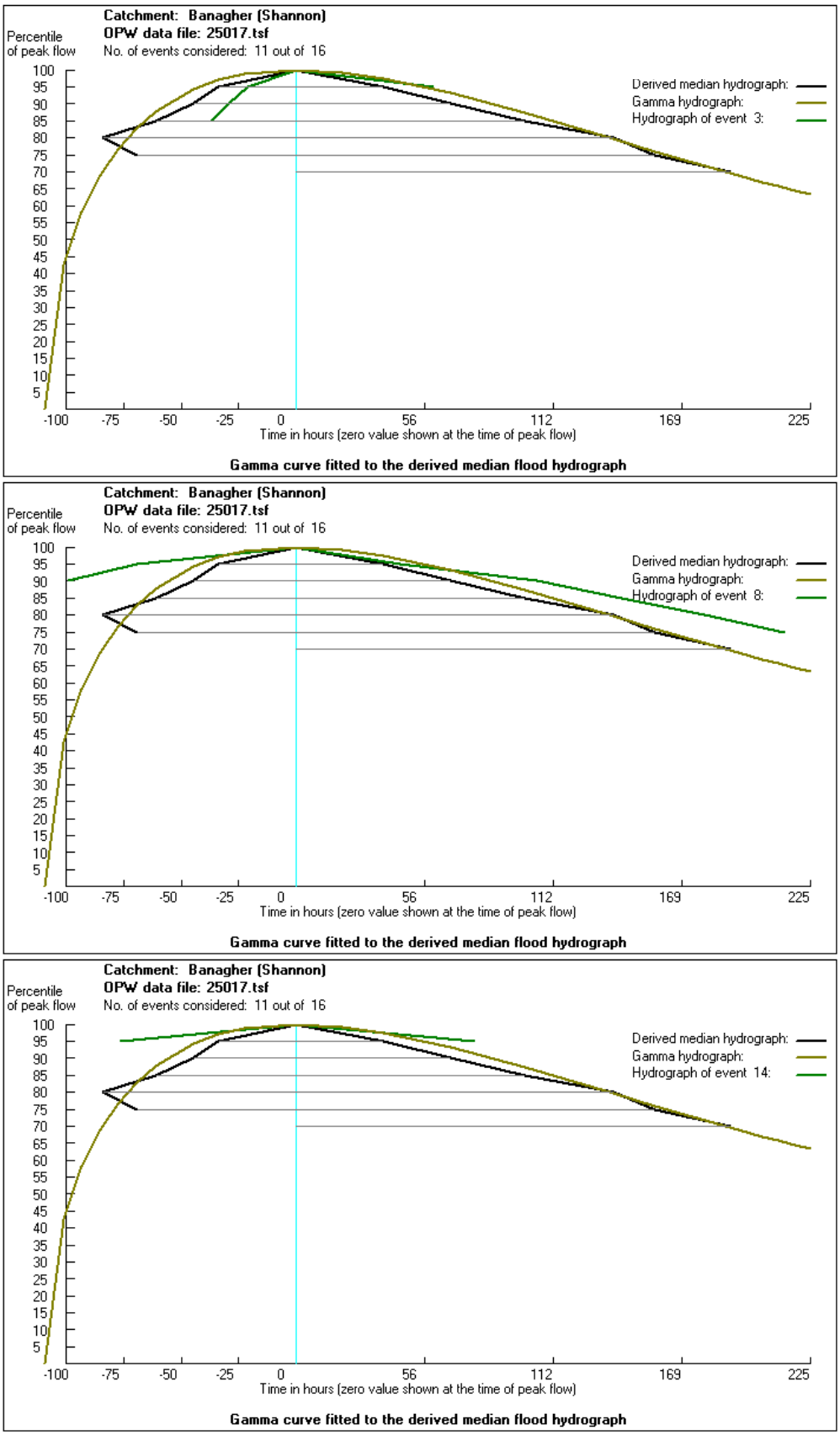

Fig. D.2.22 The derived median (best non-parametric) and Gamma-I median (best parametric) hydrographs, produced using the calibration events, shown superimposed on the observed flood hydrographs of the three verification events at Station No. 25017 (Banagher on the Shannon)

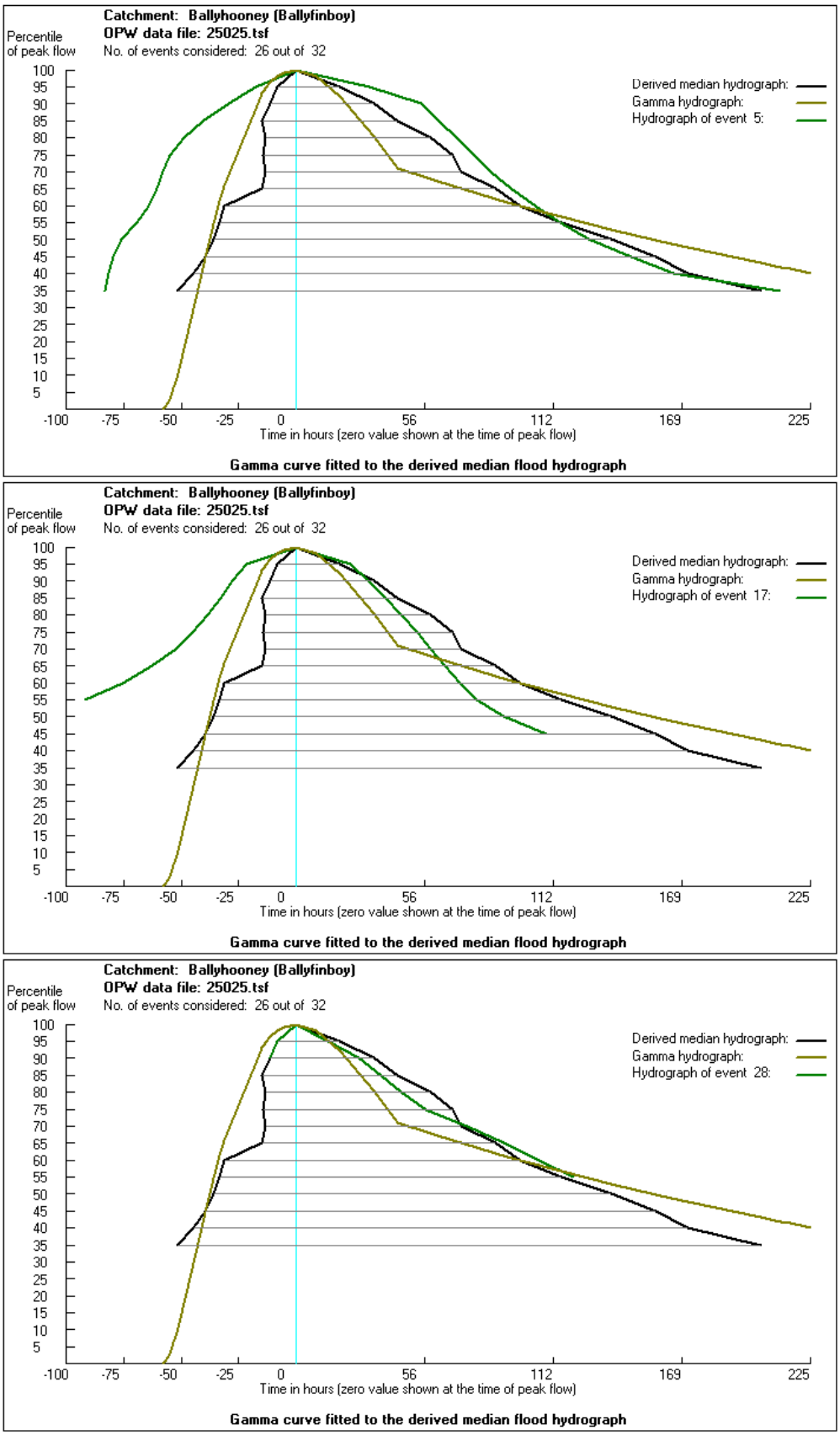

Fig. D.2.23 The derived median (best non-parametric) and Gamma-I median (best parametric) hydrographs, produced using the calibration events, shown superimposed on the observed flood hydrographs of the three verification events at Station No. 25025 (Ballyhooney on the Ballyfinboy)

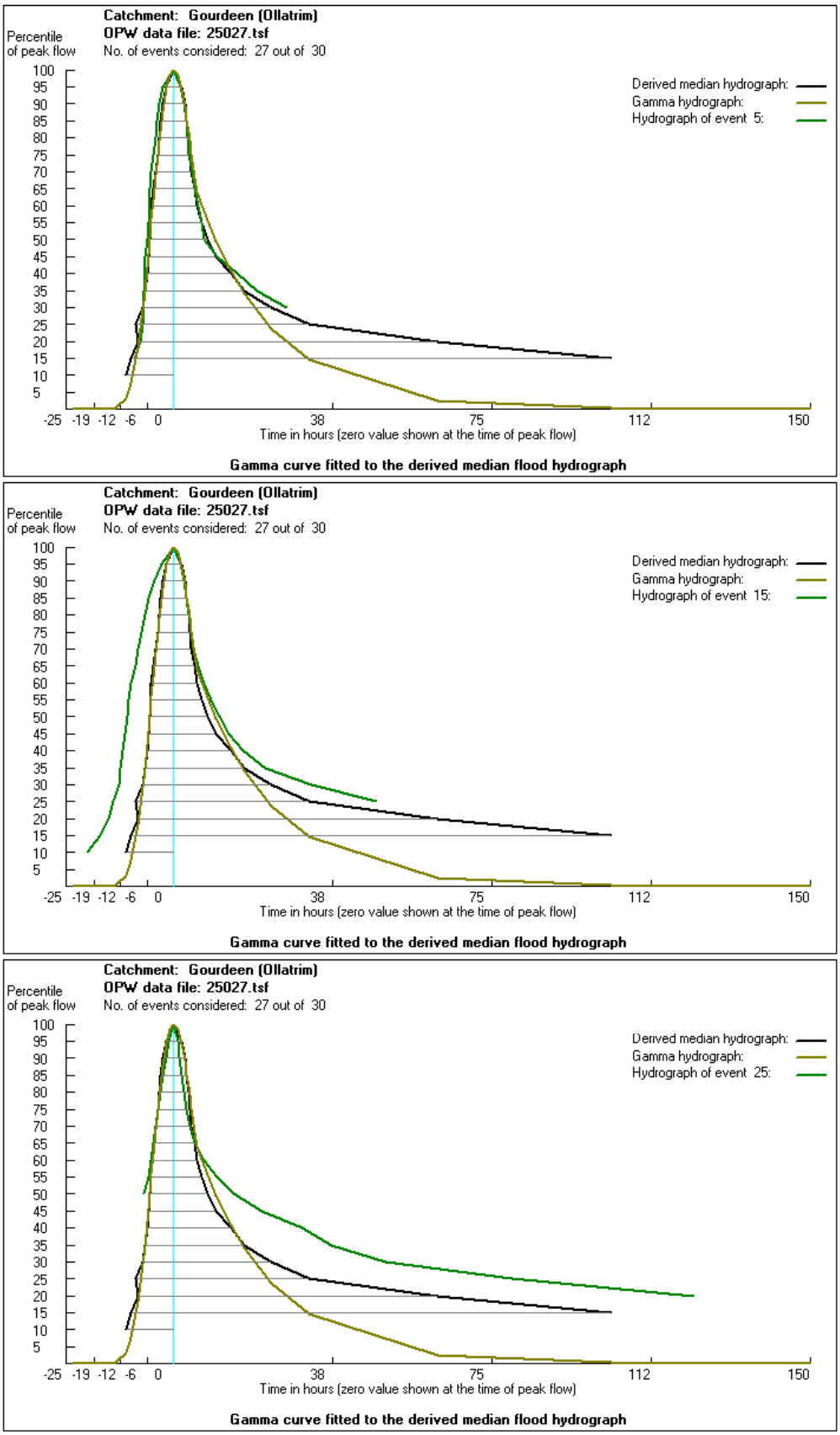

Fig. D.2.24 The derived median (best non-parametric) and Gamma-I median (best parametric) hydrographs, produced using the calibration events, shown superimposed on the observed flood hydrographs of the three verification events at Station No. 25027 (Gourdeen on the Ollatrim)

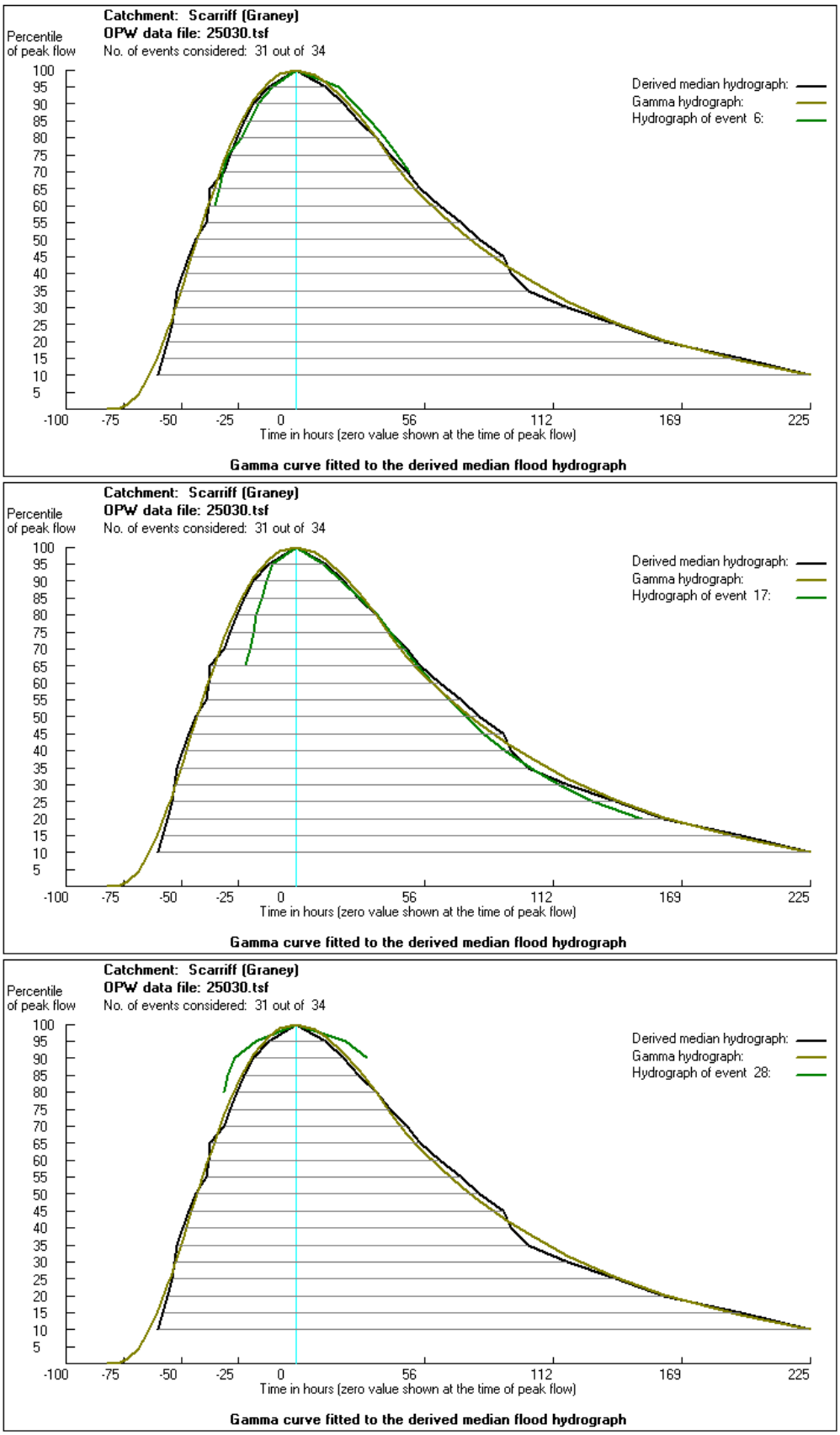

Fig. D.2.25 The derived median (best non-parametric) and Gamma-I median (best parametric) hydrographs, produced using the calibration events, shown superimposed on the observed flood hydrographs of the three verification events at Station No. 25030 (Scariff on the Graney)

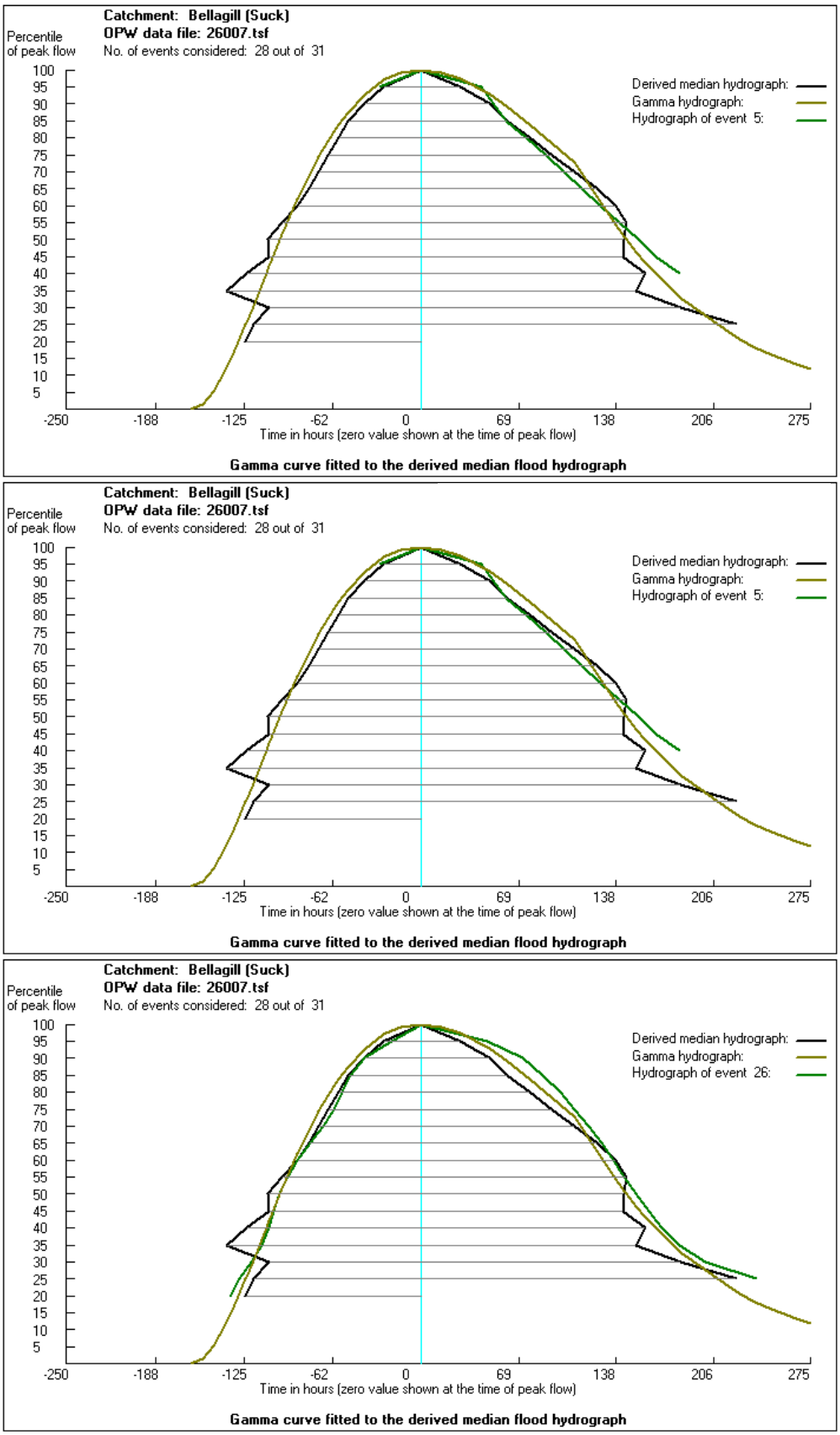

Fig. D.2.26 The derived median (best non-parametric) and Gamma-I median (best parametric) hydrographs, produced using the calibration events, shown superimposed on the observed flood hydrographs of the three verification events at Station No. 26007 (Bellagill on the Suck)

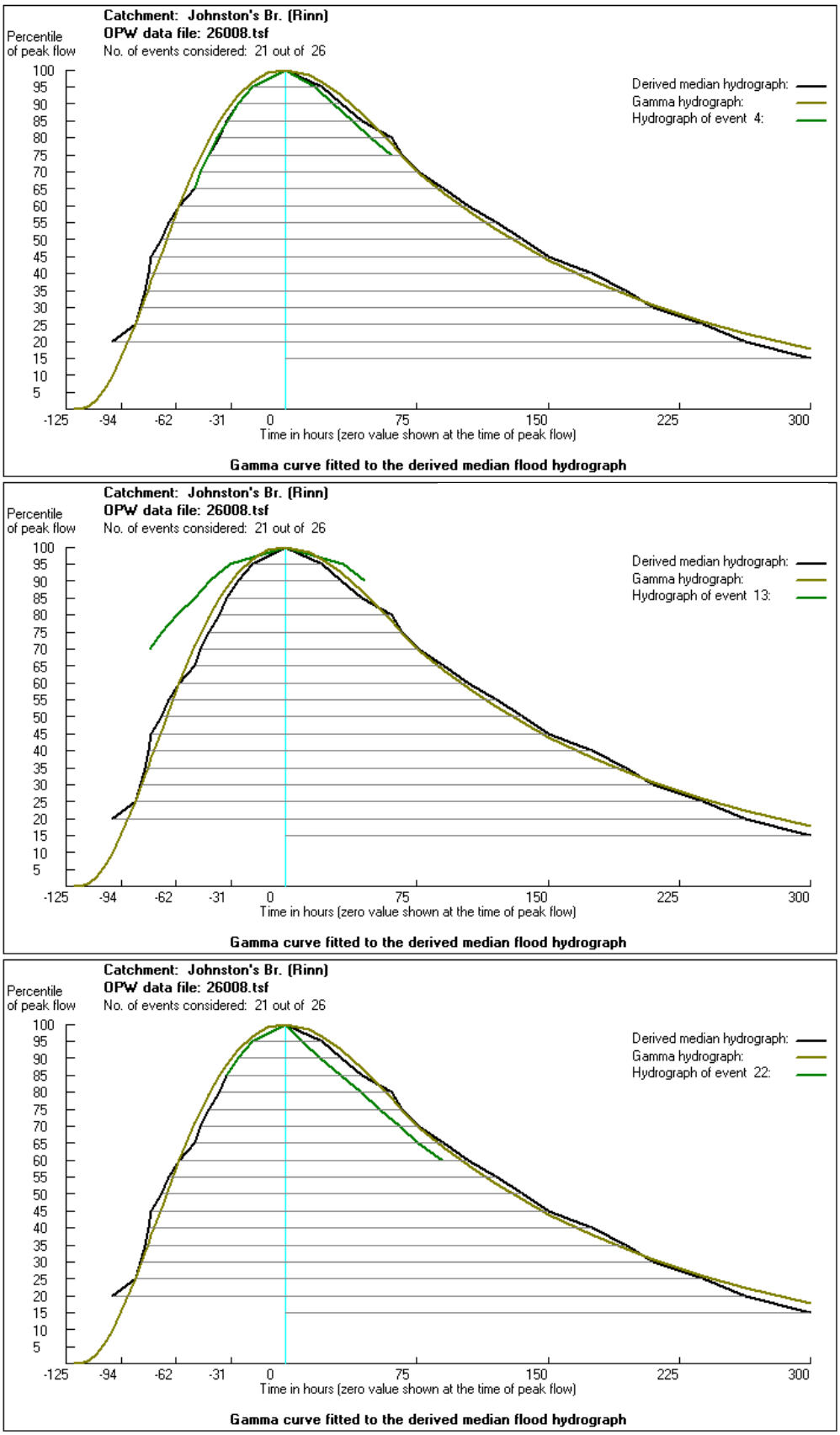

Fig. D.2.27 The derived median (best non-parametric) and Gamma-I median (best parametric) hydrographs, produced using the calibration events, shown superimposed on the observed flood hydrographs of the three verification events at Station No. 26008 (Johnston's Br. on the Rinn)

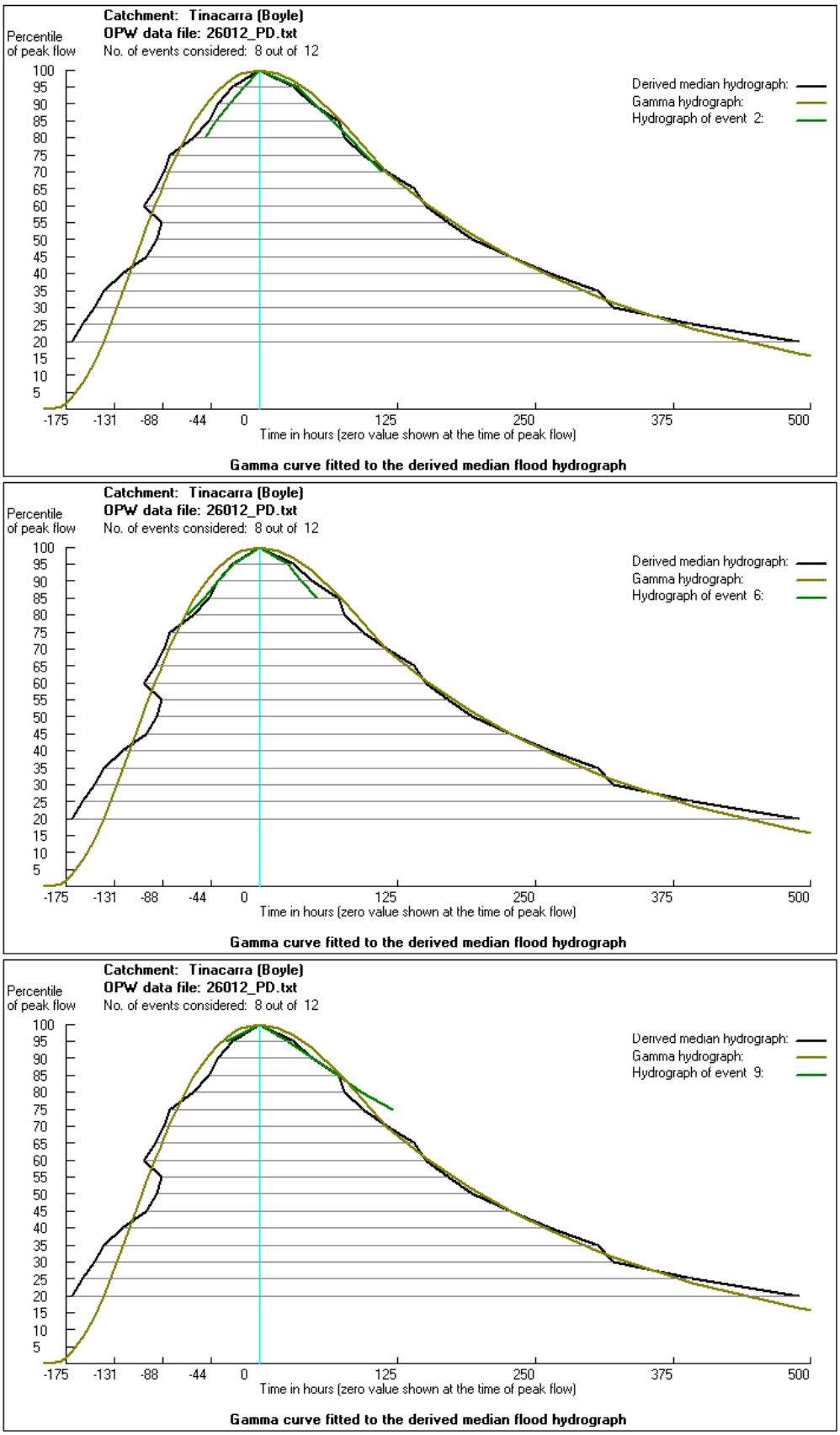

Fig. D.2.28 The derived median (best non-parametric) and Gamma-I median (best parametric) hydrographs, produced using the calibration events, shown superimposed on the observed flood hydrographs of the three verification events at Station No. 26012 (Tinacarra on the Boyle)

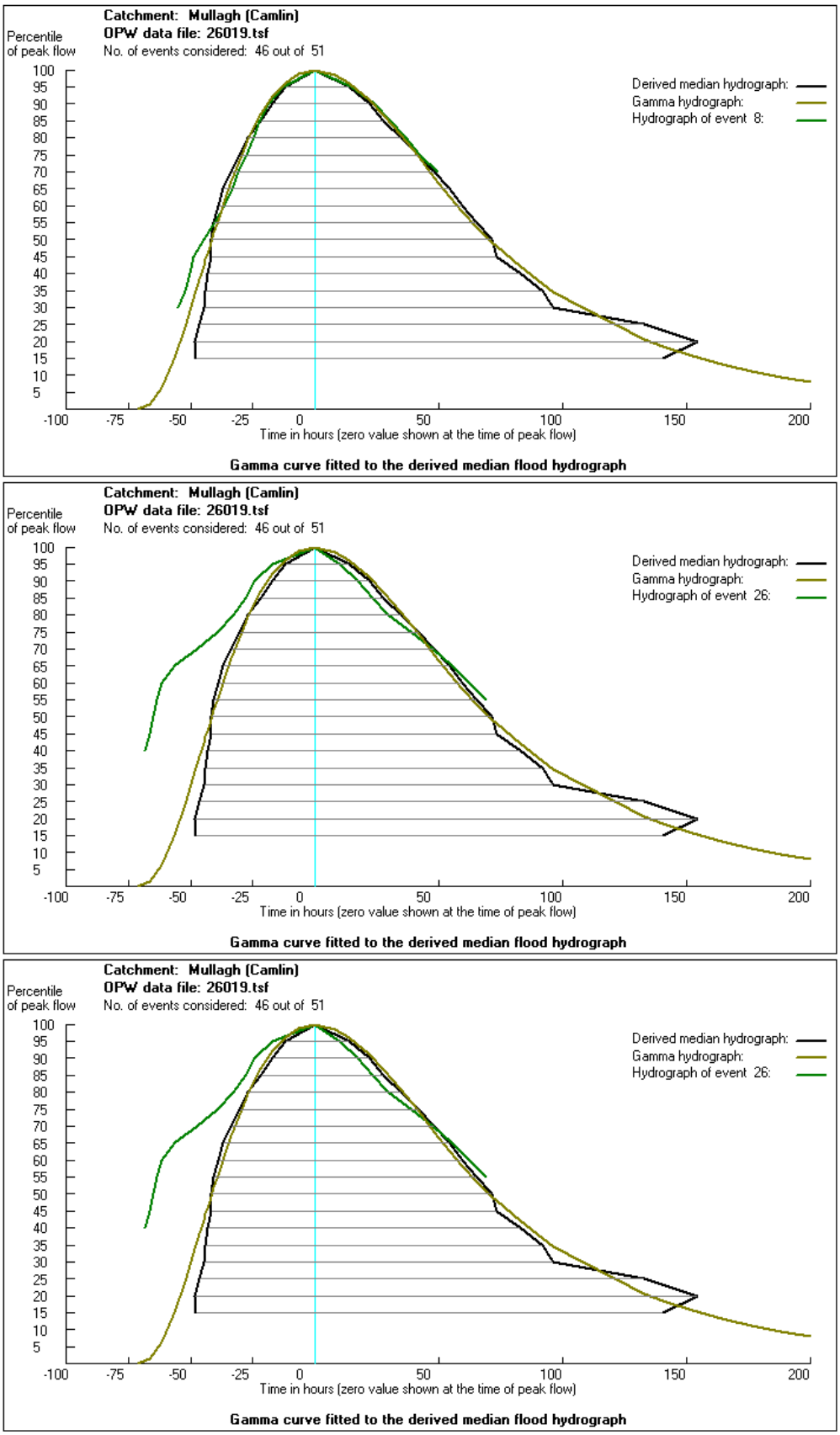

Fig. D.2.29 The derived median (best non-parametric) and Gamma-I median (best parametric) hydrographs, produced using the calibration events, shown superimposed on the observed flood hydrographs of the three verification events at Station No. 26019 (Mullagh on the Camlin)

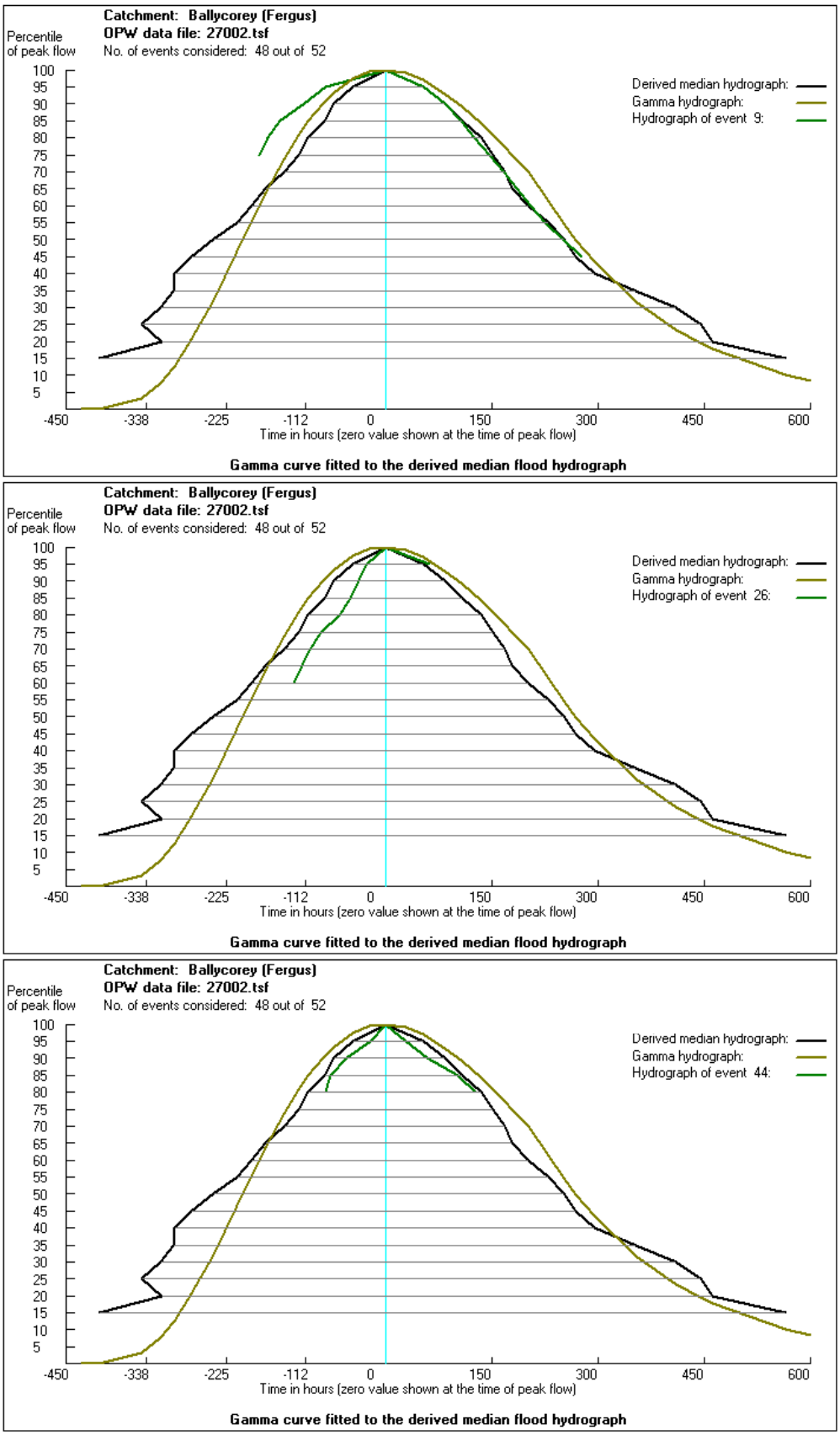

Fig. D.2.30 The derived median (best non-parametric) and Gamma-I median (best parametric) hydrographs, produced using the calibration events, shown superimposed on the observed flood hydrographs of the three verification events at Station No. 27002 (Ballycorey on the Fergus)

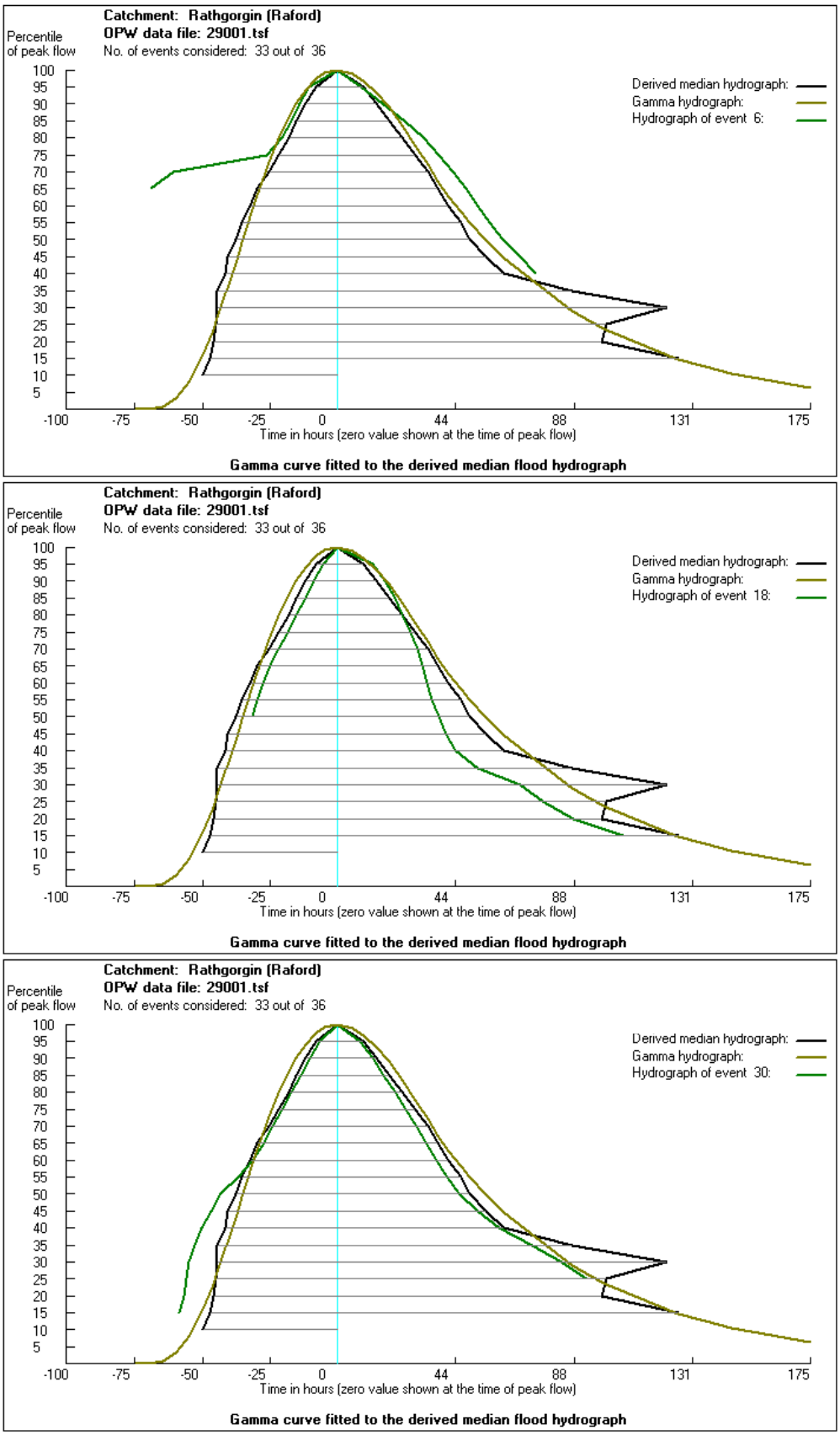

Fig. D.2.31 The derived median (best non-parametric) and Gamma-I median (best parametric) hydrographs, produced using the calibration events, shown superimposed on the observed flood hydrographs of the three verification events at Station No. 29001 (Rathgorgin on the Raford)

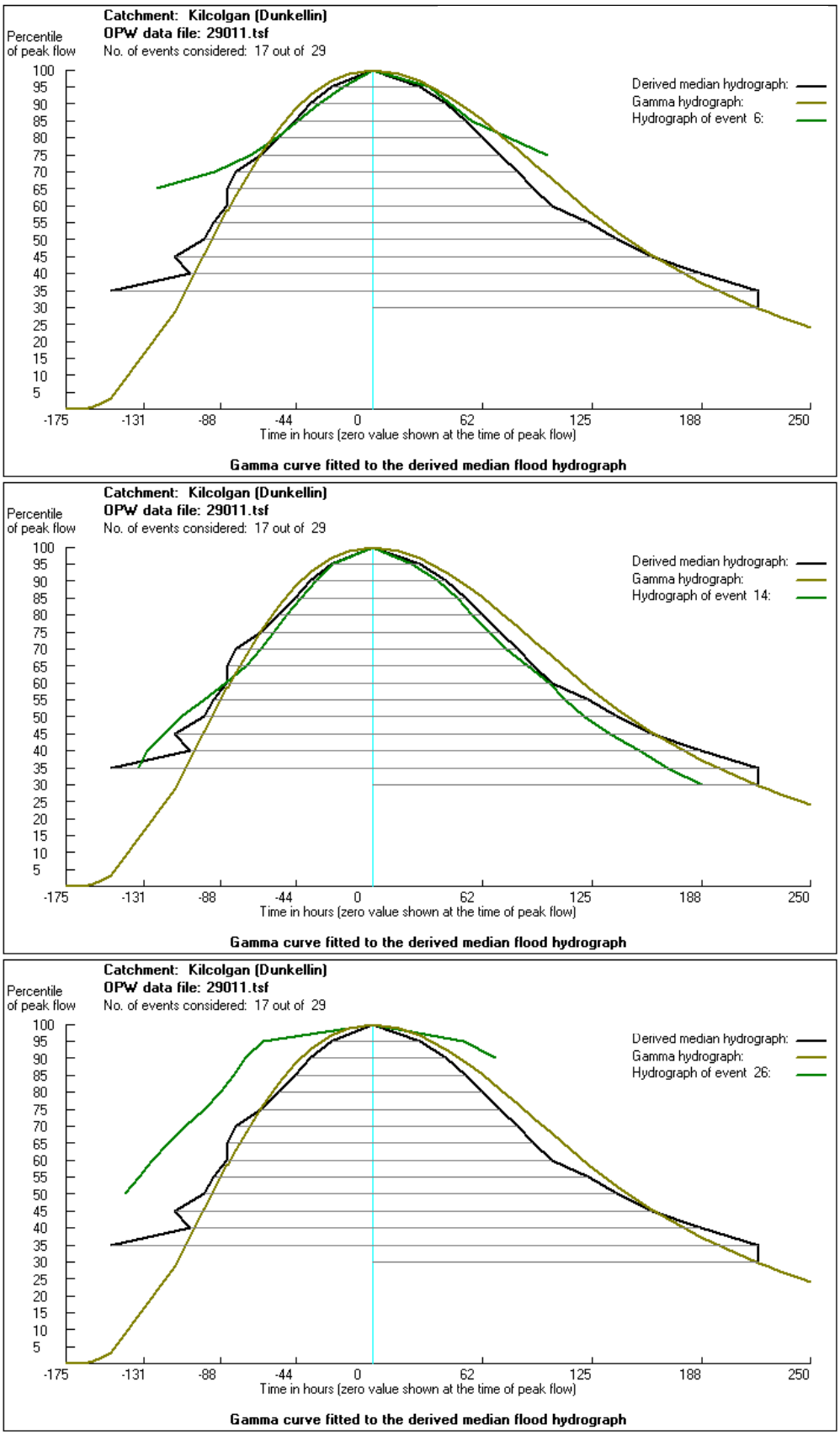

Fig. D.2.32 The derived median (best non-parametric) and Gamma-I median (best parametric) hydrographs, produced using the calibration events, shown superimposed on the observed flood hydrographs of the three verification events at Station No. 29011 (Kilcolgan on the Dunkellin)

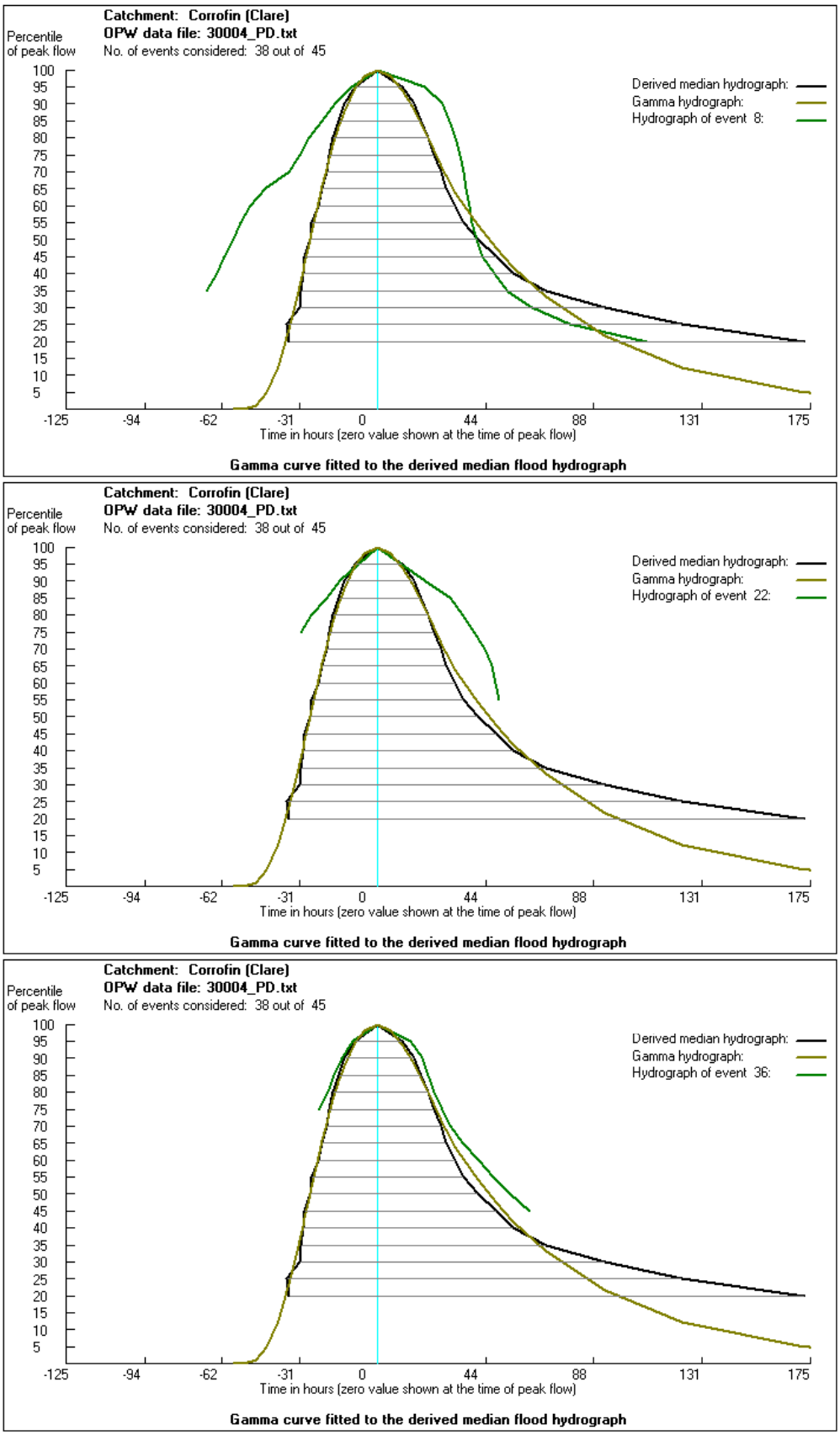

Fig. D.2.33 The derived median (best non-parametric) and Gamma-I median (best parametric) hydrographs, produced using the calibration events, shown superimposed on the observed flood hydrographs of the three verification events at Station No. 30004 (Corrofin on the Clare)

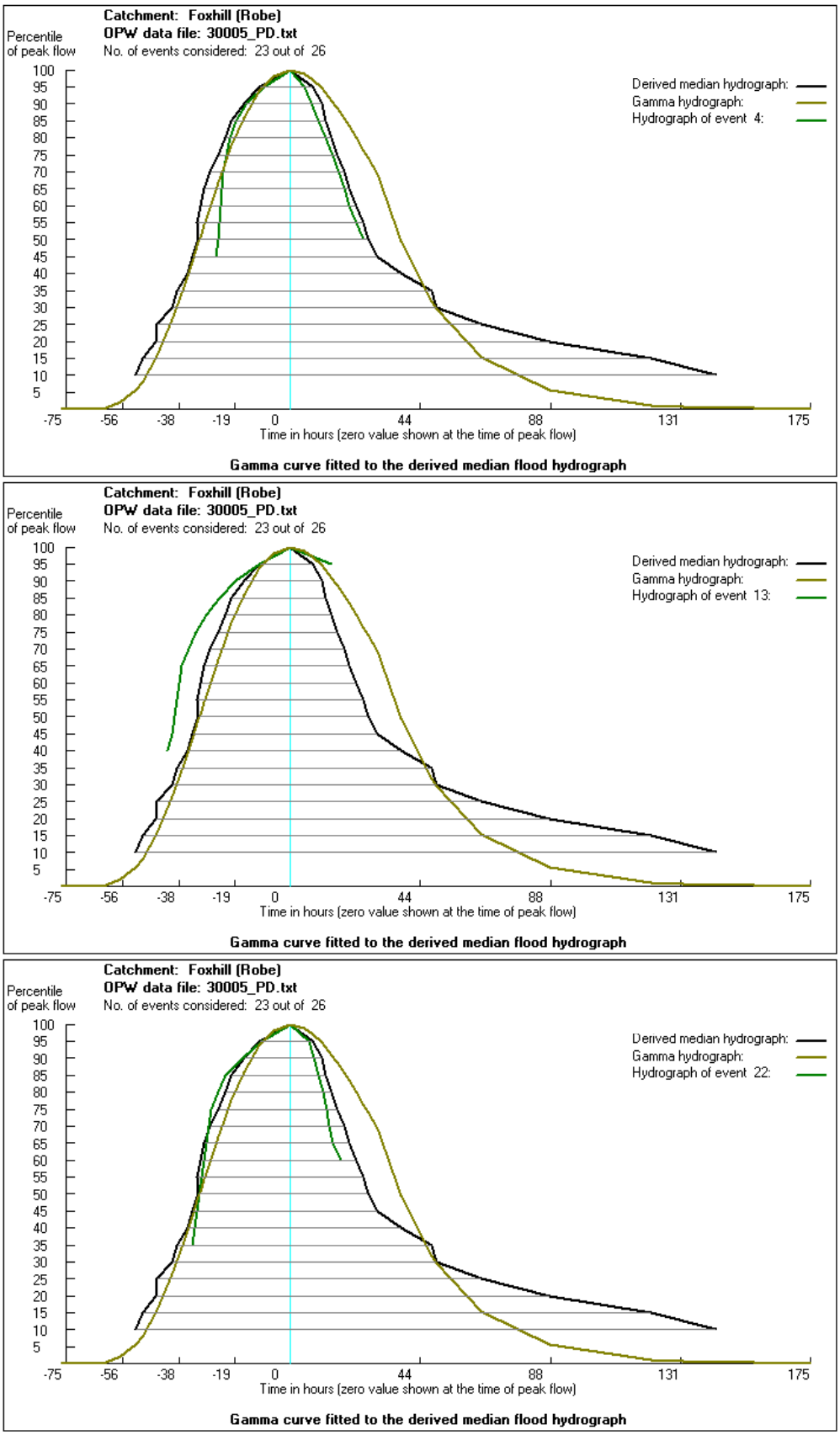

Fig. D.2.34 The derived median (best non-parametric) and Gamma-I median (best parametric) hydrographs, produced using the calibration events, shown superimposed on the observed flood hydrographs of the three verification events at Station No. 30005 (Foxhill on the Robe)

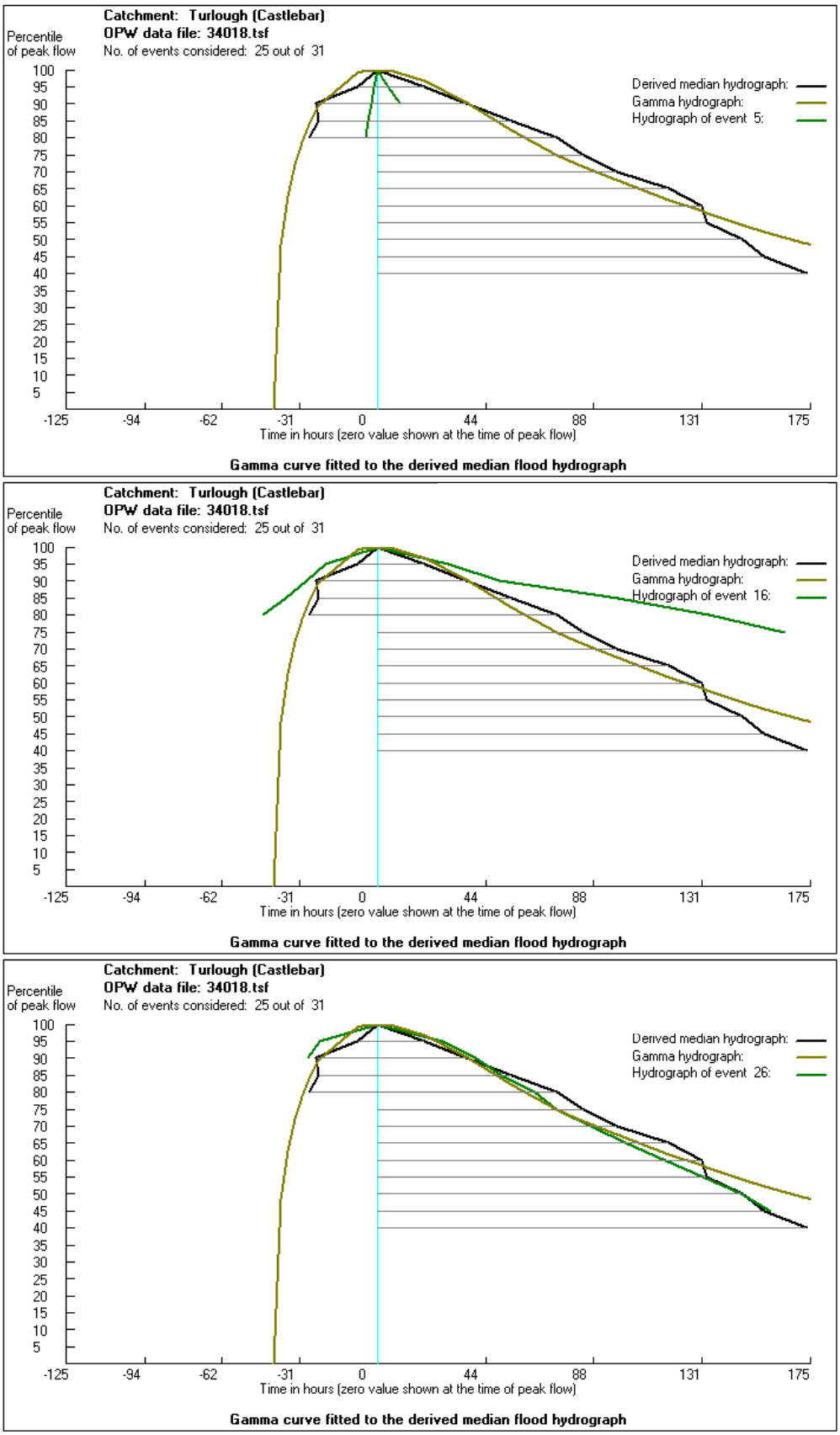

Fig. D.2.35 The derived median (best non-parametric) and Gamma-I median (best parametric) hydrographs, produced using the calibration events, shown superimposed on the observed flood hydrographs of the three verification events at Station No. 34018 (Turlough on the Castlebar)

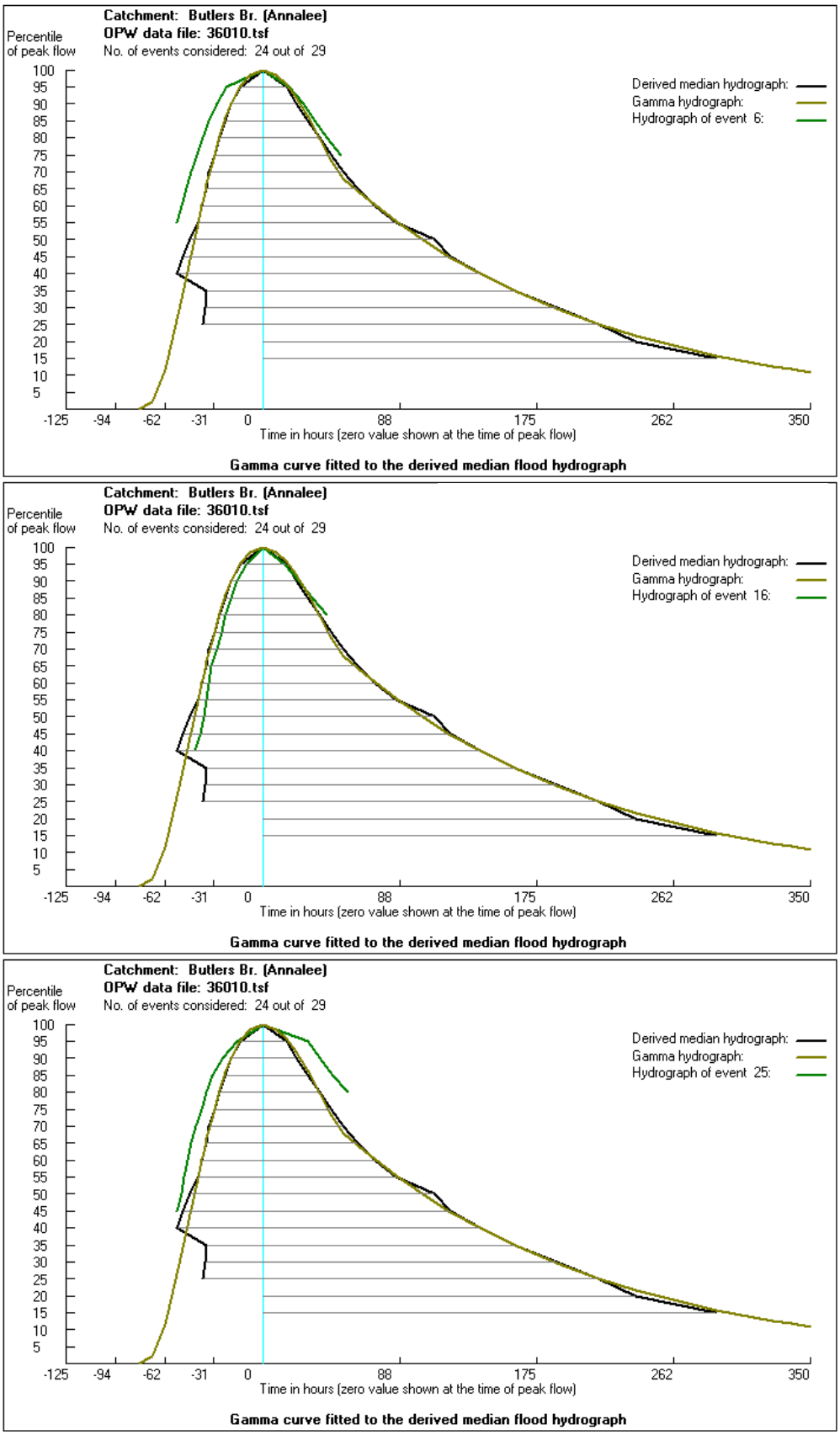

Fig. D.2.36 The derived median (best non-parametric) and Gamma-I median (best parametric) hydrographs, produced using the calibration events, shown superimposed on the observed flood hydrographs of the three verification events at Station No. 36010 (Butlers Br. on the Annalee)

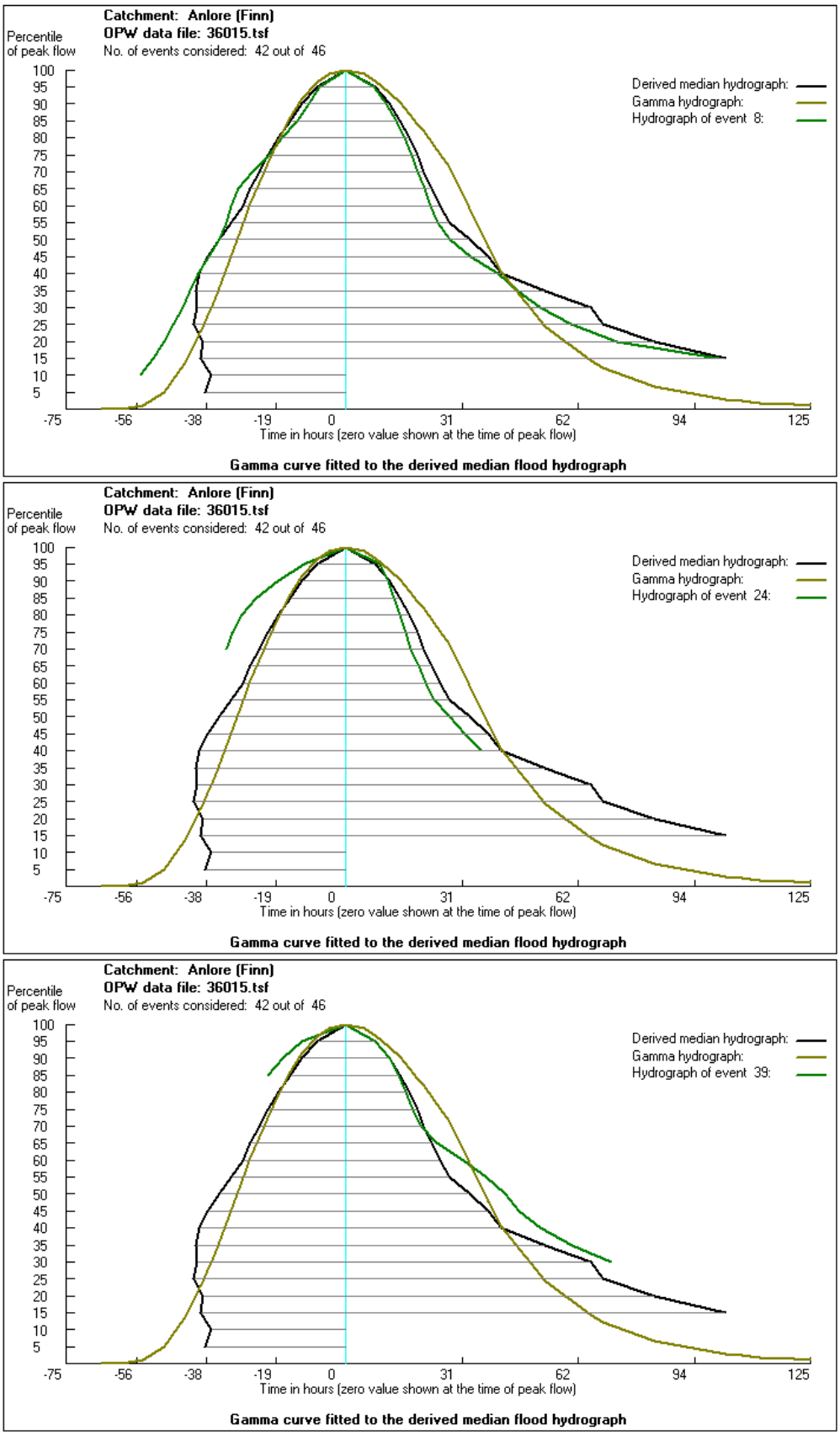

Fig. D.2.37 The derived median (best non-parametric) and Gamma-I median (best parametric) hydrographs, produced using the calibration events, shown superimposed on the observed flood hydrographs of the three verification events at Station No. 36015 (Anlore on the Finn)